Extended Release of DTPA *via* Encapsulation into Nanoparticles for the Decorporation of Deposited Radioactive Contaminants in the Lungs

by Manal Almalki

A thesis submitted to the Faculty of Graduate and Postdoctoral Affairs in partial fulfillment of the requirements for the degree of

Doctor of Philosophy

in

Chemistry

Carleton University, Ottawa, Ontario, Canada

Abstract:

Diethylenetriaminepentaacetic acid (DTPA) is a decorporation agent that can be used to enhance the release of radioactive actinides such as plutonium, americium, and curium following a radiological incident. It has also been approved by the U.S. Food and Drug Administration. In either the Zn- or Ca-form, DTPA is excreted rapidly from the body following administration. This presents a problem because repeated doses of the decorporation agent are required to remove the radioactive actinides.

In this research project, different nanocarriers for pulmonary administration have been tested to slow down the rapid excretion of DTPA following administration. DTPA-H_5 loaded polyethylene glycol (PEG) functionalized TiO_2 nanoparticles were used for the first time to sustain the release of DTPA in an *in vitro* study. However, the loading capacity of DTPA on the prepared PEG-TiO_2 remained lower than that needed for application in the decorporation of actinides. In a dialysis test, both PEG-TiO_2 nanoparticles and plain DTPA showed an extended drug release over 22 hours with a statistically significant difference in half-time between 3.5±0.3 hours and 2.5±0.2 hours, which was inadequate for our research goal of sustained release from just one single administration over two or three days.

The double-emulsion (water-in-oil-in-water) solvent evaporation technique was utilized to prepare Zn-DTPA encapsulated poly lactic-co-glycolic acid (PLGA) nanoparticles. These polymeric nanoparticles were synthesized and applied for the first time to extend the drug release of Zn-DTPA. A slow and sustained release of the encapsulated Zn-DTPA from the PLGA nanoparticles over 10 hours was obtained by dialysis with a release half time of 3.5 hours.

Liposomes from soy lecithin were selected as a nanocarrier for pulmonary delivery of Zn-DTPA. Lipid hydration, reverse phase evaporation, and mechanical sonication methods were used for the preparation of Zn-DTPA encapsulated lecithin liposomes. Liposomes had been used previously for the encapsulation of Ca-DTPA; however, lecithin was used as a source of liposomes in this project due to its low cost compared to liposomes that are prepared from individual lipids. Furthermore, Zn-DTPA was chosen as it had been reported to show less side effects compared to Ca-DTPA. In the dialysis release test, there was a non-statistically significant difference between the Zn-DTPA release from lecithin liposomes and plain Zn-DTPA in terms of the half times (6.5±0.7 and 4.2±0.3 hours, respectively) indicating a *p-value* of 0.28. However, Zn-DTPA encapsulated lecithin liposomes were chosen for an evaluation of their efficacy for the decorporation of radioactive actinides from the lungs of Long Evans rats at the Atomic Energy Canada Limited (AECL) Chalk River Laboratories.

All the DTPA loaded PEG-functionalized TiO_2, PLGA-encapsulated Zn-DTPA, and Zn-DTPA encapsulated lecithin liposomes were characterized by transmission electron microscopy and dynamic light scattering to determine their morphology and size distribution, respectively. They were spherical in shape and exhibited hydrodynamic diameters of 83(±9) nm, 379(±5) nm, and 178(± 2) nm, respectively. Their loading capacities were 21±0.3 mg/g, 106±7 mg/g, 41±5 mg/g, respectively. The extended-release of Zn-DTPA from nanoparticles into either simulated lung fluid or distilled deionized water was evaluated via dialysis or via sample and separate methods.

PREFACE

This preface provides full bibliographical details for each article included in this thesis, as well as whether the article is reproduced in whole or in part. Permission was obtained from the publishers to include the articles in the thesis. Both the thesis and the articles relevant to these chapters must be cited when citing material from this thesis.

As per the directives within Carleton University's Integrated Thesis policy, the "supervisor" (Edward P.C. Lai) and the "student" (Manal Almalki) confirm student was fully involved in setting up and conducting the research, obtaining data and analyzing results, as well as preparing and writing the material presented in the co-authored articles integrated in the thesis.

Chapter 2

Almalki M, Lai EPC, Ko R**,** Li C (2017). Polyethylene Glycol-Functionalized Titanium Dioxide Nanoparticles for Extended-Release of Diethylenetriaminepentaacetic Acid into Lung Fluid to Enhance the Decorporation of Radioactive Actinides. Journal of Nanoscience, Nanomedicine, and Nanobiology. 1: 002

Chapter 3

Almalki M, Lai EPC, Ko R, Li C (2018). Encapsulation of Zn-DTPA into Poly Lactic-co-Glycolic Acid Nanoparticles via a Modified Double Emulsion Method for Extended Release into Lung Fluid. Journal of nanomedicine. 2: 1009

These two articles were wholly reproduced and reformatted for clarity of presentation. The student performed all the work in the articles. The writing was collaborative among the co-authors.

Chapter 4

Almalki M, Lai EPC, Ko R, Li C (2020). Facile Preparation of Liposomes-encapsulated Zn-DTPA from Soy Lecithin for Decorporation of Radioactive Actinides
Manuscript submitted to the Canadian Journal of Chemistry on an exclusive basis for publication as a research article on July 7th, 2020.

Chapter 5

Conclusion

Acknowledgements

I would like to express my sincere gratitude for the tireless work of my supervisor, Dr. Edward Lai, who provided invaluable support and guidance throughout my research and studies at Carleton University. A special thanks goes to my Co-supervisor Chunsheng Li for his support, guidance and motivation. I am also very grateful to my project partner Raymond Ko for sharing experiences and knowledge as well as being always around whenever I needed him. I would like to thank all my colleagues Samar, Adam, and Ivory for sharing experiences and knowledge. I would like to extend my thanks to my thesis advisory committee, Dr. Robert Burk and Dr. Sean Barry for their support and encouragement at various stages of my studies. I would also like to thank all the members of staff at our department for their assistance and kindness during my time as a student in Ottawa. Specifically, I would like to thank Chantelle Gravelle for her support and administrative assistance over the years. I appreciate the technical support provided by Jim Logan. I am also thankful to Peter Mosher, Tanya and Susa in the science store for their kindness and dedication to their work.

I would like to extend my thanks to my supervisor at Saudi Culture Bureau Dr. Nancy Gad for her invaluable support, guidance, and motivation during my studies. My studies would not be possible without the generous support of the Saudi Ministry of Higher Education and Taibah University, who financially supported my education through a scholarship.

Finally, it is with great pleasure and sincerity that I express my gratitude to my loving and supportive family. They have been immensely patient, encouraging and loving as I worked to balance my research, studies and raising a family. In particular, my husband

Ali, who has been my rock throughout the years of my studies that have led me to this point in my career. My children, Rafaa, Zaid, and Rakan who I always looked forward to seeing and spending time with after a long day's work. My family in Saudi Arabia, including my parents, sisters and brothers, who I miss dearly, have been patient and supportive from a distance. My sincere gratitude goes to my best friend which I personally consider my own family member, Esma, for her constant support and encouragement. She has led me through tough situations in the past couple years of my studies. These are all people that have been invaluable to my journey so far, and where I get my strength

Table of Contents

List of tables

List of figures

List of abbreviations

Continuous flow	CF
Controlled release	CR
Dialysis membrane	DM
Drug delivery nanosystem	DDNS
Diethylenetriaminepentaacetic acid	DTPA
Dynamic light scattering	DLS
Fourier transform infrared spectroscopy	FTIR
Generalized arterial calcification of infancy	GACI
grays	Gy
Immediate release	IR
Intravenous	IV
Liquid chromatography- mass spectrometry	LCMS
Minimum effective concentration	MEC
Minimum toxic concentration	MTC
Polyvinyl alcohol	PVA
Pseudoxanthoma elasticum	PXE
Polyethylene glycol	PEG
Poly Lactic-co-Glycolic Acid	PLGA
Sample and separate	SS
Sievert	Sv
Simulated lung fluid	SLF
Titanium dioxide	TiO_2

Transmission electron microscopy	TEM

Chapter 1. Introduction

1.1 Radiation: types, sources, doses and health impacts

Radiation is the emission of energy in the form of particles or waves [1]. Radiation can be classified based on its effect on matter and can be categorized into two types: ionizing and non-ionizing radiation. Cosmic rays, X rays, and the emissions from radioactive materials are all examples of ionizing radiation. Non-ionizing radiation, on the other hand, includes ultrasound, ultraviolet light, radiant heat, radio waves, seismic waves, and microwaves [2]. Compared to non-ionizing radiation, ionizing radiation is considered to be much more harmful because it has enough energy to ionize atoms and induce chemical or biological changes in a living cell [3]. There are mainly four types of ionizing radiation, including alpha, beta, gamma, and neutron [4]. Radioactive materials can be found naturally in the environment in the form of gamma rays from the earth, radon decay products in the air, and various radionuclides in food or drinks [5]. Also, it can be produced artificially from other sources includes the fallout from the testing of nuclear weapons in the atmosphere, radioactive waste, and nuclear and radiological accidents [5]. When people are exposed to radiation, in order to provide appropriate medical care, the type of radiation and radiation dose must be determined. This is especially critical due to the potential negative health impacts on the public, especially pregnant women and infants [6].

Despite the importance of having nuclear power plants to meet the required energy worldwide, nuclear accidents still can happen. During nuclear accidents, a large amount of hazardous, radioactive materials may be released into the environment, including cesium-

137 (^{137}C), strontium-90 (^{90}Sr), and uranium-234/235/238 ($^{234/235/238}$U) [7]. Humans can be exposed to radioactive materials externally when radionuclides stay outside the body or internally through inhalation or ingestion of contaminated air and food, respectively [8]. Over the past, five major nuclear accidents have occurred, including Kyshtym (Russia, 1957), Windscale Piles (UK, 1957), Three Mile Island (USA, 1979), Chernobyl (Ukraine [then USSR], 1986), and Fukushima (Japan, 2011) [9]. According to the International Nuclear and Radiological Event Scale (INES)- a method that has been established to determine the extent of nuclear accidents, all of the above-mentioned nuclear accidents are level 5-7 in the scale (running from limited release of radioactive material to a major release of radioactive material) [9]. Some of the accidents have been reported to exhibit either direct or indirect health effects on children and adults living near the plants, including thyroid cancer as well as long-term psychosocial effects [9]. Currently, three nuclear power plants are in operation in Canada, with three of them are located in Ontario. Any potential accident may cause significant health problems [10]. Sheltering of the affected populations may not be enough to protect radiation-exposed people and immediate medical care may be necessary to mitigate the negative effects.

In order to determine the biological effect of any ionizing radiation, it is important to measure the absorbed dose in a human. The absorbed dose refers to the amount of the absorbed energy by unit mass of tissue and is measured in grays (Gy) and 1 gray is equal to 100 rad. [11]. The equivalent and effective doses are measured in sievert (Sv) and can be calculated from the absorbed dose to determine the potential risks that can be caused by radiation to a specific tissue or a specific radiation to the whole body, respectively. Basically, one sievert is equal to one gray multiplied by a relative biological effective

danger factor and a distribution factor of the radiation energy. Dose limits are provided by international organizations and national authorities, such as the Canadian Nuclear Safety and Commission, in regulations of radiological protection as summarized in Table 1.1 [12].

Table 1.1 Dose limits provided by Canadian Nuclear Safety and Commission, in regulations of radiological protection (Canadian Nuclear Safety and Commission, 2019).

Person	Period	Equivalent dose (mSv)	Effective dose (mSv)
Nuclear energy worker	One-year dosimetry period	500 (skin, and hand and feet)	50
Nuclear energy worker (pregnant)	Pregnancy period		4
Non-nuclear energy worker	One-year	50 (skin, and hand and feet)	1

The "4 mSv" for pregnant women refers to the dose limit after declaring pregnancy.
Equivalent dose measures the effect of ionizing radiation into a specific tissue.
Effective dose measures the effect of a specific ionizing radiation into the whole body.

When significant amounts of radioactive materials are deposited in the human body, they can cause subsequent cardiovascular effects, hypertension, stroke, central nervous system effects, and cancers as well [13]. For example, iodine-131 and strontium-90 travel to the thyroid gland and the bone tissue, respectively, causing cancers [14]. Decorporation agents that have been developed to remove radioactive materials should be employed immediately/shortly after each accident to minimize any health risks posed by the internalized radioactive materials.

1.2 Decorporation agents for radioactive actinides

Nuclear accidents and terrorist actions are considered to be the primary sources of radioactive actinides. Upon internalization into the body via inhalation, ingestion, or through open wounds, these actinides can cause significant health risks such as cancers of the lung, liver, thyroid, stomach, and bone. Removal of these actinides is the most effective method in reducing health problems associated with such contaminates [15]. Many decorporation agents for internalized radioactive contamination have been recommended by the U.S. National Council on Radiation Protection and Measurements and the International Atomic Energy Agency [16]. However, due to the limited efficacy, low specificity, and high toxicity of most of the developed drugs, only a few drugs have been approved for the decorporation therapy by the US Food and Drug Administration [16]. Molecules such as catecholates (CAM), hydroxamates, hydroxypyridonates (HOPO), 1-hydroxyethane-1, 1′-diphosphonic acid (HEDP or EHBP), and calixarenes are still in the development clinic testing their ability for the decorporation of transuranic actinides [17]. Diethylenetriaminepentaacetic acid (DTPA, in either Zn- or Ca-form) is the only decorporation agent that has been approved by the U.S. Food and Drug Administration and available in the market for decorporating actinides [18].

1.2.1 Decorporation agent: DTPA

Diethylenetriaminepentaacetic acid (DTPA, in either Zn- or Ca-form) is an effective decorporation agent with high affinity towards various metals. It increases the excretion of the internal radioactive actinides in urine via the formation of a stable soluble complex. Calcium and zinc tri-sodium salts (Ca-/Zn-DTPA) from the German

manufacturer Hameln Pharmaceuticals GmbH have been approved by FDA in 2004 for the decorporation of internalized radioactive actinides such as americium (Am), curium (Cu), and plutonium (Pu) [19]. Ca-/Zn-DTPA can decorporate only actinides, not Cs/I/Sr due to their low stability constants (e.g. 10 for Sr-DTPA). Ca-/Zn-DTPA exchange Ca or Zn for actinides of higher binding affinity to form 1:1 stable metal:chelate complex that can be eliminated by glomerular filtration into urine [20]. Table 1.2 shows the stability constants of Ca-/Zn-DTPA and actinides of interest. Accumulation of these α-emitter radioactive actinides in the liver and bone is considered to be very dangerous due to their long biological half-lives [17]. However, to reduce the absorption and increase the removal of radioactive actinides, the decorporation treatment should be initiated as soon as possible following contamination. Late decorporation therapy reduces the effectiveness of the decorporation agent as more actinides become incorporated by tissues/organs.

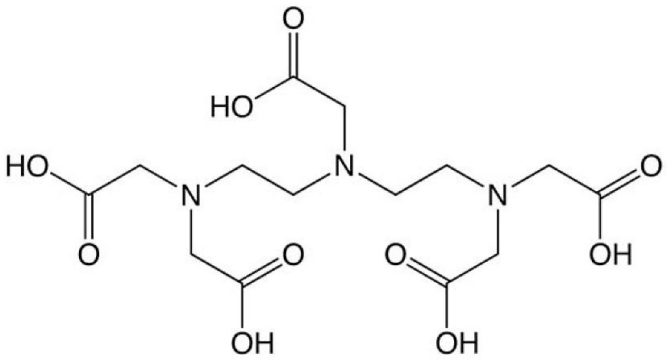

$$Zn\text{-}DTPA^{3-} + An^{n+} \longrightarrow An\text{-}DTPA^{(5-n)-} + Zn^{2+}$$

Figure 1.1 Chemical structure of DTPA.

Table 1.2 Stability constants of metal-DTPA complexes (Byegard J, 1999, Stricklin et al., 2014, Brown M, 2012.

Metal-DTPA complex	Stability constants
Ca-DTPA	10.8
Zn-DTPA	18.4
Am-DTPA	22.9
Cm-DTPA	22.9
Pu-DTPA	20.6

To measure the excretion of DTPA in plasma and urine, ^{14}C-DTPA (a radioactive nuclide) was injected into 2 subjects. As can be seen in Figure 1.2, DTPA was distributed in the plasma in the first 7 hours and 99% of the injected DTPA was accumulated in urine after 10 hours. Zn-DTPA distributed mainly in the extracellular fluid, and no accumulation of Zn-DTPA was observed in any specific organs following an intravenous administration [21]. In animal studies, an oral administration of Zn-DTPA resulted in the absorption of only 5% for the limited absorption of Zn-DTPA by the gastrointestinal tract [21]. An inhaled administration of 1 gram of Zn-DTPA into 18 patients found to be effective as an intravenous injection with the same quantity in the elimination of internalized radioactive actinides in urine [21]. Zn-DTPA shows low metabolisms changes in the body. Administration of Zn-DTPA at 583 mg to patients over 4 years did not exhibit any toxicological effects [22]. Frequent administration was found to be very effective in removing ^{241}Am from the liver, saving victims from death resulted from liver failure by radiation. Zn-DTPA can be administrated in patients who require multiple

doses and can be continued over several days, months, or even years [21]. Nebulization of three doses, 1 gram each, of Zn-DTPA (1:1 Zn-DTPA and saline) followed by 6 intravenous doses increased the plutonium excretion 45 times [21].

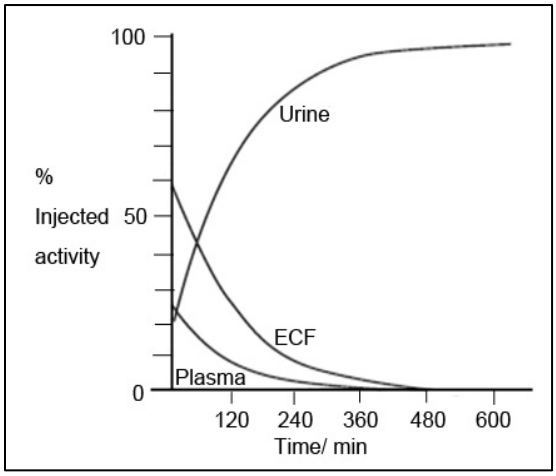

Figure 1.2 Percent distribution of ^{14}C-DTPA after injection in plasma and urine (FDA, 2013).

1.2.2 Administration of Zn-DTPA

The efficacy of DTPA for decorporation of a radioactive actinide depends on a number of factors. These include the type of radioactive actinide, the quantity of the contaminant, its chemical form, affinity for a specific target, the route of contamination, duration of exposure, part of the body exposed, physical condition and age of the patient. [11,23]. In the past, internalized radioactive actinides have been removed from exposed workers using Ca and Zn-DTPA [24,25]. The FDA recommends the use of Ca-DTPA as a first dose (1 g of DTPA/70 kg body weight for adults, and 14 mg of DTPA/kg for children not exceeding 1 g/day) in the first 24 hours after internal contamination because it is more

effective than Zn-DTPA. However, after 24 hours, if further treatment is required, Zn-DTPA exhibits similar effectiveness to Ca-DTPA. This said, if Zn-DTPA is not available during the treatment period, then Ca-DTPA can be used along with essential minerals to prevent their depletion in the body [26].

Depending on the route of contamination, Ca-DTPA and Zn-DTPA can be administrated via inhalation using a nebulizer or by intravenous injection [23]. Ca-DTPA was administrated via a nebulizer an hour after a puncture wound. This was followed by the administration of five daily treatments with Zn-DTPA [27]. The decorporation agents Ca-DTPA and Zn-DTPA were found to be very effective in the elimination of Pu and Am from the wound site [27]. The removal of the soluble Pu deposited in the lungs was significant using aerosolized Ca-DTPA compared to administration of Ca-DTPA through intravenous (IV) injection. The intrapulmonary administration of Ca-DTPA following a systemic administration of Pu exhibited similar decorporation efficacy to IV administration of Ca-DTPA [28]. A combination of pulmonary delivery and IV administration of Ca-DTPA after inhalation of Pu nitrate has been shown reduction of the pulmonary and extrapulmonary burden of Pu in animals compared to pulmonary delivery or IV administration alone [29].

1.2.3 Side effects of Zn-DTPA

The main side effect of Zn-DTPA is the depletion of certain essential nutritional metals [23]. However, compared to orally administrated Ca-DTP, Zn-DTPA is less toxic [30]. An oral administration of Zn-DTPA for one month at 30, 150 and 300 μmol/kg/day doses did not demonstrate a different degree of toxicities in beagle dogs or in rats.

However, Ca-DTPA caused slight histological changes in the small intestine, kidneys, and in the liver of beagle dogs after one injection a day over the period of one month [31]. Administration of Zn-DTPA via inhalation was shown to cause asthma exacerbation. Therefore, it is essential to monitor patients who are susceptible to asthma exacerbation during nebulized decorporation therapy [18].

1.3 Methods to improve pharmacokinetic properties of DTPA

DTPA is an ionic compound with low cell permeability which limits its decorporation efficacy of actinides that are still in the blood circulation due to the rapid clearance of DTPA [32]. Steven *et al*. studied the clearance of DTPA and found that most of the DTPA had been accumulated in urine after 24 hours of an oral administration of ^{14}C-labeled DTPA, which means that only a small amount of DTPA had been retained [33]. In this matter, DTPA cannot pass through the cell membrane to bind with actinides that are deposited in various tissues/organs [15]. Attempts, such as structural modifications of DTPA and various formulations of DTPA, have been explored to prolong DTPA circulation half-life and to improve its biodistribution.

1.3.1 Structural modifications of DTPA

The *in vivo* effectiveness of DTPA in removing actinides is limited by its charge and hydrophilicity [22]. To improve DTPA intracellular penetration, structural modification of DTPA has resulted in the formation of a lipophilic derivative of DTPA called “puchel” with two decane chains [34, 35]. However, this derivative was found to be less efficient in removing actinides in *in vivo* experiments compared to Ca-DTPA [36,37].

Puchel also induced lung inflammation and liver damage, indicating that it is more toxic than DTPA [24]. Linear alkyl groups of various lengths (from C_8-C_{22}) have been attached to triethylenetetramine hexaacetic acid (TTHA) to improve drug absorption and bioavailability [38]. Among these compounds, only C_{22}TT and C_{16}TT were able to reduce ^{241}Am and ^{239}Pu content *in vivo* in rats. However, treatment with these compounds was not as effective when compared to Ca-DTPA [27].

1.3.2 Formulations of Zn-DTPA

Several formulation approaches have been developed to improve DTPA pharmacokinetics properties. Such formulations may help reduce the number of repeated doses that are needed to reach the required decorporation efficacy. Zn-DTPA tablets containing permeation enhancers have been developed to allow oral delivery of Zn-DTPA. It has been reported that an oral administration of Zn-DTPA tablet at 1325 mg/kg/day did not exhibit any observed adverse effect when given to beagle dogs [39]. The most advanced formulation to enhance oral delivery of Zn-DTPA was achieved *via* the formation of enteric-coated Nano® DTPA capsules by the company Nanotherapeutics Inc. [40]. This formation was composed of DTPA and zinc acetate in a powder form that has shown to enhance oral bioavailability of DTPA and improved decorporation of Am-241 in dogs compared to an intravenous (IV) administration of Zn-DTPA [41]. Intravenous administration of Ca-DTPA encapsulated in conventional liposomes or polyethylene glycol (PEG)-coated stealth multilamellar liposomes were found to improve the removal of Pu significantly from rats in comparison to a plain Ca-DTPA solution [42,43]. However, the most promising result of Ca-DTPA encapsulated liposomes was obtained with

polyethylene glycol (PEG) coated unilamellar liposomes that exhibited the best decorporation efficiency of Pu compared to conventional unilamellar, conventional multilamellar, and PEG-coated multilamellar liposomes [44]. The biodistribution and fate of liposomes after injection is highly dependent on their size. The clearance of liposomes decreased as the size of liposomes became smaller. The PEG-coated unilamellar liposomes (100 nm) are able to cross the vascular endothelium and avoid the clearance by phagocytes compared to multilamellar liposomes [44]. Therefore, they remain longer in the blood circulation without being phagocyted and reach the target cells/tissues. The clearance of free DTPA from the blood circulation was 3 and 20 times faster compared to the clearance of DTPA encapsulated in conventional and PEG-coated multilamellar liposomes, respectively according to a study previously reported by Phan *et al*. in rats [44]. Compared to conventional and stealth multilamellar liposomes, stealth liposomes exhibited longer release time of DTPA as illustrated in Figure 1.3.

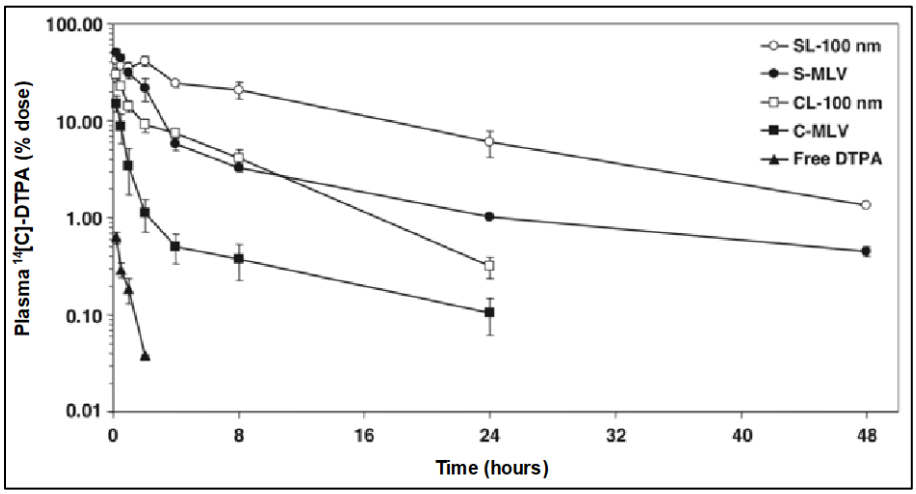

Figure 1.3 Plasma pharmacokinetics of free [^{14}C]-DTPA, conventional multilamellar liposomes, conventional unilamellar liposomes, stealth multilamellar liposomes, and stealth unilamellar liposomes over 48 h in rats (Phan *et al*., 2005).

1.4 Extended release of DTPA from nanoparticles

Several formulations of nanoparticles have been developed for the extended release of DTPA using different preparation methods with either the Ca or Zn form of DTPA. DTPA has been attached covalently to human serum albumin-based nanoparticles (HSA) and conjugated for the treatment of arterial calcification of infancy (GACI) and pseudoxanthoma elasticum (PXE). DTPA-HSA nanoparticles were found to be very effective not only in resolving existing calcification, but also in inhibiting further formation of arterial calcification. Moreover, DTPA attached HSA nanoparticles minimize the side effect that results from the systemic administration of the free DTPA due to the extended release of DTPA from the HAS nanoparticles [45]. DTPA has been covalently conjugated onto poly (γ-glutamic acid) (γPGA) and then mixed with chitosan nanoparticles (CS) for effective oral delivery of insulin. The CS/γPGA-DTPA nanoparticles prolong the bioavailability of insulin by inhibiting proteolytic degradation and improving paracellular

permeability of insulin. Incorporation of DTPA into CS/γPGA nanoparticles improves the efficacy of insulin and shows a significant and prolonged hypoglycemic effect [46]. Chitosan nanoparticles have been used to deliver Gd-DTPA as MRI contrast agents for tumor diagnosis. The chitosan-hyaluronic acid nanoparticles (GCHN) was synthesized via carbodiimide reaction of chitosan with Gd-DTPA to form (CS-DTPA-Gd). The obtained CS-DTPA-Gd and hyaluronic acid was employed to synthesize GCHN by ionic gelation. The GCHN extend the release of DTPA-Gd which prolonged the imaging time for MRI diagnosis in the B16 tumor-bearing mice model [47]. Fluorescent DTPA-silk fibroin nanoparticles radiolabeled with ^{111}In have been developed to study the biodistribution and stability of protein-derived nanoparticles. DTPA has been conjugated with radiolabeling silk fibroin nanoparticles (SFN) tagged with fluorescein isothiocyanate (FITC) to improve their stability and extends their imaging period. The conjugation of DTPA and FITC to the SFN increases the stability of SFN in aqueous media and prolong the imaging time for 24 hours [48].

1.5 Mechanisms of drug delivery systems

Drug delivery systems can be categorized based on the drug release mechanism into immediate release, delayed release, extended release, and controlled release [49]. In immediate release, where conventional dosage forms are used, the drug is released rapidly after administration [49]. Immediate release limits the efficacy of drugs that have short biological half-lives, demanding frequent administration [49]. The drug is released at a specific time after administration in delayed release. Extended release allows the drug to be released over a long period of time, which could reduce dosing frequency [49]. In

controlled release, the drug is released at a constant rate over a prolonged period. An ideal drug delivery system delivers the drug into the site of action when the drug is needed to maintain the therapeutic level [49].

Controlled release drug delivery systems have been employed to improve the pharmacokinetic profile of the therapeutic drugs [50]. These systems pose several advantages compared to immediate release dosage forms, such as maintaining drug concentration over a prolonged period of time, reducing plasma level fluctuations, enhancing drug efficiency, decreasing dose frequency, minimizing side-effects, and enhancing patient compliance [51]. The purpose of the controlled release system is to maintain the drug concentration in the plasma, tissues, or target organs at the therapeutic range [52]. The therapeutic range is the drug concentration above the minimum effective concentration (MEC) and below the minimum toxic concentration (MTC), as illustrated in Figure 1.3 [49,53]. The controlled release system follows the zero-order drug release kinetics that ideally allows a drug plasma concentration over a long period [49].

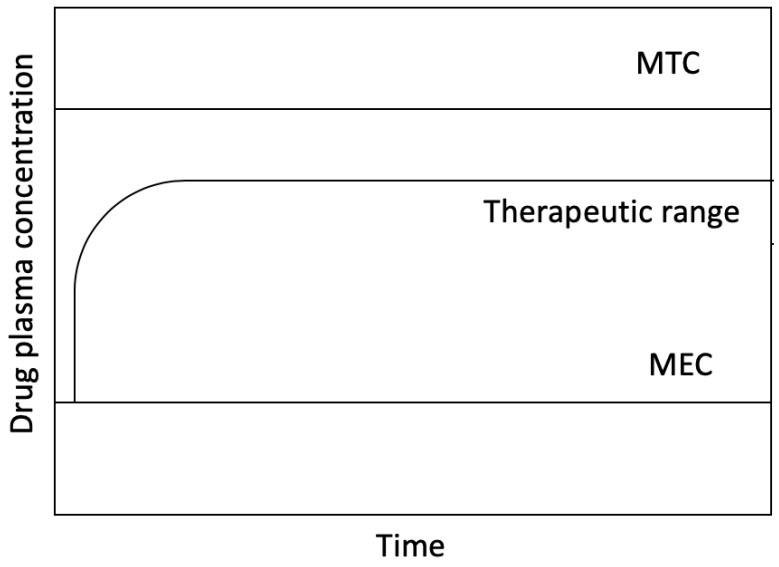

Figure 1.4 Drug plasma concentrations at the therapeutic range, minimum effective concentration (MEC) and the minimum toxic concentration (MTC) (Perrie Y 2012, Chen E *et al*., 2018).

Nanoparticles exhibit several properties that make them suitable for controlled drug release. Polymers, inorganic materials, and biomaterials have been used for the preparation of nanoparticles-based control drug release [54, 55, 56]. In these controlled release preparations, the drug is either encapsulated in the nanoparticle or dispersed throughout a matrix [49]. Drugs can be released from nanoparticles in a controlled manner following one or more mechanisms depending on the controlled-release formulation. The main mechanisms involved in the controlled release of drug are diffusion, dissolution/swelling, and osmotic pumping [57]. Diffusion-controlled drug release mechanism is the most common mechanism of drug release. When nanoparticles absorb water from the release medium, pores are formed in the matrix, resulting in drug diffusion. Drugs can be released from the nanoparticles due to dissolution of the polymer matrix containing the drug as a result of water absorption by the polymer. However, if the polymer is hydrophobic,

swelling of the polymer matrix can occur resulting in drug release without dissolution of the polymer. Osmotic pumping occurs when the polymer absorbs a large volume of the released medium which increases the pressure inside the polymer matrix. As the pressure increases, the polymer goes under rearrangement of chains. However, after some time, this pressure can overcome the polymer chain rearrangement which leads to cracks for drug release [57].

1.5.1 *In vitro* drug release test methods

Several *in vitro* methods have been developed to determine the drug release kinetics and the amount of drug released during a release test. *In vitro* drug release tests can provide valuable information regarding the performance of the formulated product. These tests are mostly performed at physiological conditions (pH 7 and 37 C^{o}) [58]. Sample and separate (SS), dialysis membrane (DM), and continuous flow (CF) methods have been used to assess the drug release from nanoparticles [58].

In the SS method, the nanoparticulate form is placed in the release media (buffer) that is kept at a constant temperature [58]. To prevent the aggregation of nanoparticles in this method and to reduce its effect on the drug release rate, agitation should be considered during the release test experiment [59]. Sampling can be performed directly from the release media or by dividing the release media into small vials that contain the same volume of the release media. At a fixed time, nanoparticles can be separated physically from the release media by centrifugation or filtration to determine the amount of drug either in the nanoparticles or in the release media [60].

The DM method is another method that has been used extensively to assess the drug release from nanoparticles [61,62,63]. In dialysis, nanoparticles in the release media (inner/donor compartment) are introduced into a dialysis tube or a dialysis bag. Then, the dialysis bag/tube is immersed into a larger container of release media (outer/acceptor compartment). During the release experiment, the drug is diffused through the dialysis membrane to the acceptor compartment. Samples are collected from the acceptor compartment and analyzed to determine the drug release profile [58]. It is crucial in dialysis to keep the outer compartment at least ten times larger than the inner compartment [58]. Dialysis is a very straightforward method in terms of setup and sampling. Also, various molecular weight cut-off (MWCO) for the dialysis membranes are available to be suitable for studying *in vitro* release of drugs with different sizes [64]. Dialysis membrane can be made from cellulosic. The soluble cellulosic can be used to form either fibers via polymer spinning or a film via polymer casting for different applications in the food, pharmaceutical, and paint industries [64].

In the CF method, the release media is circulating through an immobilized nanoparticulate dosage form in a column. The release media passes through a filter to the detector that is used to measure the drug released over time [58]. However, this method may result in erroneous data in the case of small nanoparticles. This is due to the small nanoparticles that can clog the filter in the column and build up high pressure in the system resulting in a slow flow rate [60]. A combination of CF and DM methods would be more successful in studying the drug release from nanoparticles, as this modification can help to overcome the limitations mentioned regarding the CF method [60].

1.5.2 Pulmonary Route of drug delivery

The human respiratory system is mainly consisting of two regions: the conducting airways and the respiratory region. The conducting airway is divided into the nasal cavity, trachea, and bronchi. The respiratory region comprises of respiratory bronchioles, alveolar ducts, and alveolar sacs [65]. The bronchioles and alveolar sacs represent about 95% of the lung's surface area [66].

The pulmonary route of drug delivery offers many advantages compared to other conventional administration routes (e.g. oral, nasal or parenteral routes) in the treatment of respiratory diseases [67]. These advantages include: delivering the drug into the site of action, minimizing the side effect from exposure to frequent doses by systemic administrations, less enzymatic activity (improves drug bioavailability), and rapid drug uptake due to the large absorptive surface area of the lungs (about 70-140 m^2 in adult humans) [68,69]. The pulmonary route has been used to treat various lung disorders such as a topical treatment of asthma, local infectious diseases, and pulmonary hypertension. Also, it has been utilized for the delivery of systemic drugs including insulin, human growth hormones, and oxytocin [66]. Three main types of devices have been developed to deliver drugs into the pulmonary system: metered-dose inhalers, nebulizers, and dry powder inhalers. The selection of these devices is dependent on the target lung region as these devices can produce droplets/particles with specific diameters which deliver the drugs following different mechanisms and require different drug formulations [66]. Intranasal administration and oral inhalative administration are the two modes of delivering drugs through the pulmonary route. Inhalative administration can be further classified into

intratracheal instillation and intratracheal inhalation. In animal studies, intratracheal instillation is the most common administration method where a special syringe is used to deliver the drug suspension into the lungs. The effectiveness of this method can be determined based on the pulmonary absorption of the drug, and its systemic bioavailability [70].

Nanoparticle drug formulations are considered to be an ideal approach for delivering drugs into the lungs compared to traditional aerosol powders and liquid pulmonary dose formulations. The large surface area of drug nanoparticle formulations improves solubility and bioavailability of drugs with poor water solubility [71]. Aerosolized particles deposit in the pulmonary system based on their sizes by three mechanisms: gravitational sedimentation, inertial impaction, and diffusion [66]. Particles with larger size can be deposited by gravitational sedimentation or inertial impaction mechanisms which take place due to gravitational force or hyperventilation, respectively. However, small nanoparticles can be deposited by a diffusion mechanism that occurs due to the Brownian motion [66]. Aerodynamic diameter of nanoparticles or droplets, which reflects the size, surface charge, and shape of droplets and particles, is a very critical parameter in determining the deposition site in the pulmonary system [66].

Inhalation therapy ensures direct delivery of drugs into the lungs; however, several parameters govern their delivery during their transit through the respiratory tract such as particle size and the pulmonary clearance mechanisms. To ensure proper deposition in the lungs, the particle size must be adjusted in the range of 1–5 μm, which offers the desired deposition in the smaller air ways and in the bronchioles [72]. Smaller particles that are <1

μm in size are deposited in the alveolar region but most of these particles are exhaled before reaching the site of action. On the other hand, larger particles that are >5 μm in size are deposited in the upper respiratory tract region (mouth, throat, and trachea) during inhalation [72]. In order for inhaled particles to reach lower areas of the lungs, nanoparticles must overcome the pulmonary clearance mechanisms (e.g. mucociliary escalator system and alveolar macrophages) [72]. Nanoparticles must pass through the mucus layer lining in the upper airways. This layer clears any foreign particles before they move into lower regions in the lungs by coughing or swallowing. Nanoparticles that are able to cross the mucus layer can be phagocytized by the alveolar macrophages [72]. Larger particles with sizes >6 μm are eliminated by the mucociliary system, however, smaller particles can be cleared by alveolar macrophages [72]. Many attempts have been made to justify the particle size with the pulmonary clearance mechanisms to achieve the maximum effectiveness of delivering the drug via inhalation. Table 1.2 summarized the relationship between drug deposition region, particle size, and the mechanism of deposition [72].

Table 1.3 Drug deposition region, particle size, and the mechanism of deposition (Paranjpe M *et al*., 2014).

Location	Size	Mechanism
Bronchi	5–10 μm	Impaction
Bronchioles	1–5 μm	Sedimentation
Alveoli	0.5–1 μm	Brownian motion

1.5.3 Application of nanoparticles in drug delivery

Nanoparticles are defined as particles with the size in the range of 1-100 nm. They exist naturally in the environment but also can be engineered. Applications of nanoparticles vary based on their physicochemical properties [73]. Several drugs have been discovered to treat numerous health conditions, however, some of these medications can result in severe side effects that overcome their treatment benefit. Moreover, some of these drugs have been found to be very effective in *in vitro*, but not in *in vivo* due to its degradation by endogenous enzymes [74]. Nanoparticles can be introduced into the human body via injection, inhalation, or oral intake [73]. Due to their smaller size, nanoparticles have demonstrated unique physicochemical and biological properties. They can easily pass through cell and tissue barriers and deliver the drug to the target site. Drugs can be encapsulated into nanoparticles or attached to the nanocarrier surface either physically or chemically [75]. The size and density of nanoparticles play a significant role in their transport behavior in the bloodstream. Liposomes and metal particles of different densities (1–19 g/mL) were found to exhibit different deposition rates on the blood vessel wall. Nanoparticles with a low density tend to escape the blood flow and marginate towards the vessel wall [76,77]. Nanoparticles as a drug carrier have been proven to improve the drug efficacy, reduce drug toxicity, and minimize side effects compared to the plain drug solution [78]. However, it is very critical to determine a safe dose of these nanosystems by testing them in *in vitro, ex vivo,* and *in vivo* models to avoid or reduce any toxic effects that can be caused by these systems on patients.

When these particles enter the blood circulation, the lymphatic system filters and eliminates nanoparticles from the blood capillaries [79]. This can be considered as a major limitation of drug delivery based on nanoparticles. However, the clearance of nanoparticles is dependent on the size and surface characteristics of particles [73]. The particle size can influence on their distribution into various organs, toxicity, and targeting abilities [73]. Smaller particles tend to remain longer in the circulation whereas larger particles are removed faster [80]. It has been shown that nanoparticles measuring 100 nm exhibited a 2.5-fold and 6-fold greater uptake by target cells compared to particles with 1 μm and 10 μm, respectively [81]. Surface properties of nanoparticles form another aspect that can be manipulated to improve the nanoparticles bioavailability, stability, and to reduce the clearance of nanoparticles by the lymphatic system [82]. Hydrophobic nanoparticles interact strongly with the cell membrane compared to hydrophilic nanoparticles, which lead to higher cell uptake before reaching the target site. [83]. However, surface modification of hydrophobic nanoparticles with hydrophilic polymers such as polyethylene glycol (PEG), poly (N-vinyl-2-pyrrolidone) (PVP), poly (amino acids) and dextran extend the circulation time of nanoparticles in the blood [80]. This modification decreases the interaction between hydrophobic nanoparticles and lipid bilayer which may increase the chance of nanoparticles to reach the desired site [79]. It has been reported that PEGylated nanoparticles referred to as "stealth" nanoparticles can escape the reticuloendothelial system (RES) [84].

Inorganic nanoparticles, polymeric nanoparticles, and liposomes have been used successfully as drug carriers [85]. Doxorubicin-polyethylene glycol-titanium dioxide nanoparticles (DOX-PEG-TiO_2) were found to inhibit the tumor growth in the orthotopic

breast tumor-bearing mice. DOX-PEG-TiO_2 nanoparticles improved the anti-tumor activity of DOX due to their controlled release compared to free DOX. The modified TiO_2 nanoparticles with PEG were found to be safe for use as a drug carrier and did not exhibit any observed side effect [86]. Poly lactic-*co*-glycolic acid (PLGA) nanoparticles have been utilized to treat various lung diseases, as they can deliver drugs into the target site in a controlled manner. For example, inhalable rifampicin-PLGA particles have been reported to reduce the lung bacterial burden 10-fold compared to a plain rifampicin solution. Animals treated with rifampicin-PLGA particles exhibited less inflammation and lung damage compared to those treated with plain rifampicin [87]. Inhalable liposomes have been applied extensively for the delivery of anticancer drugs to treat lung cancer patients. It has been found that 50% of liposomes administrated intratracheally in mice remained in their lungs for 24 hours. Arikace (a liposomal formulation of amikacin) has been used to treat lung infection via inhalation in cystic fibrosis patients and it is in phase III clinical trial. Hence, liposomes prolong drug retention time and increase drug accumulation [88].

1.6 Liquid chromatography-mass spectrometry

Liquid chromatography-mass spectrometry (LC-MS) is used to separate individual components in a complex mixture based on their mass-to-charge ratio (m/z). The coupling of chromatography with MS provides high sensitivity and high specificity compared to conventional chromatographic detectors [89]. LC-MS has been utilized for the analysis and identification of endogenous components such as proteins, peptides, carbohydrates, DNA, and drugs or metabolites [90]. Moreover, it has been used widely to perform pharmacokinetic studies of pharmaceuticals due to its shorter analysis time, its high

sensitivity, and specificity [91]. It can be used to measure the amount of a drug that got cleared from the plasma and organs in a certain amount of time. This is useful to determine the drug half-life and the subsequent doses. LC-MS has been used to identify and establish the structure of new drugs that have been synthesized or isolated from different natural sources. Moreover, LC-MS applications in drug development include metabolite identification, impurity identification and *in vivo* drug screening, natural product dereplication, bio-affinity screening [92]. The basic components of this system include: the autosampler, HPLC column, the ionization source (LC-MS interface), the mass analyzer, the electron detector, and electrical current signal output [93].

While many ionization sources are readily available to integrate LC with MS, electrospray ionization (ESI) and atmospheric pressure chemical ionization (APCI) are the most commonly used techniques [94]. These techniques can be used for the analysis of small, large, polar, and nonpolar molecules [95]. They can generate ions at high voltage and high heat at atmospheric pressure. In ESI, charged droplets are formed from the eluent that pass through an electrode which is at high potential. Then, these droplets are evaporated by heated nitrogen drying gas and pass through a metal capillary kept at a high voltage field (3–5 kV). Later, the ionized analytes are moved to the high vacuum of the MS with the help of small apparatus and focusing voltage [89]. Electrospray ionization can be operated in either negative or positive modes to detect negative or positive ions that are corresponding to the deprotonated or protonated of analytes, respectively [89]. In APCI, the eluent is introduced into a capillary and is vaporized by the application of a nebulizing gas and heat instead of electric potential. Then a corona discharge is used to ionize the eluent molecules which transfer the charge to the analyte molecules via charge transfer

reactions or molecular association [96]. Both ESI and APCI are soft ionization methods. This means that during the formation of ions, only small energy can transfer to these ions. This prevents the fragmentation of the generated ions into smaller mass ions. Therefore, the generated ions are either $[M+H]^+$, $[M-H]^-$, or adduct ions like $[M+Na]^+$ in the mass spectrum [96]. Furthermore, many mass analyzers have been developed to increase the capabilities of LC-MS analysis such as quadrupole, time-of-flight (TOF), and ion-trap mass analysers. In quadrupole, ions separation is performed via the application of radiofrequency voltages along four parallel metal rods. Ions of a non-collisional or stable trajectory, pass through the quadruple, reaching the detector whereas unstable or collisional trajectory ions touch the quadruple rods, become discharged and not detectable [96]. Quadruple analysers work at <4000 m/z with scan speeds up to 1000 m/z per sec [89]. Quadrupole analysers can be set in a scan mode or selected ion monitoring (SIM) where multiple mass to charge ratios or single mass to charge ratio ions are monitored, respectively [89]. The detection limit of target analyte improves during single ion monitoring as more time can be spent detecting ions produced only by the target analyte instead of other ions [89]. Ions generated in the ion source are accelerated with high voltage in the time of flight. Ions travel in a flight tube based on their charge to mass ratio. Heavier ions have low travel speed and become slower; hence they reach the detector at last compared to lighter ions. The mass to charge ratio of ions can be calculated by determining the time that ions take to reach the detector along with other experimental parameters. This technique scans all ions very fast with high accuracy and sensitivity [89]. In the ion trap analyzers, ions of a specific mass to charge ratio are trapped between three hyperbolic electrodes by the application of radiofrequency voltages. To obtain a mass spectrum of specific ions, non-selected ions are

ejected from the trap. Multiple fragmentation and isolation can be achieved by trap analyzer resulting in MS^n capabilities [89].

Several steps are involved in the LC-MS analysis including sample separation into individual components with LC column, followed by ionization and quantification with MS [97]. Individual components can be separated based on their affinity to the stationary phase packed in the column and the used mobile phase. Components that exhibit higher affinity to the stationary phase are separated at last. Then, the separated components are nebulized forming ions in the gas phase at atmospheric pressure. The formed ions are separated according to their mass to charge ratio by the mass analyzer. Finally, the separated ions are directed to the detector for quantification. A computer system can be utilized to record and process data for the generation of a mass spectrum [96].

In LC-MS, certain flow rates and mobile phases must be used during analysis. A lower flow rate, in the range of 0.05-0.2 mL/min, is recommended as it results in complete ionization and higher sensitivity [89]. As the flow rate increases above 0.2 mL/min, the MS sensitivity decreases. The main solvents used in reversed-phase LC coupled with MS is water combined with either methanol or acetonitrile [89]. To improve the ionization of the analyte of interest, mobile phase modifiers can be added into the mobile phase such as ammonium acetate, acetic acid and formic acid [91]. Column with 1.0- or 2.1-mm diameters can be used with low flow rate for higher sensitivities and resolutions [89].

1.7 Objective of this research project

It is well known that DTPA (DTPA, in either Zn- or Ca-form) is an effective decorporation agent that has been used to eliminate actinides from the human body via the formation of stable complexes that can be excreted in urine. However, the decorporation efficacy of Ca-trisodium and Zn-trisodium DTPA is limited by its low tissue distribution. Hence, DTPA is only able to remove radioactive actinides that are still in the blood circulation or extracellular fluid. Moreover, DTPA has short retention where frequent administration of DTPA is required to achieve the desired decorporation adequacy, which results in the depletion of essential elements in patients of radiation incidents.

The primary goal of this research work is to improve the pharmacokinetic properties of DTPA by the formation of DTPA loaded PEG-functionalized TiO_2 nanoparticles, PLGA-encapsulated Zn-DTPA, and Zn-DTPA encapsulated lecithin liposomes. This combination between nanoparticles as a drug delivery carrier and the decorporation agent DTPA may increase DTPA decorporation efficacy by offering the following advantages:

I. Improve the ability of DTPA to cross cell membrane to remove intracellular actinides.
II. Increase the DTPA retention time in patients which reduce the frequency of doses and minimize the side effects of DTPA.
III. Allow for extended release of DTPA into the lungs to maintain the drug concentration at the therapeutic level.

Chapter 2: Polyethylene Glycol–Functionalized Titanium Dioxide Nanoparticles for Extended Release of Diethylenetriaminepentaacetic Acid into Lung Fluid to Enhance the Decorporation of Radioactive Actinides

Modified from original manuscript, published as:
Almalki M[1], Lai EPC[1*], Ko R[2], Li C[2] (2017). Polyethylene Glycol–Functionalized Titanium Dioxide Nanoparticles for Extended Release of Diethylenetriaminepentaacetic Acid into Lung Fluid to Enhance the Decorporation of Radioactive Actinides. Journal of Nanoscience, Nanomedicine and Nanobiology. 1: 002

[1]Department of Chemistry, Carleton University, Canada
[2]Radiation Protection Bureau, Health Canada, Canada

Abstract

Titanium dioxide (TiO_2) nanoparticles have been used widely as a nanocarrier in drug delivery systems due to their high delivery efficiency and controlled release of therapeutic drugs. Diethylenetriaminepentaacetic acid (DTPA-H_5) is an attractive decorporation agent that can enhance the excretion of radioactive actinides such as plutonium, americium, and curium that are incorporated into the lungs after a radiological incident. However, DTPA is excreted in a short period of time after administration. In this project, biocompatible polyethylene glycol (PEG) functionalized TiO_2 nanoparticles were used to load DTPA to increase its residence time in the human body. The prepared DTPA-loaded PEG-functionalized TiO_2 nanoparticles were characterized by transmission electron microscopy, Fourier transform infrared spectroscopy, and dynamic light scattering. The prolonged retention of DTPA from PEG-functionalized TiO_2 nanoparticles were also evaluated via dialysis experiments. Liquid chromatography-mass spectrometry analysis of

the dialysates showed an extended release of DTPA into simulated lung fluid. This approach was used for the first time to sustain the release of DTPA in an *in vitro* study.

2.1 Introduction

During radiological accidents, inhalation of radioactive actinides could be the main route of internal contamination [17]. During the radioactive decay harmful ionizing radiation, such as alpha particles, beta particles, and gamma rays are emitted [98]. The quantity of radionuclides inhaled, the type of radiation, and the proximity of contamination to organs in the human body determine the degree of hazard. Cellular exposure to ionizing radiation leads to the generation of reactive oxygen species (ROS) that can damage biological macromolecules via the radiolysis of intracellular H_2O [99,100,101].

To reduce the ionization radiation damage to the human body systems, chelation therapy may be required. Decorporation leads to the removal of internal radioactive actinides from the body following a radiological incident. Diethylenetriaminepentaacetic acid (DTPA-H_5) is recognized as a chelating agent that accelerates the excretion of actinides. It works best when given shortly after radioactive actinides enter the body. DTPA comes in three forms: calcium DTPA, zinc DTPA, and sodium DTPA. All forms are very effective in enhancing the elimination of actinides such as plutonium and americium [102]. DTPA catches these actinides in the body and turns them into a stable coordination complex form that can be excreted in the urine [103]. The efficacy of DTPA as a decorporation agent is limited by several factors. DTPA exhibits low distribution in tissues due to their low permeability. Therefore, it can only chelate actinides that are still in the blood or extracellular fluid. Moreover, it has a residence time as short as 90 minutes

in humans due to fast clearance mechanisms [104]. Therefore, repeated daily doses over several weeks may be required to achieve the desired decorporation. However, such a frequent dosage of DTPA can cause severe toxic effects by the depletion of essential elements such as magnesium, manganese, calcium and zinc [105].

Systemic delivery of DTPA has traditionally been used for the decorporation of radioactive actinides. However, due to its low local concentration in the lungs, the clinical application remains largely unsatisfactory for treating inhaled actinides [106]. Achieving a sustained presence of the chelating agent in the lungs is very challenging [107]. Drug delivery to the lungs through inhalation is considered to be particularly advantageous due to a high-localized concentration of the agent and relatively low side effects [106].

Nanoparticles, also known as ultrafine particles, come together to compose what is known as nanomaterials (NMs). The physicochemical properties of nanoparticles are dependent on their particle size, chemical composition, electronic charge, surface structure, crystalline phase, solubility, shape and aggregation [108]. Nanotechnology has emerged as a highly valuable, useful and versatile technology. It has found application in catalysis, cosmetics, drug carriers, food additives and sunscreen. Complimentary to the development of nanotechnology, drug delivery nanosystems (DDNSs) is gaining more attention by researchers and scientists worldwide [109, 110, 111]. Among NMs, titanium dioxide nanoparticles (TiO_2 NPs) are one of the most used drug delivery nanosystems [112]. TiO_2 has been used as a drug carrier for various drugs such as daunorubicin, sodium phenytoin, temozolomide, and valproic acid. TiO_2 showed a high delivery efficiency, and sustained drug release over days, weeks, or months. This can decrease the exposure time to the drug

which lead to less side effect [113,114,115,116].

Many industries make use of TiO_2 nanoparticles and can be found in food products, various medicines and as well as cosmetics [117,118,119]. TiO_2 nanoparticles efficacy can be attributed to their ability to reach various parts of the body. This can be accomplished through exposure routes, which include inhalation, ingestion, and gastrointestinal tract absorption [120]. DDNSs have a unique potential to not only enhance drug bioavailability, but also to extend the period of drug release and enhance the drug targeting [121].

Polyethylene glycol (PEG) is a polyether compound with many medical applications due to its biocompatible and biodegradable properties [122]. The attachment of PEG to the surface of nanoparticles increases their biocompatibility [123]. Jugan *et al.* and Yaling *et al.* performed a study on the influence of TiO_2 nanoparticles on human lung cells and mouse liver cells [124]. This study confirmed that the toxicity of TiO_2 is reduced when functionalized with polymers [125]. Nanoparticles that are not functionalized with PEG are recognized as foreign products and ejected from the blood circulation by macrophage cells that exist within the reticuloendothelial system. The TiO_2 nanocarrier has been used successfully for the controlled release of anticancer drugs such as paclitaxel [126,127].

In this study, we loaded DTPA onto PEG-functionalized TiO_2 nanoparticles in order to achieve effective delivery and sustained release of this agent into the lungs. The prepared DTPA-loaded PEG-functionalized TiO_2 nanoparticles were characterized by different analytical techniques. To confirm our hypothesis of extended release, DTPA released from the PEG-TiO_2 into simulated lung fluid was monitored via dialysis

experiments. The loading capacity of DTPA on PEG-functionalized TiO_2 nanoparticles was determined by LC-MS analysis.

2.2 Materials and Methods

Titanium dioxide nanoparticles (20 nm), polyethylene glycol (molecular weight or degree of polymerization Mn6000), Diethylenetriaminepentaacetic Acid (DTPA-H_5), penta sodium salt of diethylenetriaminepentaacetic Acid (DTPA-Na_5), calcium chloride, iron (III) chloride hexahydrate, magnesium chloride, potassium chloride, sodium chloride, sodium citrate dehydrate, sodium hydrogen carbonate, sodium sulfate, dihydrate sodium acetate, disodium hydrogen phosphate, D-mannitol and formic acid were purchased from Sigma-Aldrich and are ACS grade or greater. Regenerated cellulose dialysis membranes (MWCO 3.5 kDa) were purchased from Thermo Fisher Scientific.

2.2.1 Adsorption test of DTPA-Na_5/DTPA-H_5 into PEG functionalized TiO_2 nanoparticles

A solution of DTPA-Na_5 (1 mL, 1000 mg/L) was mixed with different concentrations of PEG-functionalized TiO_2 nanoparticles (0, 0.0058, 0.0233, 0.0583, and 0.175 g/mL) and adjusted to final volumes of 1.5 mL. Also, another solution of DTPA-H_5 (1 mL, 1000 mg/L) was mixed with a new batch of PEG-functionalized TiO_2 nanoparticles in the same aforementioned concentrations. The mixtures were left overnight to interact followed by centrifugation at 4500 rpm for 1 h at 18 $^{\circ}$C. Liquid chromatography-mass spectrometry (LC-MS) analysis of the supernatants was performed to determine any free DTPA.

2.2.2 Preparation of DTPA-H_5-PEG Functionalized TiO_2

TiO_2 nanoparticles (20 nm) were mixed with 1% polyethylene glycol (PEG) solution in distilled deionized water, and the mixture was magnetically stirred overnight as illustrated in Figure 2.1. The resulting PEG-functionalized TiO_2 nanoparticles were mixed with an aqueous solution of DTPA-H_5 and the mixture left under shaking for overnight. DTPA-H5 loaded PEG-functionalized TiO_2 nanoparticles were collected by centrifugation at 4500 rpm for 1 h at 18 $^{\circ}$C and washed with water [126,127]. A pre-frozen solution of DTPA loaded PEG functionalized TiO_2 was mixed with a 5% solution of D-mannitol before freeze-drying in a Labconco model 7753020 freeze dryer operating at a temperature of -53^{0}C [98]. Mannitol was used as a dispersant to prevent the aggregation of DTPA loaded PEG functionalized TiO_2 during the freeze-drying process. DTPA loaded PEG-functionalized TiO_2 nanoparticles were obtained as dry powders.

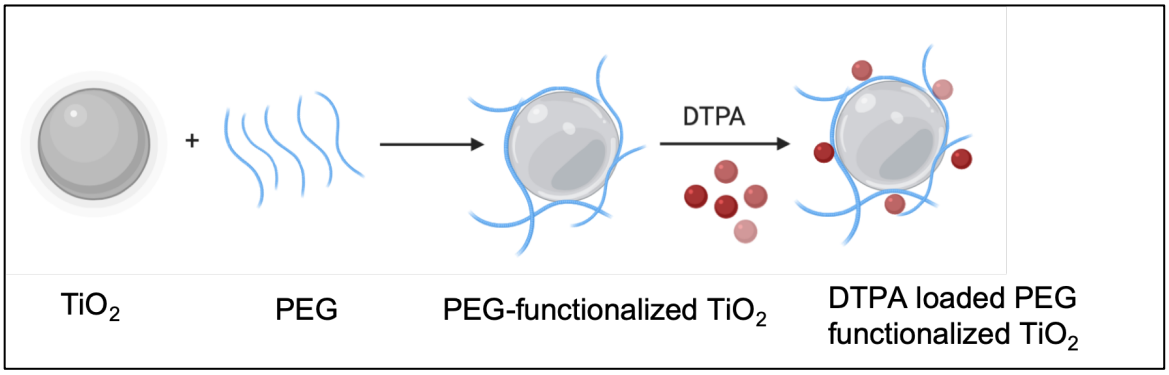

Figure 2.1 Preparation of DTPA-H_5-PEG functionalized TiO_2 nanoparticles.

2.2.3 Characterization of nanoparticles by transmission electron microscopy

Transmission electron microscopy (TEM) was used to characterize the TiO_2 nanoparticles, before and after functionalization with PEG and loading of DTPA on a FEI Tecnai G2 F20 microscope operating at 200 kV.

2.2.4 Characterization of nanoparticles by Fourier transform infrared spectroscopy

The chemical structures of TiO_2 nanoparticles and surface modified nanoparticles were characterized using an ABB (Bomem MB series, Quebec, Canada) Fourier transform infrared (FTIR) spectrometer. Disc samples were prepared by grinding 2 mg of nanoparticles with 200 mg of spectrophotometric-grade KBr. All FTIR spectra were obtained in the spectral region of 600-4000 cm^{-1}.

2.2.5 Characterization of nanoparticles by dynamic light scattering

Dynamic light scattering (DLS) was used to measure the hydrodynamic size distribution of TiO_2 nanoparticles and DTPA loaded PEG-TiO_2 nanoparticles suspended in 10 mM potassium nitrate buffer. DLS analysis of each suspension was performed using a Brookhaven Instruments nano DLS particle size analyzer (Holtsville, NY, USA). Each suspension was measured in ten replicates of 10 s each for higher accuracy [102,128].

2.2.6 Loading Capacity of PEG-functionalized TiO_2

The prepared PEG-functionalized TiO_2 nanoparticles at different concentrations 0.0084, 0.0168, 0.0252, 0.0336, 0.042, 0.084, 0.126, and 0.168 g/mL were mixed with 1 mL of DTPA-H_5 at 1000 mg/L. The mixtures were left overnight under shaking to interact followed by centrifugation. LC-MS analysis of the supernatants was performed to determine the PEG-TiO_2 capacity. The capacity of polyethylenimine functionalized TiO_2 nanoparticles (PEI-TiO_2) was determined following the same procedure.

2.2.7 *In vitro* release of DTPA loaded PEG-functionalized TiO_2

Simulated lung fluid (SLF) was prepared with pH 7.4 for *in vitro* release tests based on Marques *et al.* description (Gamble's solution) [129]. DTPA loaded PEG-functionalized TiO_2 nanoparticles were dispersed in 10 mL of SLF, followed by transferring to dialysis membrane tubing (MWCO 3500). Then, the dialysis tubing was immersed in a beaker containing 50 mL of lung fluid. The dialysis process was performed at 37±1°C under magnetic stirring. At appropriate time intervals, a dialysate sample was taken and replaced by the same volume of SLF to keep the dialysis volume constant. The *in vitro* release tests were conducted for 28-50 hours using the experimental setup shown in Figure 2.2. Finally, all the dialysate samples were analyzed by LC-MS to determine the concentration of released DTPA versus the dialysis time.

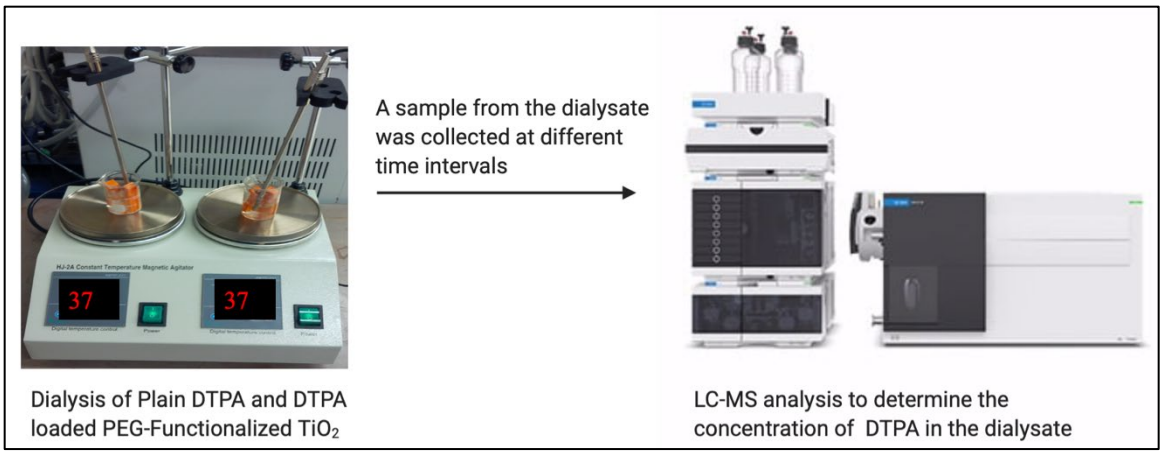

Figure 2.2 Dialysis set up used for the *in vitro* release of DTPA and DTPA-loaded PEG-functionalized TiO_2.

2.2.8 Determination of DTPA concentration by liquid chromatography-mass spectrometry

Liquid chromatography-mass spectrometry (LC-MS) was used to determine the DTPA concentration released during the dialysis experiments. DTPA standard solutions and dialysate samples were mixed with Fe^{3+} ions to form a stable $[M{-}H^{+}]^{-}$ cluster ion. All Fe-DTPA standards and dialysate samples were diluted with 1:1 ratio of 0.1% formic acid before the analysis. A C18 column was used in LC (50 mm x 2.1 mm) maintained at room temperature. The mobile phase was prepared by mixing 98% A and 2% B at a flow rate of 0.4 mL/min: (A) 0.1% formic acid in ultrapure water and (B) 0.1% formic acid in acetonitrile. Mass spectrometric analysis was performed using an Agilent Technologies model 6460 triple quad MS/MS system that was equipped with an ESI source operating in the negative mode. The operating parameters were: nitrogen gas flow rate = 9.8 L/min, gas temperature = 300°C, nebulizer pressure = 15 psi, capillary voltage = 4000 V, fragmentor voltage = 135 V, and cell accelerator voltage = 7 V. Single ion monitoring was set up to record the peak at m/z = 445.

2.3 Results and discussion

When a solution of DTPA-Na_5 or DTPA-H_5 was added into two batches of PEG-functionalized TiO_2 nanoparticles, most of the DTPA-H_5 was adsorbed into the nanoparticles as indicated by decreases in the DTPA concentration that remained in the supernatant liquid (Figure 2.3). However, all the DTPA-Na_5 was found to remain in the supernatant liquid as illustrated in Figure 2.4. No change in the DTPA concentration was observed even with 1 week of contact time with varying amounts of functionalized nanoparticles. Samples prepared with the addition of DTPA-H_5 to the functionalized TiO_2 nanoparticles showed a significant decrease in the DTPA peak area as the concentration of PEG-TiO_2 nanoparticles increased. The latter result suggested strong binding of DTPA-H_5 with PEG-functionalized TiO_2 nanoparticles compared to DTPA-Na_5. The formation of hydrogen bonds was a key factor for the interaction between DTPA-H_5 and PEG. The ability of DTPA-H_5 to act as a hydrogen acceptor/donor allows the formation of hydrogen bonds between its carboxylate groups and the hydroxyl groups of PEG as well as its carboxylic acid groups and the ether repeating units of PEG. This can explain the higher adsorption of DTPA-H_5 into the PEG-functionalized TiO_2 compared to DTPA-Na_5. Moreover, the low adsorption of DTPA-Na_5 could be due to the high affinity of $DTPA^{5-}$ toward Na^+ ions compared to PEG. Kubota *et al*. found that DTPA in its acidic form was retained in the blood circulation for a longer time compared to its salt forms which were excreted very fast via urine [130]. Based on this result; DTPA-H_5 has been used for further experiments.

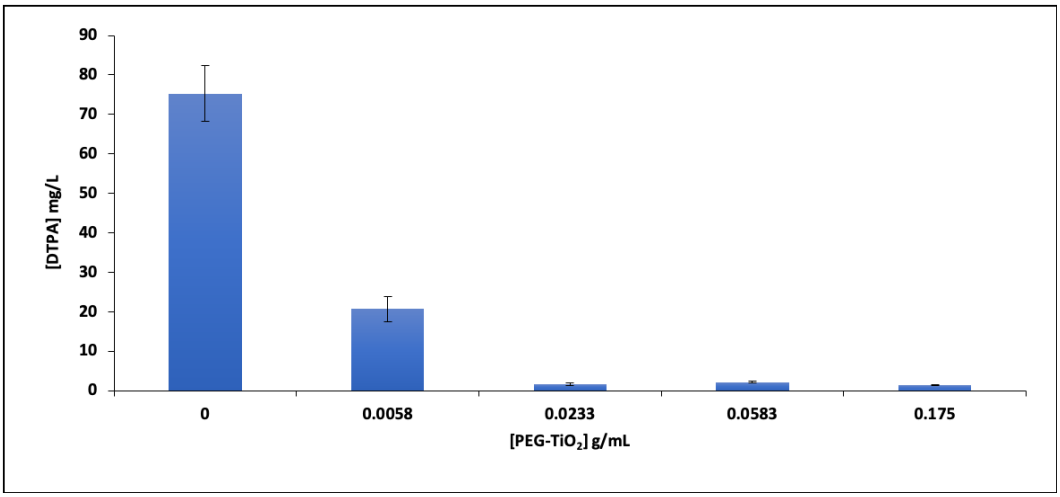

Figure 2.3 Adsorption test of DTPA-H_5 into PEG-functionalized TiO_2 nanoparticles by monitoring the concentration of DTPA remaining in the supernatant liquid. Data are presented as mean ± SD (n=3).

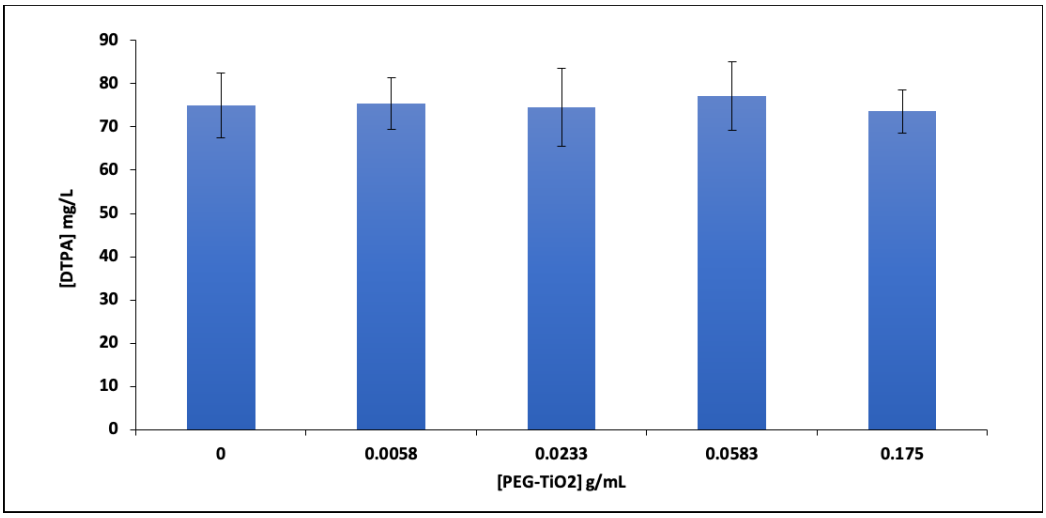

Figure 2.4 Adsorption test of DTPA-Na_5 into PEG-functionalized TiO_2 nanoparticles by monitoring the concentration of DTPA remaining in the supernatant liquid. Data are presented as mean ± SD (n=3).

The TEM images in Figure 2.5 show an average particle size of 17-21 nm for TiO_2 nanoparticles and 25-37 nm for DTPA loaded PEG-functionalized TiO_2. This increase in size could be attributed to DTPA loading and PEG functionalization of TiO_2 nanoparticles. Energy dispersion x-ray (EDX) has been used to confirm our results. The atomic

percentage of C increased in the DTPA loaded PEG-functionalized TiO_2 nanoparticles when compared to the PEG-functionalized TiO_2 nanoparticles before DTPA loading.

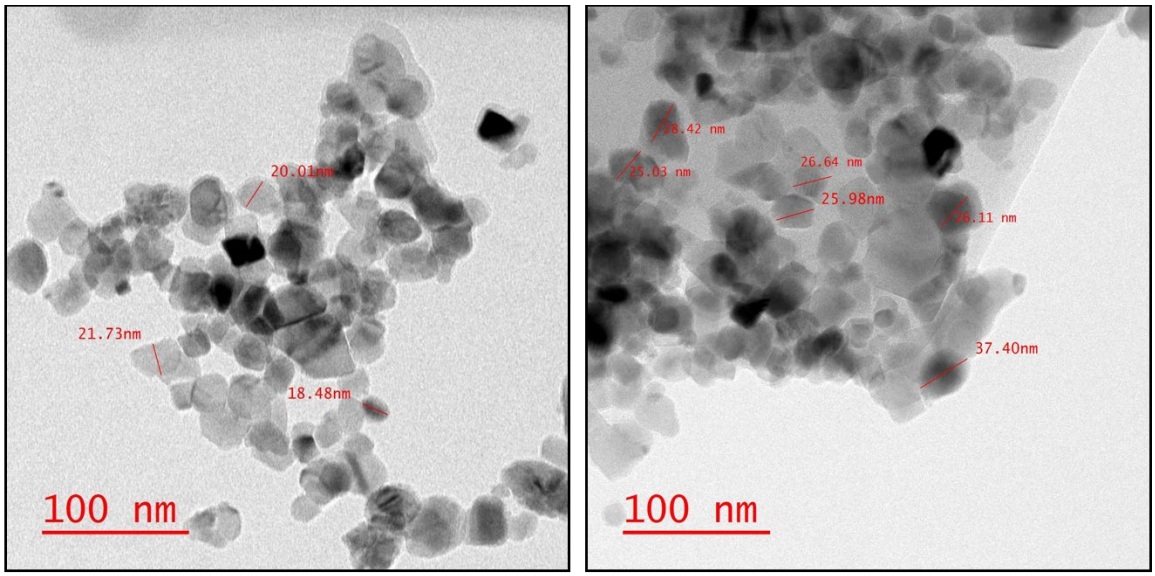

Figure 2.5 TEM images: (a) TiO_2 nanoparticles, and (b) DTPA-loaded PEG-functionalized TiO_2 nanoparticles. The TEM instrument offers a point resolution of 0.27 nm and a magnification ranging from 21x to 700,000x.

Figure 2.6 exhibits the FTIR of TiO_2, DTPA, PEG, and DTPA loaded PEG functionalized TiO_2. The presence of characteristic absorption peaks of the TiO_2, PEG, and DTPA in the DTPA loaded PEG functionalized TiO_2 suggested the loading of DTPA into the PEG functionalized nanoparticles. The band at 602 cm^{-1} in the TiO_2 (2.6a) corresponds to Ti-O stretching vibration, shifted into 707 cm^{-1} in the DTPA loaded PEG functionalized TiO_2 (2.6d). The intense band in the PEG at 2889 cm^{-1} (2.6c) which, corresponds to the C-H stretching vibrations, shifted into 2866 cm^{-1} in the DTPA loaded PEG functionalized nanoparticles. The bands in the DTPA (2.6b) that appears at 1733 and 1698 cm^{-1},

corresponding to the COO^- and C=O functional groups respectively, are shifted to 1728 and 1636 cm^{-1} in the DTPA loaded PEG functionalized TiO_2.

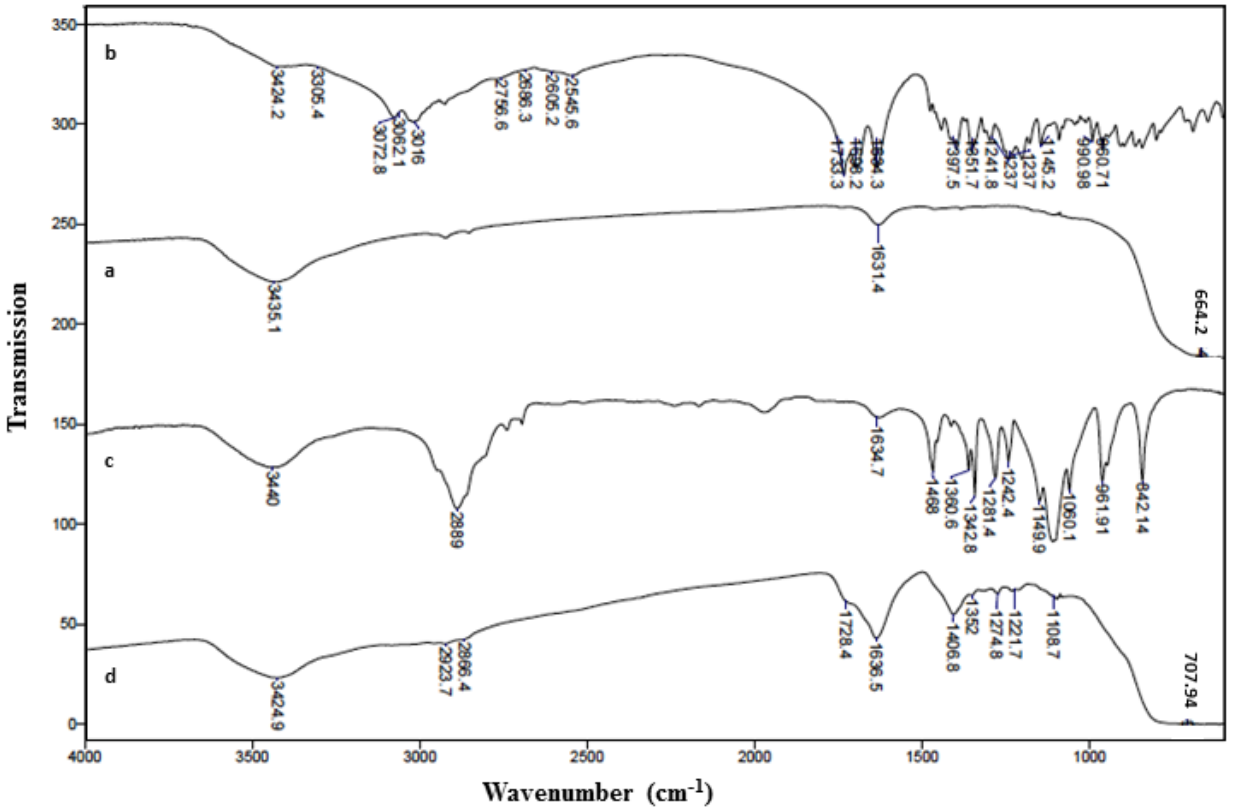

Figure 2.6 FTIR spectra: (a) TiO_2 nanoparticles, (b) DTPA, (c) PEG, and (d) DTPA loaded PEG-functionalized TiO_2 nanoparticles.

Dynamic light scattering of the TiO_2 nanoparticles exhibited a hydrodynamic diameter of 66 nm. The DTPA loaded PEG-TiO_2 showed a significant increase in their hydrodynamic diameter (83 nm) compared to the bare TiO_2 nanoparticles as illustrated in Table 2.1. This increase confirmed the successful formation of DTPA-loaded PEG-functionalized TiO_2 nanoparticles.

Table 2.1 Hydrodynamic diameter of TiO_2 nanoparticles and DTPA loaded PEG functionalized TiO_2 nanoparticles. Data are given as mean ± SD (n=10).

Sample	Hydrodynamic diameter (nm)
TiO_2	66 ± 9
DTPA-PEG-TiO_2	83 ± 9

The binding capacity experiment showed a decrease in the DTPA peak area as the PEG functionalized TiO_2 nanoparticles concentration increased from 0.0056 to 0.028 g/mL. The DTPA concentrations in the supernatant decrease, which means more DTPA, have been adsorbed into the surface of PEG-TiO_2. However, no significant change in the adsorption was observed when the PEG-functionalized TiO_2 concentration increased from 0.056, to 0.084 g/mL indicating equilibrium has been reached (Figure 2.7a). The capacity of PEG-functionalized TiO_2 nanoparticles was determined to be 21 mg DTPA/g of PEG-TiO_2 nanoparticles based on LC-MS analysis. To increase the loading capacity of PEG-functionalized TiO_2 nanoparticles, TiO_2 were functionalized with various 2%, 3%, and 4% concentrations (w/v) of PEG. However, the resulted PEG-functionalized TiO_2 nanoparticles didn't exhibit higher capacity than the nanoparticles that functionalized with 1% PEG concentration. The low capacity of the functionalized TiO_2 is due to the polymer functionalization into the nanoparticles surface as PEG coated TiO_2 nanoparticles may decrease the interaction between DTPA and TiO_2. However, the use of coating polymer was essential for the reduction of TiO_2 nanoparticles toxicity and clearance by macrophage system. In an attempt to improve the loading capacity of functionalized TiO_2 nanoparticles, polyethylenimine (PEI) was used to functionalize the TiO_2 surface in a similar way to PEG. Theoretically PEI is a positively charged polymer at neutral pH. Therefore, electrostatic

attractions between PEI and negatively charged DTPA could lead to more loading of DTPA into the PEI-functionalized TiO_2 nanoparticles. However, PEI-functionalized TiO_2 nanoparticles did not exhibit efficient loading of DTPA compared to PEG-functionalized TiO_2 nanoparticles, as shown in Figure 2.7b. About 50% of the DTPA was initially adsorbed into the PEI-functionalized TiO_2 nanoparticles at 0.0056 g/mL. When more PEI-functionalized TiO_2 nanoparticles were added from 0.0112 g/mL up to 0.084 g/mL, the concentration of DTPA only decreased slightly, corresponding to a modest increase in DTPA loading from 21 mg/g to 25 mg DTPA/g of PEI-functionalized TiO_2 nanoparticles. Hence, the DTPA encapsulation efficiency of PEI-functionalized TiO_2 nanoparticles is not as good as PEG-functionalized TiO_2 nanoparticles. Neither PEG-TiO_2 nor PEI-TiO_2 nanoparticles showed any affinity toward gadolinium Gd^{+3}, which had previously been used as a model trivalent ion. Therefore, decorporation of radioactive actinides will rely totally on the loaded DTPA when these functionalized TiO_2 nanoparticles are introduced to the contaminated lungs [131].

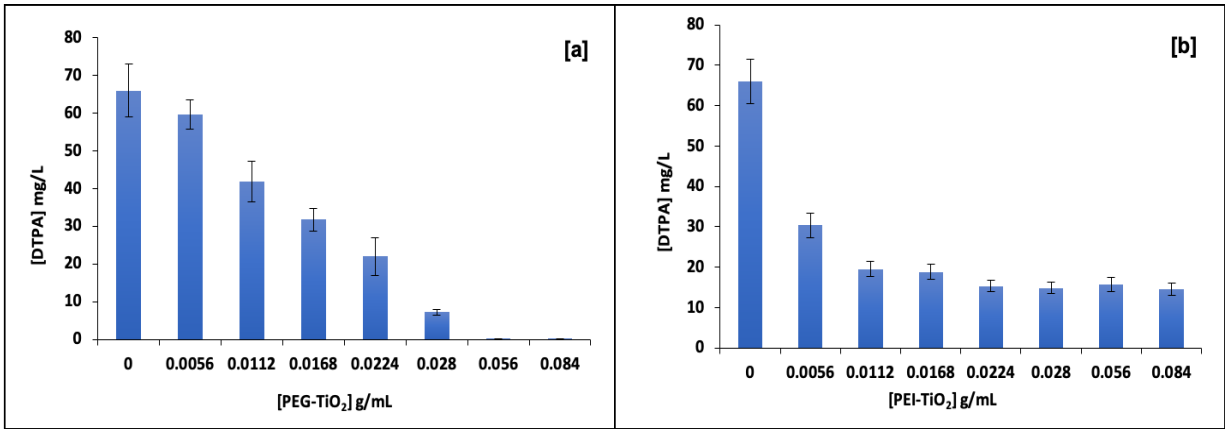

Figure 2.7 DTPA-H_5 binding capacities: (a) PEG-functionalized TiO_2 nanoparticles; (b) PEI-functionalized TiO_2 nanoparticles. Data are presented as mean ± SD (n=3).

2.3.1 Drug release profile

DTPA has high affinity toward divalent ions that are present in the lung fluid. This can lead to the formation of several DTPA complexes. Therefore, the released DTPA in the dialysate samples was determined by LC-MS upon the formation of a stable Fe-HDTPA$^-$ complex due to the highest affinity of DTPA^{5-} towards the Fe^{3+} metal ion compared to various metal ions such as Ca^{2+}, Cd^{2+}, Co^{2+}, Cu^{2+}, Mn^{2+} and Zn^{2+} [132,133] as shown in equation 1. As shown in Figure 2.8a, the Fe-HDTPA peak appeared at a short retention time of 0.555 minutes. A linear trend line equation obtained by running a series of Fe-HDTPA$^-$ standard solutions was used to determine the unknown DTPA concentration in each dialysate as shown in Figure 2.8b.

$$Fe^{3+} + DTPA^{5-} \xrightarrow{\text{Low pH}} \text{Fe-HDTPA}^- \qquad \text{(Equation 1)}$$

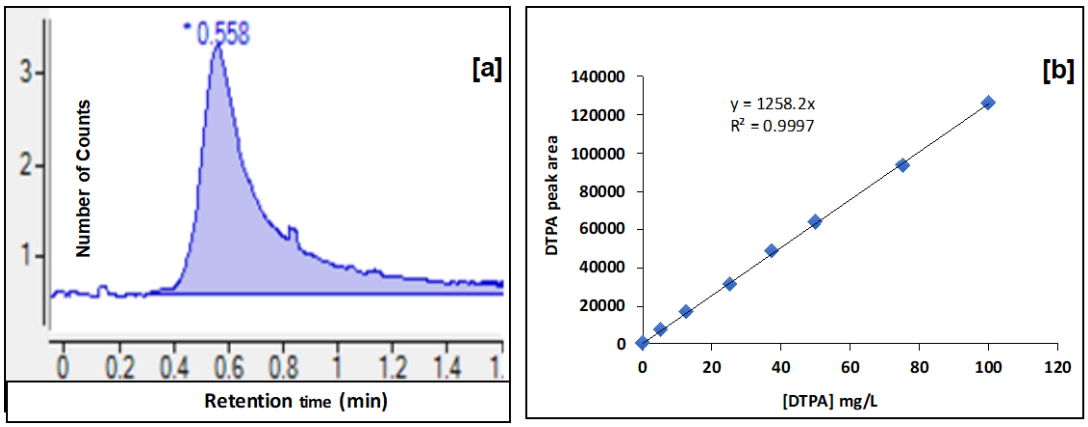

Figure 2.8 (a) Liquid chromatogram of Fe-HDTPA at a retention time of 0.555 min using selected ion monitoring at m/z = 445. (b) Standard calibration curve of Fe-HDTPA peak areas versus DTPA concentrations.

The drug release profile of DTPA-H_5 from PEG functionalized titanium dioxide nanoparticles into simulated lung fluid is given in Figure 2.9. The drug release profiles exhibit a rapid release of drug in the initial stage that looks like a first order process,

followed by a slow release of drug. Drug release profile (14 mg of DTPA-H_5 in 950 mg of PEG-TiO_2) shows 88% release of DTPA-H_5 occurs over 22 hours with a release half-time of 4 hours. In the initial stage the cumulative amounts of DTPA-H_5 released rapidly reach 12.5 mg/L in the first 3.4 h. The cumulative amounts of DTPA-H_5 increase slowly to reach 20 mg/L within the next 8 h. At 21 h the accumulative drug released increased from 20 to 23.8 mg/L to reach its maximum concentration. After 21 h there was no significant increase in the cumulative DTPA amounts. Due to this promising result, drug release of DTPA-H_5 loaded PEG-TiO_2 was performed in the presence of plain DTPA-H_5 as a control. The plain drug concentration was equal to the concentration of DTPA-H_5 loaded into the PEG-TiO_2. The DTPA-H_5 released from PEG-TiO_2 showed a slower drug release compared to the plain drug. The drug release profile of (70 mg/L of DTPA) shows a complete release of DTPA occurs around 22 h as shown in Figure 2.10. The 50 % of the total DTPA-H_5 concentration was released from the PEG-TiO_2 at 210 minutes, while 50% of the plain drug released at 150 minutes. The release half-time of DTPA-H_5 released from PEG-TiO_2 nanoparticles is 60 minutes longer than the plain drugs' release half-time.

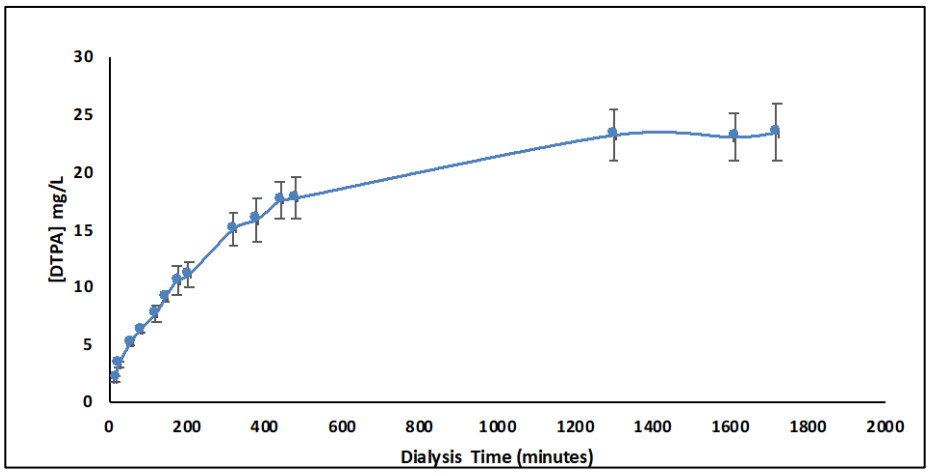

Figure 2.9 Drug release profile of DTPA-loaded PEG-functionalized TiO_2 nanoparticles. Data are presented as mean ± SD (n=3)

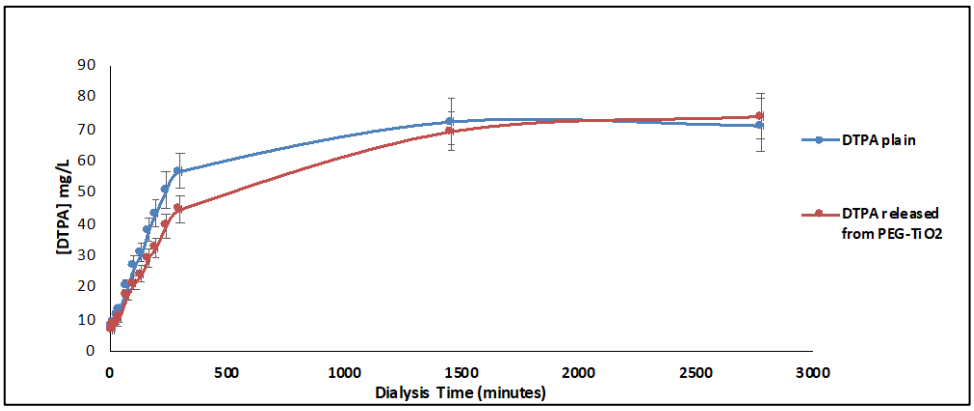

Figure 2.10 Drug release profile of plain DTPA and DTPA-loaded PEG-functionalized TiO_2 nanoparticles. Data are presented as mean ± SD (n=3).

The initial burst release of the drug could be attributed to the DTPA-H_5 that adsorbed onto the surface of PEG. Then, the drug molecules that interact strongly with the PEG-TiO_2 or entrapped between the polymer chains are released. In order to improve the drug release, it is very important to understand factors that affect the drug release such as drug solubility, particles size, and polymer-drug interaction [134]. Decreasing or increasing the amount of PEG can help to speed up or slow down the release of DTPA-H_5 from PEG-TiO_2, respectively. Having a low amount of PEG may speed up the drug release from TiO_2 as DTPA-H_5 will be adsorbed onto the surface of PEG. PEG is a hydrophilic polymer which can absorb water to form pores in the swollen polymer matrix that facilitates the diffusion of DTPA. Hydrophilic drugs need a larger amount of polymer to extend their release from the nanocarrier. Usually, for the modification of the TiO_2 surface, people used 1% of PEG to avoid encapsulation of the drug. This means that increasing the amount of PEG can lead to the encapsulation of DTPA into the polymer matrix instead of being only adsorbed onto the surface of PEG coated TiO_2. Hence this approach may slow down the release of DTPA-H_5 from PEG-coated TiO_2.

2.4 Conclusion

Polyethylene glycol functionalized titanium dioxide nanoparticles have been developed successfully for use as a drug carrier. The loading capacity of DTPA on the prepared PEG-TiO_2 remains lower than the desired for application in decorporation. However, the prepared DTPA loaded PEG-TiO_2 showed a slower drug release compared to DTPA itself, indicating a promising future for further development. The use of DTPA loaded PEG-functionalized TiO_2 as a decorporation nano-system for radioactive actinides will be tested in the future.

2.5 Connection to chapter 3

The PEG/TiO_2 and PEI/TiO_2 nanoparticles are limited by their low capacity which may not meet the desired therapeutic efficacy required for the decorporation of radioactive actinides deposited in the lungs. Event though, the PEG-functionalized TiO_2 exhibited an extended drug release compared to the plain drug, the release of DTPA was fast. These limitations could be overcome by the preparation of Zn-DTPA encapsulated poly lactic-*co*-glycolic acid (PLGA) nanoparticles in **Chapter 3** as they exhibited a higher loading capacity and extended drug release compared to TiO_2 nanoparticles.

Chapter 3: Encapsulation of Zn-DTPA into Poly Lactic-*co*-Glycolic Acid Nanoparticles via a Modified Double Emulsion Method for Extended Release into Lung Fluid

Modified from original manuscript, published as:
Almalki M[1], Lai EPC[1*], Ko R[2], Li C[2] (2017). (2018). Encapsulation of Zn-DTPA into Poly Lactic-*co*-Glycolic Acid Nanoparticles via a Modified Double Emulsion Method for Extended Release into Lung Fluid. Encapsulation of Zn-DTPA into Poly Lactic-*co*-Glycolic Acid Nanoparticles via a Modified Double Emulsion Method for Extended Release into Lung Fluid. Journal of nanomedicine. 2: 1009
[1]Department of Chemistry, Carleton University, Canada
[2]Radiation Protection Bureau, Health Canada, Canada

Abstract

Diethylenetriaminepentaacetic acid (DTPA), in either Zn- or Ca-form, is an approved chemical agent for decorporation of internalized actinides. During a radiological or nuclear incident, inhalation of radioactive actinides into the lungs is one of the main paths of hazardous exposure. High affinity of DTPA toward actinides makes it a suitable actinide decorporation agent that accelerates their excretion from the lungs. Polymeric nanoparticles are ideal for use in prolonging drug release, as they are biocompatible, non-toxic, and have been approved for therapeutic use by the Federal Drug Administration. Poly lactic-*co*-glycolic acid (PLGA) was chosen for this research as previous literature has shown that PLGA nanoparticles would delay the drug release of other therapeutic agents. PLGA nanoparticles encapsulated Zn-DTPA (PLGA-encapsulated Zn-DTPA) were synthesized for the first time to extend the DTPA release in human lungs. Since the physicochemical properties of a particle such as its size and shape can influence its uptake by lung cells and tissues *in vivo*, the synthesized PLGA-encapsulated Zn-DTPA were characterized by transmission electron microscopy, Fourier-transform infrared

spectroscopy, and dynamic light scattering. The loading capacity of Zn-DTPA in the PLGA nanoparticles achieved in this formulation was determined to be 106(±7) mg/g through use of liquid chromatography-mass spectrometry (LC-MS). Extended release of Zn-DTPA from the PLGA nanoparticles into simulated lung fluid was confirmed *via* dialysis experiments using continuous ultraviolet (UV) absorbance monitoring. LC-MS was also used to demonstrate the extended release of DTPA from these PLGA nanoparticles; a statistically significant increase of half-time was achieved compared to that obtained for Zn-DTPA itself. As the dialysis lung fluid volume increased, longer release half-times were observed for both Zn-DTPA and PLGA-encapsulated Zn-DTPA. Furthermore, as expected, decreasing the concentration of Zn-DTPA in dialysis experiments increased the release half-time, which indicated a second-order process. The purpose of this study was to extend the drug release through an optimized formulation of PLGA-encapsulated Zn-DTPA as compared to the free DTPA treatment in *in vitro* study.

3.1 Introduction

Over the past two decades, pharmaceutical research has focused on developing new drug delivery systems that offer high therapeutic potential by delivering the drug effectively at the target site to enhance both treatment efficacy and drug tolerability [135,136]. Drug delivery with nanoparticles enables the medicine to be released over a long period of time [137,138]. Thanks to their controllable physical properties, synthetic polymeric nanoparticles can improve drug delivery by releasing therapeutic agents over long time periods to avoid causing toxic effects [139, 140]. These physical properties, such as nanoparticle size and stability, can be controlled through optimization of various synthesis parameters such as drug to polymer mass ratios, organic solvents, and surfactants [141]. The U.S. Food and Drug Administration and the European Medicines Agency have approved the use of polymeric nanoparticles for therapeutic drug delivery [142,143]. Among various synthetic polymers, poly lactic-*co*-glycolic acid (PLGA) is widely used in the preparation of nanoparticles. PLGA exhibits attractive properties including low cytotoxicity, high biocompatibility and sustained drug release for extended period [144]. Different forms of PLGA nanoparticles can be prepared by varying the ratio of lactic acid and glycolic acid, the two monomers that form PLGA [145]. PLGA nanoparticles have been applied successfully for the extended drug release of anticancer drugs [146]. Although PLGA nanoparticles have been used successfully in various medical applications, formation of reproducible PLGA nanoparticles remains a challenge [147].

Radioactive actinides such as thorium-232 (^{232}Th), Uranium-238 (^{238}U), Plutonium-239 (^{239}Pu) and Americium-241 (^{241}Am) can enter the human body during

nuclear accidents. The internalized actinides would continue to decay, emitting ionizing radiation that may cause cancer or other severe damages to the biological system. Removal of these actinides requires decorporation therapy [148,149]. An effective decorporation agent should exhibit several properties under physiological conditions, including (i) functional groups that can chelate the actinides with high selectivity, (ii) low affinity to elements essential to the human body, (iii) good biocompatibility, (vi) availability to the contaminated individuals shortly after a nuclear incident [17,150,151].

An effective decorporation agent of actinides is diethylenetriaminepentaacetic acid (DTPA), in either Zn- or Ca-form [152]. It is usually administered through injection, but due to low retention of the agent in the human body, frequent injections of DTPA are needed which can cause severe side effect through depletion of essential metals in the body [153,154]. DTPA binds with actinides forming stable complex structures which can be excreted rapidly from the human body via urine [155]. A previous study showed that an early treatment with DTPA resulted in a marked decorporation of inhaled soluble Pu and Am in the livers and bones of rats [156.157].

Inhalation drug delivery can be considered as the best way of treating lung contamination, which enhances the drug bioavailability in the lungs, compared to other systemic methods [106,158]. Particle size plays a significant role in whether the particles can access the deposition site in the lower respiratory system (including bronchioles and alveoli) for the removal of the actinides [159]. In order to reach the lower respiratory system, the aerodynamic diameter of inhalable nanoparticles must be within an optimal size range of 1-5 μm. Particles with sizes larger than 5 μm tend to deposit in the

mouth, hence decreasing the therapeutic dose that reaches the lungs. On the other hand, particles smaller than 1 μm may escape from the lower respiratory tract during the exhalation cycle [160, 161].

Mucus, consisting mostly of water and protein, creates a tangled network of gel-like substance within the lungs [162]. When drug molecules are administered by inhalation through the mouth or nose, they must pass through the mucosal surface in order to reach the underlying cells; however, most drugs interact with mucus which prevents their delivery into the target site, resulting in less therapeutic effects. As such, developing a new therapeutic delivery system that can pass through mucus without any interaction is demanded for better therapeutic efficacy [163]. PLGA nanoparticles coated with PEG showed a rapid penetration through mucus in *in vitro* studies [164].

Different methods including sample and separate, continuous flow and dialysis membrane have been used to determine the release rate of drug from nanoparticles [58]. Dynamic dialysis is the most common *in vitro* method to evaluate drug release from nanoparticle delivery systems [165]. The donor compartment contains nanoparticles in the donor fluid, which pass through the dialysis membrane into the receptor compartment. A dialysis membrane is used to separate molecules *via* diffusion based on their difference in size. The membrane is manufactured with pores that allow only molecules under a certain size to pass through the membrane. Molecules that are larger than the membrane pores will be retained on the sample side. The increase of drug concentration in the acceptor lung fluid could be used to estimate the drug release kinetics [166,167]. However, dialysis can also lead to inaccurate data interpretation about nanoparticle release half-time [168]. The

drug release during dialysis is governed by two steps: drug release from nanoparticles, and drug diffusion through the dialysis membrane. The observation of slow dialysis release may be due only to a slow diffusion through the dialysis membrane but a mistaken to be a slow release from the nanoparticles. Drug release kinetics is important for drug carrier design and drug development since it advances our understanding of dosage form behavior and defines a parameter to evaluate the safety and efficiency of drug administration. *In vitro* release kinetics is being vastly used to evaluate *in vivo* behavior and to test drug carrier performance [169].

To address the issue with the depletion of essential metal-requiring biomolecules that can be resulted from the long-term use of a chelation agent such as DTPA, Zn- DTPA encapsulated PLGA nanoparticles (for sustainable drug release) was prepared via double emulsion method in this study. The prepared PLGA-encapsulated Zn-DTPA were characterized by various instrumental analysis techniques. Dialysis and sample and separate methods were used to study the drug release from the PLGA nanoparticles *in vitro*. The PLGA nanoparticles exhibited a sustained release of Zn-DTPA. Binding capacity of PLGA NPs was determined by LC-MS analysis.

3.2 Materials and Methods

Poly lactic-co-glycolic acid (PLGA) (lactide:glycolide ratio of 50:50, MW: 24,000-38,000), acetone (ACE), Dichloromethane (DCM), Tween 80, and polyvinyl alcohol , magnesium chloride, potassium chloride, sodium chloride, sodium citrate dehydrate, sodium hydrogen carbonate, sodium hydroxide, sodium sulfate, dihydrate sodium acetate, and disodium hydrogen phosphate were purchased from Sigma-Aldrich, and were ACS

grade or greater (Millwaukee, Wisconsin, USA). Pentetate zinc trisodium (Zn-DTPA) (200 mg/mL) was purchased from Heyl Chemisch-pharmazeutische Fabrik, Berlin. Regenerated cellulose dialysis membrane (MWCO: 6-8 kDa) was purchased from Thermo Fisher Scientific (Waltham, Massachusetts, USA). Distilled deionized water was used throughout this work.

3.2.1 Preparation of PLGA-encapsulated Zn-DTPA

A double-emulsion (water-in-oil-in-water (W/O/W)) solvent evaporation technique was used to prepare the PLGA-encapsulated Zn-DTPA as illustrated in Figure 3.1[170]. Two hundred mg of PLGA was dissolved in 10 mL of an organic mixture of acetone and dichloromethane with 1:1 (v/v) ratio containing Tween 80 (5% by volume) as an emulsifier. Zn-DTPA (2.5 mL at 200 mg/mL) was diluted with 2 mL of distilled deionized water and homogenized with the polymer solution by sonication for 5 minutes. The obtained primary W/O emulsion was further added to 40 mL of water with homogenization (for 5 minutes) to form the double emulsion (W/O/W). The resulting emulsion was added gradually into 200 mL of water containing polyvinyl alcohol 0.1% (w/v) as a surfactant under stirring. Stirring was continued for 12 hours to solidify the nanoparticles and evaporate the remaining organic solvents [147, 171]. The nanoparticles were collected after centrifugation at 600 rpm for 15 minutes at 18 $^{\circ}$C. The products were dried by lyophilization in a Labconco model 7753020 freeze dryer (Kansas City, MO, USA) operating at a temperature of -53 $^{\circ}$C. PLGA nanoparticles as a control were prepared following the same above procedure in the absence of Zn-DTPA.

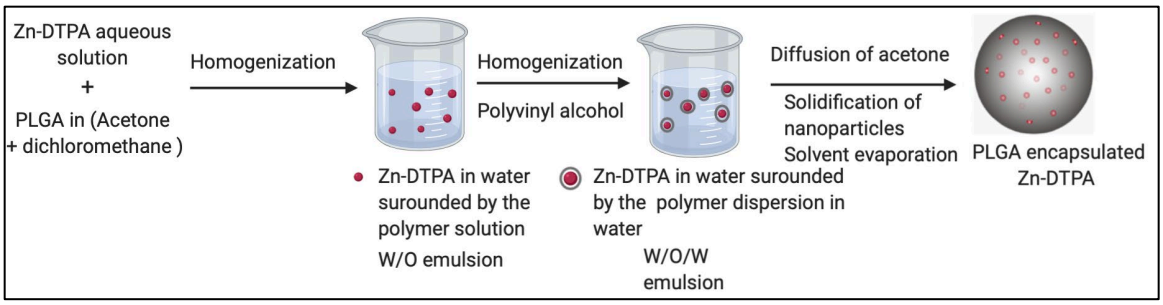

Figure 3.1 Preparation of PLGA-encapsulated Zn-DTPA via a modified double emulsion method.

3.2.2 Characterization of nanoparticles by transmission electron microscopy

Transmission electron microscopy (TEM) was used to characterize the PLGA nanoparticles and PLGA-encapsulated Zn-DTPA on a FEI Tecnai G2 F20 microscope (Hillsboro, OR, USA) operating at 200 kV.

3.2.3 Characterization of nanoparticles by Fourier-transform infrared spectroscopy

The chemical structures of PLGA nanoparticles and PLGA-encapsulated Zn-DTPA were characterized using an ABB (Bomem MB series, Quebec, Canada) Fourier-transform infrared (FTIR) spectrometer. Disc samples were prepared by grinding 2 mg of nanoparticles with 200 mg of spectrophotometric-grade KBr. All FTIR spectra were obtained in the spectral region of 600-4000 cm^{-1}.

3.2.4 Characterization of nanoparticles by dynamic light scattering

Dynamic light scattering (DLS) was used to measure the hydrodynamic size distribution of PLGA nanoparticles and PLGA-encapsulated Zn-DTPA suspended in 10 mM potassium nitrate buffer. DLS analysis of each suspension was performed using a

Brookhaven Instruments nano DLS particle size analyzer (Holtsville, NY, USA). Each suspension was measured in ten replicates of 10 s each for high accuracy.

3.2.5 Determination of PLGA nanoparticles loading capacity

The content of Zn-DTPA in PLGA nanoparticles prepared using Zn-DTPA was determined by LC-MS. After centrifugation, PLGA-encapsulated Zn-DTPA were collected, dried, and re-suspended in 0.1% formic acid to determine the amount of the drug in PLGA nanoparticles. The concentration of Zn-DTPA in the PLGA nanoparticles was calculated from a standard curve, prepared by known concentrations of Zn-DTPA.

3.2.6 Determination of Zn-DTPA by automatic UV monitoring system

The effect of different volumes of lung fluid inside the dialysis bags on the drug release rate was investigated on Zn-DTPA itself and PLGA-encapsulated Zn-DTPA. A drug release automatic monitoring system (DREAMS) was adapted from the design by Xie *et al.* to study the continuous release of Zn-DTPA from the PLGA nanoparticles by measuring the increasing UV absorbance during dialysis as shown in Figure 3.2 [167]. In this system, a beaker (the acceptor compartment) contained a constant volume of lung fluid (120 mL under magnetic stirring) at 37°C. A regenerated cellulose dialysis bag that is made from the transformation of natural cellulose to a soluble cellulosic (the donor compartment) containing either Zn-DTPA or PLGA-encapsulated Zn-DTPA dispersed in various volumes of lung fluid (0.5, 5, 7, 10 and 15 mL) was immersed in the acceptor compartment. A mini pump transported the lung fluid from the acceptor compartment to the UV detector.

As the Zn-DTPA concentration increased in the acceptor compartment due to the dialysis from the donor compartment, the UV absorbance increased proportionally.

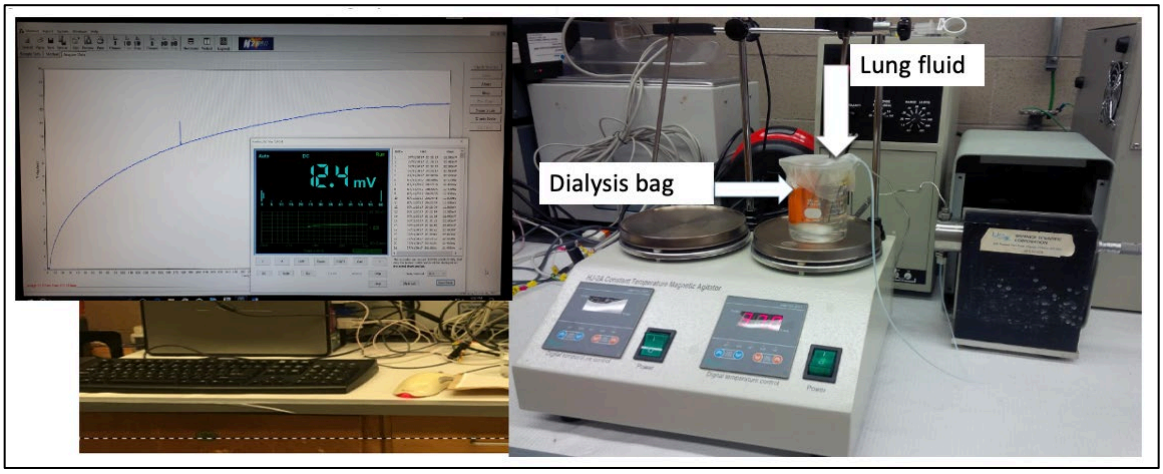

Figure 3.2 A drug release automatic monitoring system (DREAMS) used to study the effect of different volumes of lung fluid inside the dialysis bags on the plain Zn-DTPA and PLGA-encapsulated Zn-DTPA release half-time.

3.2.7 Effect of different concentrations of Zn-DTPA on the release half-time

Several quantities of Zn-DTPA (3, 10, and 20 mg) were dispersed in 6 mL lung fluid at a concentration (0.5, 1.7, and 3.3 mg/mL), respectively inside dialysis bag that were then immersed in 120 mL of lung fluid in a beaker to study the effect of different concentrations of the plain drug on the release half-time. A DREAMS was used for this experiment. The release half-times of different concentrations of Zn-DTPA were compared with each other based on their UV detector signals at 10 hours since their signals at 10 hours were assumed to be at equilibrium (no changes observed afterward).

3.2.8 *In vitro* release of PLGA-encapsulated Zn-DTPA *via* dialysis

Gamble's solution was prepared with pH 7.4 for use as simulated lung fluid (SLF) for *in vitro* release tests [129]. PLGA-encapsulated Zn-DTPA were dispersed in 6 mL of SLF, and the dispersion was transferred into a dialysis membrane tube. Subsequently, the dialysis membrane tube was immersed in a beaker containing 120 mL of SLF. The dialysis process was performed at 37±1°C under magnetic stirring on a constant temperature magnetic hotplate. A DREAM was used to carry out this release test experiment.

3.2.9 *In vitro* release of PLGA-encapsulated Zn-DTPA *via* sample and separate method

PLGA-encapsulated Zn-DTPA (266 mg) were dispersed in 32 mL lung fluid (Gamble's solution) and kept under stirring for 5 minutes. Then, 0.4 mL of the dispersed nanoparticles was transferred into 1.5 mL centrifugation tubes. At appropriate time intervals, the dispersed nanoparticles were centrifuged, and 20 µL of the supernatant was transfer into a vial and diluted with 100 µL of iron (III) chloride solution at 5 mg/mL and 880 µL of 0.1% formic acid to obtain 1 mL as a total volume [172]. Samples were complexed to Fe-HDTPA^{-} due to the highest affinity of DTPA^{5-} towards the Fe^{3+} metal ion compared to various metal ions such as Ca^{2+}, Cd^{2+}, Co^{2+}, Cu^{2+}, Mn^{2+} and Zn^{2+} that are present in the lung fluid [173]. The *in vitro* release test was conducted for 16 hours. Liquid chromatography-mass spectrometry (LC-MS) (single ion monitoring) was used to determine the concentration of Zn-DTPA released from PLGA nanoparticles and Zn-DTPA standard solutions upon the formation of Fe-HDTPA^{1-}, at m/z 445. A C18 column was used in LC (50 mm x 2.1 mm, 1.8 micron) maintained at room temperature. The mobile

phase was prepared by mixing 98% of the solvent A (0.1% formic acid in ultrapure water) and 2% of the solvent B (100 % acetonitrile) at a flow rate of 0.4 mL/min. Mass spectrometric analysis was performed using an Agilent Technologies model 6460 triple quad MS/MS system equipped with an electrospray ionization (ESI) source operating in the negative mode. The operating parameters were nitrogen gas flow rate = 9.8 L/min, gas temperature = 300°C, nebulizer pressure = 15 psi, capillary voltage = 4000 V, fragmentor voltage = 135 V, and cell accelerator voltage = 7 V.

3.3 Results and discussion

The resultant PLGA-encapsulated Zn-DTPA were characterized and examined for extended drug release in the *in vitro* study. They were characterized to determine if there was any difference between those with encapsulated Zn-DTPA and those without (as a control), in terms of their TEM morphologies and DLS size distributions. The PLGA nanoparticles exhibit a particle size of 88±5 nm as shown in the TEM images (Figure 3.3). The PLGA-encapsulated Zn-DTPA showed a significant increase in the particle size (105±7 nm). This increase could be attributed to the encapsulation of Zn-DTPA in the PLGA nanoparticles. As can be seen, PLGA nanoparticles and PLGA-encapsulated Zn-DTPA exhibited a spherical shape. The size of PLGA-encapsulated Zn-DTPA (30-500 nm in diameter) was optimal for the penetration through mucus in the lungs [174].

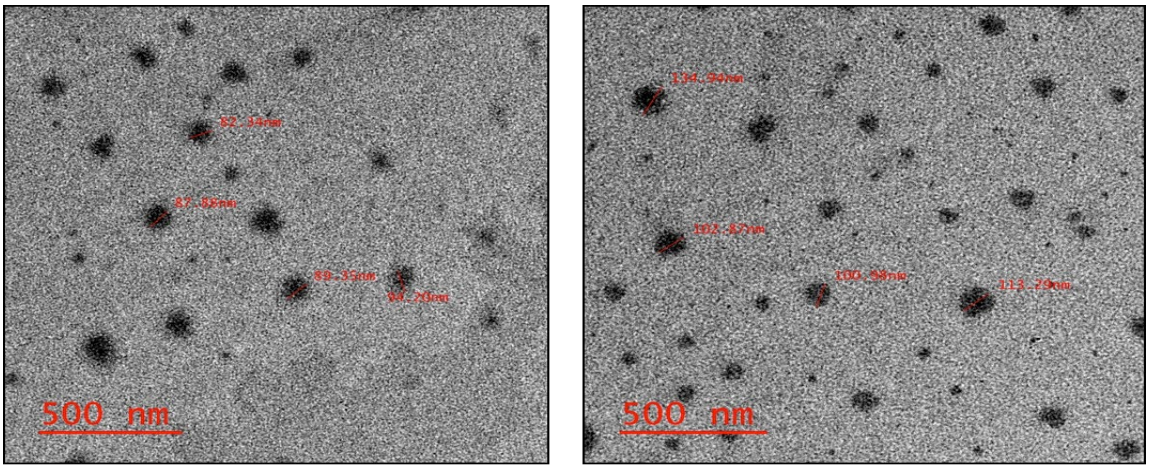

(a) (b)

Figure 3.3 TEM images of (a) PLGA nanoparticles, and (b) PLGA-encapsulated Zn-DTPA.

The size of polymer nanodroplet depends on the sonication power. High sonication power would lead to the formation of smaller particle sizes, as the organic and aqueous phases are totally homogenized [145]. The PLGA nanoparticles and PLGA-encapsulated Zn-DTPA exhibited large hydrodynamic diameters of 472.4 and 643.4 nm, respectively, at a sonication power of 100 W (100% of power). As the sonication power was increased (300 W at 50%) using an ultrasonic homogenizer with a probe, the PLGA nanoparticles exhibited a smaller hydrodynamic size of 331 nm. The PLGA-encapsulated Zn-DTPA showed significant increases in their hydrodynamic diameters compared to the PLGA nanoparticles that were prepared at an identical sonication power, as listed in Table 3.1. It could be implied that the encapsulation of Zn-DTPA into the PLGA nanoparticles would result in increasing the hydrodynamic size [145].

Table 3.1 Hydrodynamic diameters of PLGA nanoparticles and Zn-DTPA encapsulated PLGA nanoparticles. Data are given as mean ± SD (n=10).

Sample	Hydrodynamic diameters (nm)	Polydispersity
PLGA nanoparticles (low intensity sonication)	427±32	0.3
PLGA-encapsulated Zn-DTPA (low intensity sonication)	643±54	0.3
PLGA nanoparticles (high intensity sonication)	331±6	0.3
PLGA-encapsulated Zn-DTPA (high intensity sonication)	379±10	0.3

Figure 3.4 shows the FTIR spectra of Zn-DTPA, PLGA, and PLGA-encapsulated Zn-DTPA. The broad strong characteristic peak at 3425 cm^{-1} corresponds to N–H stretching for the pure Zn-DTPA (3.4a) and a peak at 2940.4 cm^{-1} is originated from C-H stretching vibration. The strong characteristic peaks at 3448 cm^{-1} and 1757 cm^{-1} correspond to O-H and C= O stretching, respectively for the PLGA (3.4b). The FTIR spectra of the Zn-DTPA-encapsulated polymeric nanoparticles (3.4c) shows a peak at 3497 cm^{-1} which could be assigned to N-H or O–H stretching vibration. The band in the PLGA at 2953 cm^{-1} corresponding to the C-H stretching vibrations shifted to 2921 cm^{-1} in PLGA-encapsulated Zn-DTPA. The band at 1442.8 cm^{-1} in the PLGA corresponding to C-H bending shifted into 1458.9 cm^{-1} in PLGA-encapsulated Zn-DTPA. No significant shifts were observed for other bands, which suggests the encapsulation of Zn-DTPA into the nanoparticles via physical interaction because no chemical bonding was evident to shift any IR bands.

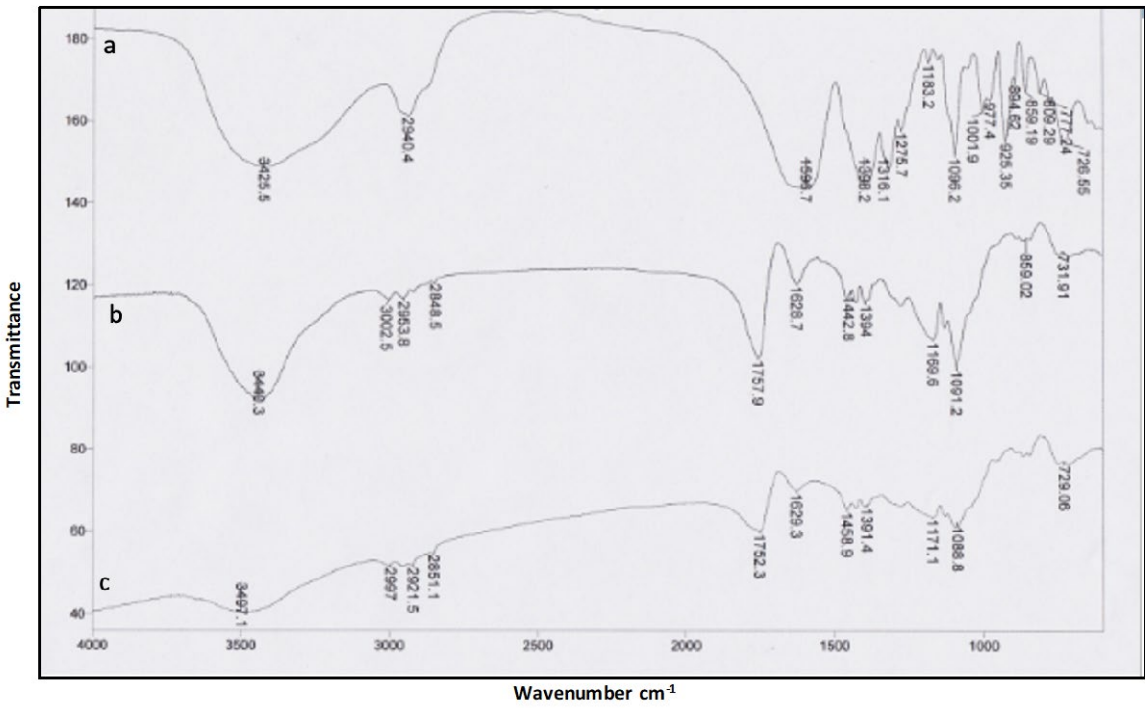

Figure 3.4 FTIR spectra of (a) Zn-DTPA, (b) PLGA, and (c) PLGA-encapsulated Zn-DTPA.

The encapsulation of hydrophilic drugs into the polymeric nanoparticles via the double emulsion method exhibit several limitations such as low drug loading and low encapsulation efficiency. The hydrophilic drugs penetrate rapidly from the inner aqueous phase to the external aqueous phase resulting in low encapsulation. To overcome these limitations, a modified double-emulsion solvent diffusion/evaporation technique was used in which acetone was a co-solvent. Due to the miscibility of acetone in water, it can diffuse from the inner to the external aqueous phase inducing nanoparticle solidification. This prevents the hydrophilic drug to penetrate to the external phase leading to higher drug loading [170]. The prepared PLGA nanoparticles exhibited a drug loading capacity of 106(±7) mg/g based on LC-MS analysis, and the capacity was calculated from the following equation:

Drug loading (%) = (mass of trapped drug in the nanoparticles / mass of polymeric nanoparticles) × 100 (Equation 1)

The drug released in lung fluid was monitored at a wavelength of 210 nm as Zn-DTPA showed the highest absorbance at this wavelength as shown in Figure 3.5. Changing the volumes inside the dialysis bags influenced the drug release rates in both plain and Zn-DTPA released from PLGA nanoparticles as illustrated in Figure 3.6. As the inside volume increased, longer release half-times were observed. This could be attributed to the longer diffusion distances for DTPA molecules inside larger lung fluid volumes. Therefore, the optimum volume of lung fluid inside the dialysis bag, which had less effect on the drug release rate, was obtained in order to find an accurate release half-time. Increasing the inside volume from 0.5 to 15 mL increased the release half-time of the plain drug from 5 to 43 minutes while the release half-time of the Zn-DTPA released from the PLGA nanoparticles increased from 18 to 96 minutes at the same volumes. This proved a delayed and extended drug release from the PLGA nanoparticles.

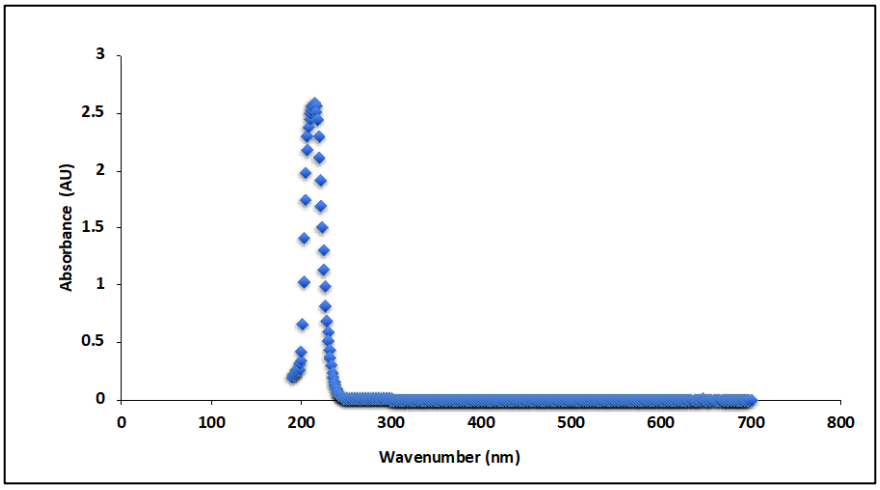

Figure 3.5 The UV spectrum of Zn-DTPA in lung fluid.

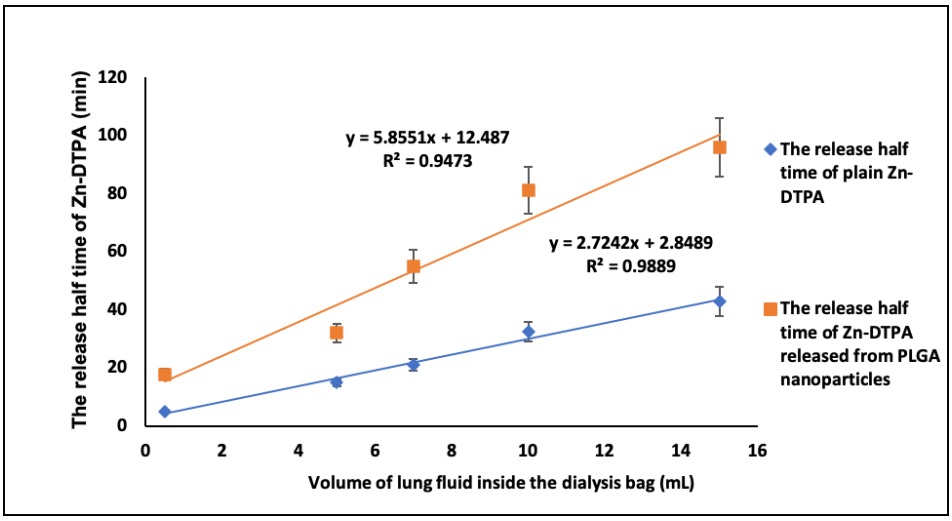

Figure 3.6 Effect of lung fluid volume inside the dialysis bag on the release half-time of plain Zn-DTPA, and PLGA-encapsulated Zn-DTPA. Data are presented as mean ± SD (n=3).

Figure 3.7 shows the drug release of plain Zn-DTPA at concentrations of 0.5, 1.7, and 3.3 mg/mL. As the concentrations of the drug inside the dialysis bag increased from 0.5 to 3.3 mg/mL, the release half-time corresponding UV signal (when half of the Zn-DTPA was released) decreased from 2.4 to 1.7 hour resulting in an average release half-time of 2 ± 0.4 hours. The diffusion rate of the drug was reduced when the concentrations of Zn-DTPA decreased leading to longer release half-time.

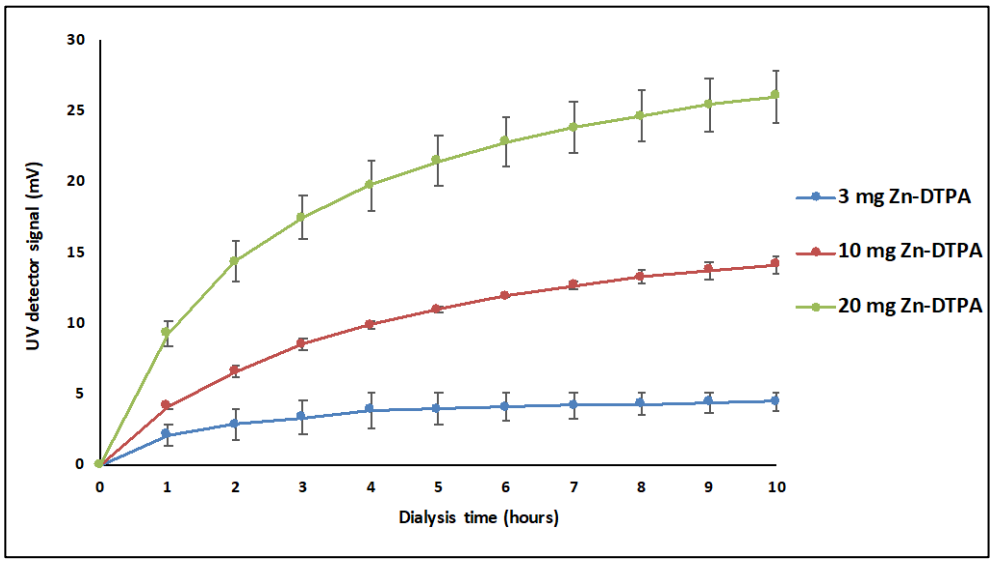

Figure 3.7 Effect of different quantities of Zn-DTPA on the release profiles. Data are presented as mean ± SD (n=3).

3.3.1 *In vitro* release of Zn-DTPA

There are mainly three possible mechanisms for the drug molecules to be released from PLGA nanoparticles used in the drug delivery system including diffusion through water-filled pores, diffusion through polymer matrix, and dissolution of the encapsulating polymer [175]. In order to control the drug release, it is very important to determine factors that affect the drug release rate. Several factors influence the drug release rate from polymeric nanoparticle, namely environmental conditions, physicochemical processes within PLGA matrices, polymer-drug interaction, drug-drug interaction, or a combination of these factors [142,175].

Encapsulation of Zn-DTPA into PLGA nanoparticles did not alter the drug chemical structure since the released drug formed Fe-HDTPA$^-$ that was detected by LC-MS (single ion monitoring) at the same molecular ion (m/z = 445). Therefore, the chemical

structure and function of DTPA remained unchanged, and the encapsulation should not reduce its therapeutic efficacy in decorporating actinides. For instance, Ca-DTPA had previously been encapsulated into liposome (or lipid nanoparticles) and showed even higher efficacy for the removal of actinides in animal experiments compared to that of the free DTPA [42]. The liposomes improved the therapeutic efficacy through an extended drug release resulting in a gradual decorporation and removal of actinide residues from patient organs [43]. Administration of therapeutic agents via inhalation can result in higher distribution of the drugs in the lungs compared to other routes. However, inhalable therapeutic agents may be eliminated rapidly by alveolar macrophages upon deposition into the lungs [174]. Encapsulation of the anti-inflammatory drug PS341 into PLGA nanoparticles increased its bioavailability and half-life upon accumulation in the lungs compared to the plain PS341 [176].

Figure 3.8 shows the drug release profile of PLGA-encapsulated Zn-DTPA at a mass ratio of 2.5:1. The *in vitro* drug release experiment in the simulated lung fluid was performed for 16 hours via dialysis at pH 7.4 and 37°C in order to test the extended drug release of PLGA nanoparticles. The drug release profiles exhibit a fast release within the first hour, followed by a sustained release over the next 15 hours. However, the extended drug release could also be due to the use of the dialysis membrane and not only due to the PLGA nanoparticles. As such, to confirm the extended drug release of PLGA nanoparticles, sample and separate method was used as an alternative method. In this method, the PLGA-encapsulated Zn-DTPA was dispersed into lung fluid without any barrier (like a dialysis membrane). Then, the dispersed sample was transferred into 1.5 mL centrifugation tubes. At appropriate time intervals, the divided samples were centrifuged,

and analyzed to assess the release of Zn-DTPA from PLGA nanoparticles. Figure 3.9 shows the drug release profile of PLGA-encapsulated Zn-DTPA from sample and separate method. In this experiment, the PLGA nanoparticles were collected after centrifugation along with 10 mL of residual supernatant. The free Zn-DTPA, which left in the supernatant before freeze-drying process can account for the initial rapid rise in DTPA concentration. This free Zn-DTPA could serve as an urgent dose for victims after a nuclear accident, followed by a slow and sustained release of encapsulated Zn-DTPA from the PLGA nanoparticles over 10 hours. After that, the Zn-DTPA concentration did not change significantly in the next 6 hours. The half time of Zn-DTPA released from PLGA nanoparticles was 3.5 hours, which confirmed extended drug release from the PLGA nanoparticles.

Increasing the relative PLGA concentration/ratio to the Zn-DTPA may slow down the drug release. However, higher concentration of PLGA in an organic solvent will increase the viscosity of the organic phase, which increases the viscous forces resisting droplet breakdown. This will result the formation of bigger oil droplets and larger nanoparticles that can slow down the drug release due to the longer diffusion distance for drugs to reach the release medium. However, large nanoparticles are not favoured as smaller nanoparticles can stay longer in the air circulation and reach lower regions in the lungs. On the other hand, decreasing the polymer concentration may result in a faster release due to the formation of smaller nanoparticles which has been proven to have a fast release.

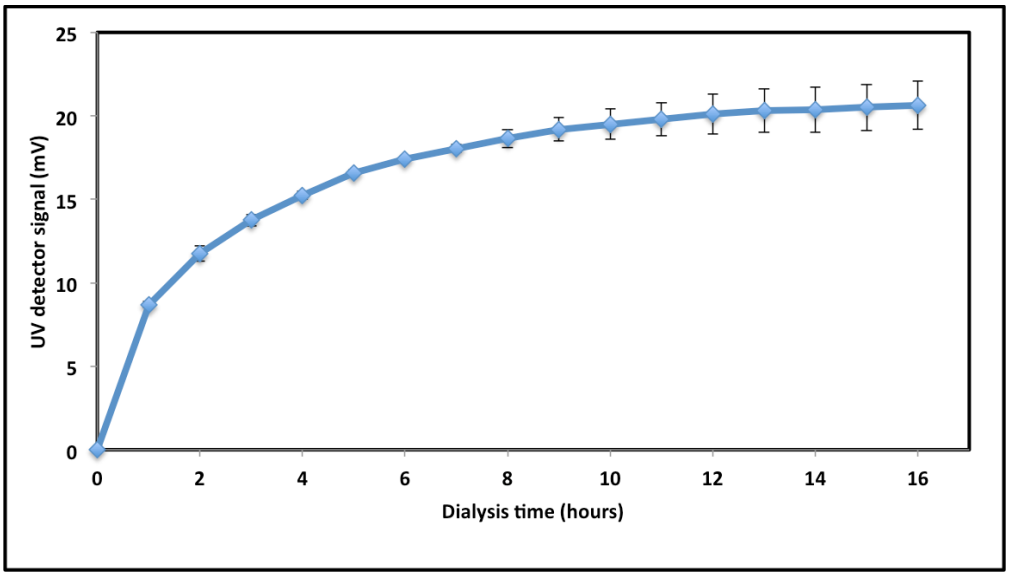

Figure 3.8 Drug release profile of PLGA-encapsulated Zn-DTPA from the dialysis method with UV detection. Data are presented as mean ± SD (n=3).

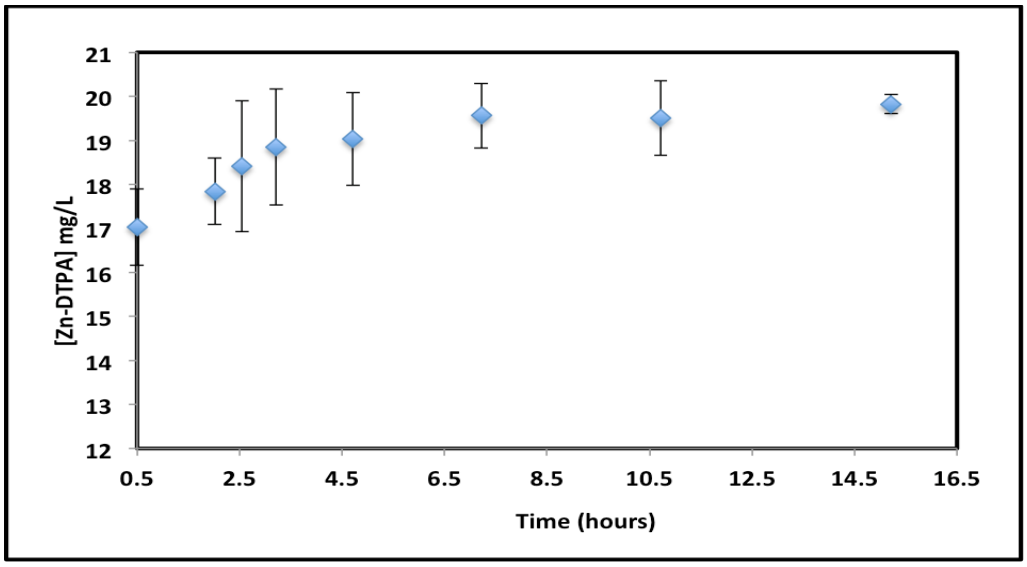

Figure 3.9 Drug release profile PLGA-encapsulated Zn-DTPA from the sample and separate method with LC-MS detection. Data are presented as mean ± SD (n=3).

PLGA nanoparticles were not used as a control during the drug release experiment because PLGA nanoparticles with encapsulated Zn-DTPA were placed in a dialysis bag

and only Zn-DTPA could diffuse through the membrane to reach the acceptor compartment for UV detection. Also, LC-MS analysis was performed in the single ion-monitoring mode to detect only Zn-DTPA as Fe-HDTPA (at m/z 445) after PLGA nanoparticles were sedimented by microcentrifugation. Thus, PLGA nanoparticles could not interfere with the UV detection of any released Zn-DTPA. PLGA is safe and nontoxic after hydrolysis *in vivo;* the US Food and Drug Administration have approved it [177]. The unloaded PLGA nanoparticles exhibited negligible cytotoxicity in *in vitro* studies wherein mouse embryonic fibroblasts NIH3T3, a highly sensitive cell line, were treated with PLGA nanoparticles followed by resazurin-based assay [178, 179]. PLGA nanoparticles of various sizes remain in the mice lungs for seven days without any clearance but they did not trigger the immune system [180].

3.4 Conclusion

To the best of our knowledge, PLGA nanoparticles were employed for the first time for the encapsulation of Zn-DTPA, a hydrophilic drug. The double-emulsion solvent diffusion/evaporation technique was used successfully for the encapsulation of Zn-DTPA into PLGA nanoparticles. The PLGA-encapsulated Zn-DTPA exhibited a spherical shape with a mean diameter of 105 ± 7 nm and a hydrodynamic size of 372 ± 5 nm. Several characteristic peaks of Zn-DTPA in the FTIR spectra of the PLGA-encapsulated Zn-DTPA revealed the encapsulation of Zn-DTPA into the PLGA nanoparticles. The concentration level of the drug inside the dialysis bag would affect the release half-time. These polymeric nanoparticles were synthesized and applied for the first time for the extended drug release of hydrophilic drug in *vitro* and exhibited a drug loading capacity of 106(±7) mg/g. DTPA

release from nanoparticles was found to be significantly slower compared to the plain drug based on half time differences. At this stage, our research mainly focused on the preparation of different types of nano-carriers for the extended release of Zn-DTPA. However, more research is needed to investigate the performance of PLGA-encapsulated Zn-DTPA in *in vivo* experiments and also to examine the effects of modification of the PLGA nanoparticles on loading capacity and release kinetics of the drug. The carrier that exhibits an optimally extended drug release profile will be examined further through release experiments in cell lines and animal pharmacokinetic models with comparison to the plain drug.

3.5 Connection to chapter 4

It was very challenging to synthesize reproducible PLGA-encapsulated Zn-DTPA, which may have been due to centrifugation of PLGA-encapsulated Zn-DTPA. Even low centrifugation speeds and short times might lead to the disruption, which can affect the structural integrity and the amount of the encapsulated drug in the resultant nanoparticles as shown in Figure 3.10. Damage to PLGA nanoparticles inflicted by centrifugation may also have been responsible for the fast release of the drug from these nanoparticles. However, as centrifugation was vital for the collection of PLGA-encapsulated Zn-DTPA after preparation, the removal of unwanted free Zn-DTPA, as well as residual organic solvent that are present in the supernatant, the damage caused by this method is unavoidable. Lecithin liposomes were prepared in **chapter 4** to overcome the limitations of PLGA nanoparticles. They had exhibited high stability and prolonged drug release compared to PLGA nanoparticles, based on previous scientific literature.

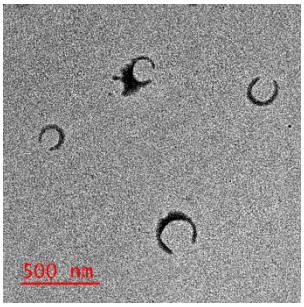

Figure 3.10 TEM images of broken PLGA-encapsulated Zn-DTPA.

Chapter 4: Facile Preparation of Liposomes-encapsulated Zn-DTPA from Soy Lecithin for Decorporation of Radioactive Actinides

Manal Almalki[1], Edward P.C. Lai[1*], Raymond Ko[2], Chunsheng Li[2]

[1]Department of Chemistry, Carleton University, Ottawa, Canada

[2]Radiation Protection Bureau, Health Canada, Ottawa, Canada

*Corresponding author: Edward P.C. Lai, Department of Chemistry, Carleton University, 1125 Colonel by Drive, Ottawa, ON K1S 5B6, Canada, Tel: (613) 520-2600 ext. 3835; E-mail: edward.lai@carleton.ca

Abstract:

Diethylenetriaminepentaacetic acid (DTPA) is an attractive decorporation agent that can enhance the excretion of radioactive actinides such as plutonium, americium, and curium after a radiological incident. However, DTPA is excreted in a short period of time after administration. Several formulations have been developed to improve DTPA pharmacokinetics properties. In this project, liposomes were prepared facilely from soy lecithin as a nanocarrier for pulmonary delivery of Zn-DTPA. Lipid hydration, reverse phase evaporation, and mechanical sonication were three methods evaluated for the preparation of liposomes-encapsulated Zn-DTPA (lipo-Zn-DTPA). Mechanical sonication was the method of choice due to simple apparatus and facile preparation. Lipo-Zn-DTPA exhibited a hydrodynamic diameter of 178(± 2) nm and a spherical shape. The loading capacity and encapsulation efficiency of Zn-DTPA were 41(±5) mg/g and 10(±1)%, respectively. Lyophilization of lipo-Zn-DTPA for extended storage did not affect the amount of encapsulated drug or damage the structure of liposomes. An *in vivo* cytotoxicity test confirmed no serious adverse effect of lipo-Zn-DTPA in rats.

4.1 Introduction

Encapsulation of therapeutic drugs by nanoparticles or nanostructures offers several advantages that make it a suitable formulation for a range of pharmaceutical applications. Liposomes are artificial vesicles comprised of a phospholipid bilayer [181]. They can be prepared by hydration of lipids to form at least one phospholipid bilayer with an enclosed aqueous core [182]. The properties of liposomes (surface charge, size, and fluidity) depend on lipid composition and the method of preparation [183,184,185]. A water-soluble molecule can be encapsulated in the aqueous core while hydrophobic molecules can be entrapped in the lipid bilayer [186]. Liposomes have been used as carriers to facilitate the processing of various bioactive molecules in food, cosmetic, pharmaceutical, and farming products [187,188,189,190,191,192]. Encapsulating drugs in liposomes has proven to be a promising technique in drug delivery due to their biocompatibility, biodegradability, and non-immunogenicity for systemic and non-systemic administrations [193,194,195,196]. In therapeutic medicines, liposomes can protect the encapsulated drug from decomposition by enzymes, bile salts, intestinal flora, and free radicals in the human body [197,198]. Hence, liposomes can increase the efficacy, stability, bioavailability and bioactivity of the encapsulated drug [199,200,201]. Several liposomal drug products (including Exparel, Marqibo, treprostinil, irinotecan/floxuridine, and cytarabine/daunorubicin) have been developed following the successful formulation of liposomal doxorubicin for approval by FDA [202,203,204,205,206]. Clinically, liposomes have been applied for the successful treatment of various cancer and pulmonary diseases for the benefits of sustained release and reduced dosing frequency in the administration of various drugs [207,208,209,210,211,212]. For instance, paclitaxel

encapsulation in liposomes formulated from soy lecithin shows an extended stable release compared to the plain paclitaxel [213]. Liposomes can release the encapsulated drug into cells through different mechanisms including interactions with the cell-surface component, exchange of lipid component with the cell membrane, and electrostatic attraction [214,215]. Liposomes prepared from natural unsaturated phospholipids such as lecithin possess a more permeable bilayer structure compared to that made from saturated phospholipids such as dipalmitoylphosphatidylcholine [216]. Lecithin is a combination of phospholipids found in many naturally occurring sources such as soybean, egg, milk, and sunflower. Large quantities of lecithin are commercially available at a low cost, which potentially allows for the large-scale production of lecithin liposomes [217].

Diethylenetriamine pentaacetate (DTPA, in either Zn- or Ca- form) is a chelation agent that has been used for the removal of radioactive actinides such as plutonium (Pu), americium (Am), and curium (Cm) [218,219,220]. These salts, Zn-DTPA and Ca-DTPA, have been approved by the FDA for the removal of radioactive contaminants from the human body. The formation of soluble/stable complexes between DTPA and radionuclides leads to the chelation and excretion of radioactive contaminants. Zn-DTPA and Ca-DTPA are available as a solution for intravenous injection, or as a dry powder for inhalation *via* a nebulizer for intrapulmonary administration [155,221]. However, the *in vivo* effectiveness of DTPA in removing actinides is limited by its short retention time of 94 minutes in humans, and repeated daily doses over several days or weeks may be required in order to reach the desired decorporation efficacy [17, 222]. Moreover, DTPA has a low distribution into tissues, which limits its efficacy in removing intracellular actinides. As a nanocarrier, liposomes can penetrate the tissue membrane and deliver DTPA into the cells effectively.

Indeed, encapsulation of DTPA in liposomes improves DTPA biodistribution and prolongs its retention time in the human body compared to plain DTPA [42,223].

Individuals can be internally exposed to radionuclides during nuclear research operation in medicine, industries or accidents. Nuclear accidents can be considered to be the worst-case scenario as it can happen suddenly and cause multiple risks including mechanical injury, thermal trauma, external irradiation, superficial contamination, and contamination by radioactive material [224]. Inhalation of radioactive materials is one of the main routes of exposure to internal contamination. The inhaled contaminants can deposit in the respiratory system, being dissolved slowly, and cause damages to internal organ tissues. Victims of radiation incidents should be provided with an immediate decorporation therapy in order to prevent any unnecessarily prolonged irradiation, blood absorption of actinides, and rapid transfer to liver or bone that can cause a higher health risk [225,226,227,228,229]. It is very important to develop a quick method, simple procedure, and cheap source of lipids to make lipo-Zn-DTPA available for all survivors shortly after a nuclear attack. Inhalation drug delivery can localize the DTPA in the lungs, which enhance the decorporation efficacy of actinides compared to other systemic methods [230]. Liposomes can improve the therapeutic efficacy of the inhaled drug by enhancing the drug bioavailability in the lungs and reducing the adverse effect of repeated doses of drug that can result in the dangerous depletion of essential elements by DTPA [231]. They are safe for pulmonary administration as their composition is very similar to the pulmonary surfactants [232,233]. It has previously been reported that inhalation of hydrogenated soy phosphatidylcholine did not induce any pathological effects on alveolar macrophages in

animal models [234]. After actinides are inhaled, they deposit in the epithelial lining fluid that covers the respiratory system regions before transferring into blood and other compartments [235]. Soluble actinides transfer from the lungs to the blood circulation much faster compared to less soluble actinides [235]. Lipo-Zn-DTPA penetrates into pulmonary cells *via* fusion, endocytosis, adsorption, or lipid exchange to form complexes with actinides that have accumulated in cells [236,237]. The formed actinide-DTPA complexes translocate to the extracellular compartment and will be eliminated in urine, which is considered to be the main excretion pathway for actinide-DTPA complexes [238].

This study was mainly focused on the preparation of lipo-Zn-DTPA from commercially available lecithin that is composed of soybean phospholipids. An affordable ultrasonic homogenization system was used for high-throughput liposome preparation. Lipo-Zn-DTPA was prepared by three methods: lipid hydration, reverse phase evaporation, and mechanical sonication. The influence of each preparation method on particle size, size distribution, loading capacity, and encapsulation efficiency was thoroughly investigated. Dynamic light scattering was used to determine particle size, and size distribution of the prepared lipo-Zn-DTPA. Dialysis was used to determine the loading capacity and encapsulation efficiency of liposomes. The stability of lipo-Zn-DTPA was studied after lyophilization for long-term storage.

4.2 Materials and Methods

Soy lecithin in oil form was obtained from Vita Health Products (Winnipeg, Manitoba, Canada). Chloroform, sucrose, and Triton X-100 of ACS grade or higher were

purchased from Sigma-Aldrich (Oakville, Ontario, Canada). Pentetate zinc trisodium (Zn-DTPA) (200 mg/mL) was purchased from Heyl Chemisch-pharmazeutische Fabrik (Berlin, Germany). Cellulose ester dialysis membrane (MWCO: 8-10 kDa) and Millipores Sigma™ Amicon™ Ultra Centrifugal Filter Units (3 kDa) were purchased from Thermo Fisher Scientific (Waltham, Massachusetts, USA). Distilled deionized water (DDW) was used throughout this work

4.2.1 Preparation of liposomes-encapsulated Zn-DTPA

Figure 4.1 shows three methods that were followed for the preparation of liposomes and lipo-Zn-DTPA in our research work.

4.2.1.1 Lipid hydration method

To prepare lipo-Zn-DTPA, a lipid hydration method was adopted from Bangham *et al.* [239]. Lecithin (240 mg) dissolved in chloroform (3 mL) was dried using a rotary evaporator. The dry lipid film was hydrated with an aqueous solution (5 mL) of Zn-DTPA (20 mg/mL). The lipo-Zn-DTPA kept under rotation for 30 minutes, followed by sonication for 30 minutes to disperse lipo-Zn-DTPA. Finally, an ultrasonic probe (300 W at 40%) was used to homogenize the mixture (5 minutes).

4.2.1.2 Reverse phase evaporation method

A solution of lipid (240 mg) in chloroform (3 mL) was mixed with an aqueous solution (5 mL) of Zn-DTPA (20 mg/mL), in accordance with the method developed by Cortesi *et al.* [240]. An ultrasonic probe was used to homogenize the mixture (5 minutes).

The organic solvent was eliminated using a rotary evaporator (30 minutes), followed by sonication. Lastly, the mixture was homogenized again for five minutes.

4.2.1.3 Mechanical sonication method

A mechanical dispersion method was adopted from Dwivedi *et al.* to prepare lipo-Zn-DTPA [241]. A solution of lipid (240 mg) in chloroform (3 mL) was left in the fume hood overnight to evaporate chloroform. Lipid hydration followed upon the addition of an aqueous solution of Zn-DTPA (5mL at 20 mg/mL). An ultrasonic probe was applied (5 minutes) to homogenize the formation of lipo-Zn-DTPA.

Liposomes, for use as a reference in transmission electron microscopy and dynamic light scattering, were prepared using the same lipid hydration, reverse evaporation and mechanical sonication methods in the absence of Zn-DTPA.

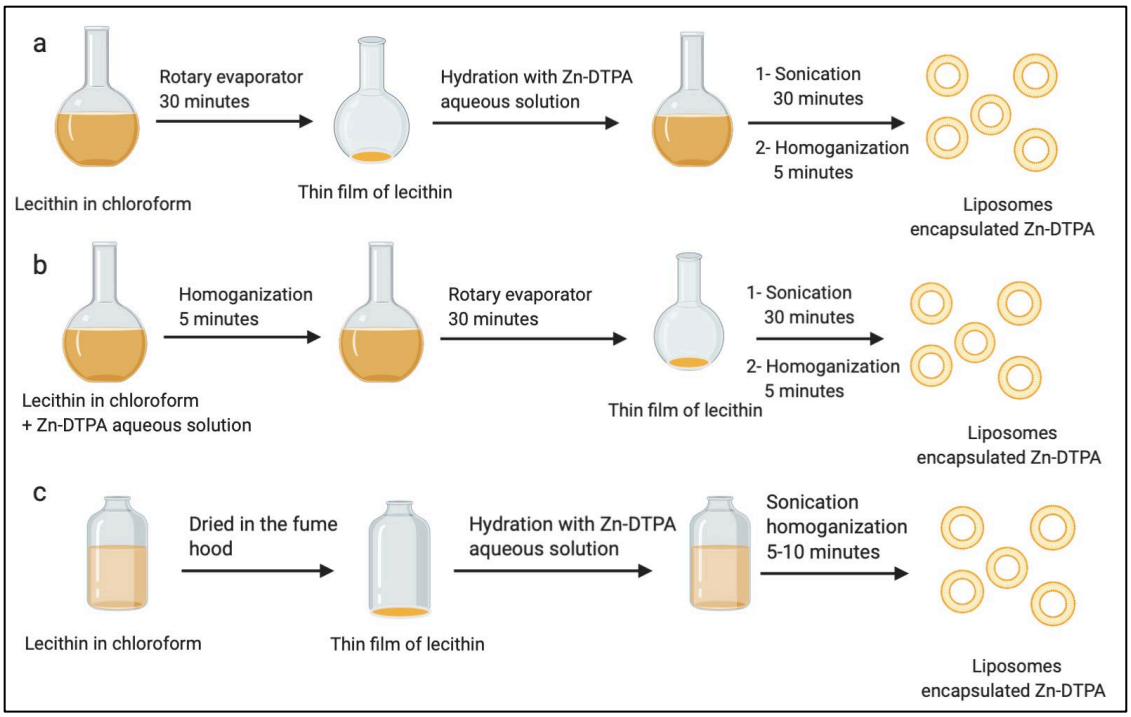

Figure 4.1 Preparation of liposomes encapsulated Zn-DTPA by three methods: (a) lipid hydration, (b) reverse phase evaporation, and (c) mechanical sonication.

4.2.2 Characterization of liposomes by transmission electron microscopy

Transmission electron microscopy (TEM) was used to determine the size distribution and morphology of liposomes and lipo-Zn-DTPA on a FEI Tecnai G2 F20 microscope (Hillsboro, OR, USA) operating at 170 kV.

4.2.3 Characterization of liposomes by dynamic light scattering

Dynamic light scattering (DLS) was used to measure the hydrodynamic diameter and size distribution of liposomes and lipo-Zn-DTPA suspended in DDW. DLS analysis of each suspension was performed using a Brookhaven Instruments nanoDLS particle size analyzer (Holtsville, NY, USA). Each suspension was measured in ten replicates of 10 s each for high accuracy.

4.2.4 Determination of liposomes-encapsulated Zn-DTPA loading capacity and release profile by dialysis

The content of Zn-DTPA in liposomes was determined *via* dialysis. Plain Zn-DTPA or lipo-Zn-DTPA were loaded into a 5-mL dialysis tube for immersion in 150 mL of DDW (acceptor compartment) at 25^{o}C ± 2^{o}C to avoid any potential evaporation of DDW during the dialysis experiments. At appropriate time intervals of 12, 24, and 48 hours, a sample of the dialysate was collected (for LC-MS analysis) before the dialysis tube was transferred to a new beaker containing 150 mL of fresh DDW. The loading capacity of liposomes for Zn-DTPA encapsulation was calculated based on the following equation:

Loading capacity =

$$\left(\frac{(\text{ZnDTPA released from plain (control)} - \text{ ZnDTPA released from liposomes (not encapsulated) mg})}{\text{Mass of lecithin g}}\right)$$

(Equation 1)

where Zn-DTPA released was the total amount of Zn-DTPA released over 48 h. The efficiency of Zn-DTPA encapsulation by liposomes was calculated based on the following equation:

Encapsulation efficiency percentage =

$$\left(\frac{(\text{ZnDTPA encapsulated})}{(\text{ZnDTPA initial amount})}\right) \times 100$$ (Equation 2)

For the *in vitro* release experiments, plain Zn-DTPA or lipo-Zn-DTPA were placed in a 5-mL dialysis tube and immersed in 150 mL of DDW at 25^{o} ± 2^{o}C. At hourly time intervals over the course of the first 7 hours, dialysate samples were collected. Then,

dialysate samples were collected at 21, 43, 67 and 91 hours. After each dialysate collection, the dialysis tube was transferred to a new beaker containing 150 mL of fresh DDW. All dialysate samples were analyzed by LC-MS.

4.2.5 Stability studies of liposomes-encapsulated Zn-DTPA *via* membrane filtration

The stability of lipo-Zn-DTPA in terms of drug content over time was performed using a microcentrifuge filter device. A suspension of lipo-Zn-DTPA (5 mL) were divided into ten 0.5-mL aliquots put in different microcentrifuge tubes. The microcentrifuge tubes were kept under rotation at 110 rpm to ensure the homogeneity of lipo-Zn-DTPA during the experiment. At hourly time intervals over 100 hours, lipo-Zn-DTPA were transferred from one of the microcentrifuge tubes to a microcentrifuge filter device, followed by centrifugation at 14800 rpm for 10 minutes. That speed (14800 rpm) was the highest speed available from our centrifuge, and this time (10 minutes) was the minimum time required to get enough filtrate for LCMS analysis. The concentration of Zn-DTPA in each filtrate was measured by LC-MS to determine if there was any Zn-DTPA released from the liposomes. A control experiment following the same above procedure was carried out using plain Zn-DTPA.

4.2.6 Freeze-drying of liposomes-encapsulated Zn-DTPA

A suspension of lipo-Zn-DTPA (5 mL, at 60 mg Zn-DTPA/mL) was mixed with 1-gram of sucrose at a mass ratio of 1:5 lipid: sugar, respectively [242]. Sucrose had previously been proven to be an excipient that could prevent the aggregation of lipo-Zn-DTPA during the freeze-drying process. The mixture was frozen at -80 ^{o}C for 45 minutes

and lyophilized at -55 ^{o}C for 48 hours in a Labconco model 7753020 freeze dryer (Kansas City, MO, USA). The non-lyophilized liposomes and lyophilized liposomes were mixed with 6% Triton X-100 and heated at 60 ^{o}C in a water bath for 30 minutes to break down the liposomes. The concentrations of free Zn-DTPA and encapsulated Zn-DTPA that released from liposomes during the disruption process were determined in non-lyophilized and lyophilized liposomes by LC-MS

4.2.7 LC-MS analysis

For analysis by liquid chromatography-mass spectrometry (LC-MS), 100 µL of each dialysate was transferred into a glass vial and diluted with both 100 µL of iron (III) chloride solution at 5 mg/mL and 800 µL of 0.1% formic acid [172]. The LC-MS was operated in the single ion monitoring mode to determine the concentration of DTPA as Fe-HDTPA^{1-}, at m/z 445. LC was performed on a C18 column (50 mm x 2.1 mm, 1.8 microns) maintained at room temperature with a mobile phase of 0.1% formic acid at a flow rate of 0.4 mL/min. Samples were complexed to Fe-HDTPA^{-} due to the highest affinity of Zn-DTPA^{3-} towards the Fe^{3+} metal ion [173]. The mass spectrometry analysis was performed using an Agilent Technologies model 6460 triple quad MS/MS system equipped with an electrospray ionization (ESI) source operating in the negative mode. The operating parameters were nitrogen gas flow rate = 9.8 L/min, gas temperature = 300°C, nebulizer pressure = 15 psi, capillary voltage = 4000 V, fragmentor voltage = 135 V, and cell accelerator voltage = 7 V.

4.2.8 Cytotoxicity studies

The cytotoxicity of an aqueous solution of Zn-DTPA and lipo-Zn-DTPA were studied *in vivo* in rats. Eight male Long Evans rats weighing 400 g were used to examine the possible toxicity of Zn-DTPA and lipo-Zn-DTPA. An aqueous solution of Zn-DTPA or lipo-Zn-DTPA were given daily to two different groups of rats (n= 4, 0.3 mL at 3.3 mg DTPA/mL) over five days *via* intranasal instillation. Then, the euthanasia procedure of the rats was achieved through cardiac puncture and their lungs were removed for histopathology to study the effect of Zn-DTPA and lipo-Zn-DTPA on the respiratory system.

4.3 Results and discussion

The prepared lipo-Zn-DTPA were characterized by TEM and DLS to confirm their spherical morphology and to confirm their particle size distribution compared with liposomes without encapsulated Zn-DTPA. Any changes in liposomes morphology such as size, shape, or surface area upon encapsulation of drug were found to activate the immune system leading to rapid clearance of liposomes [243,244]. As a result of this, the US Food and Drug Administration highly recommended the characterization of liposomes morphology [245,246]. The unloaded liposomes and the lipo-Zn-DTPA exhibited particle sizes in the range of 80-100 nm, as illustrated by TEM analysis (Figure 4.2). These images showed that the particle sizes of unloaded liposomes and lipo-Zn-DTPA were not significantly different. To promote the accumulation of the liposomes in the lungs and enhance the potential of capturing radioactive actinides, Muraki *et al.* had previously investigated whether 80-100 nm of liposomes were suitable for intratracheally

administration. Liposomes-encapsulated fluorescent dye-labeled drug measuring 40, 80 and 180 nm were administrated intratracheally to the lungs of a pulmonary hypertension rat for evaluating their biodistribution. The fluorescent imaging analysis showed that only liposomes of 80 nm were accumulated in the rat lungs [247]. The TEM images showed that both unloaded liposomes and lipo-Zn-DTPA were spherical in shape, without any noticeable aggregation.

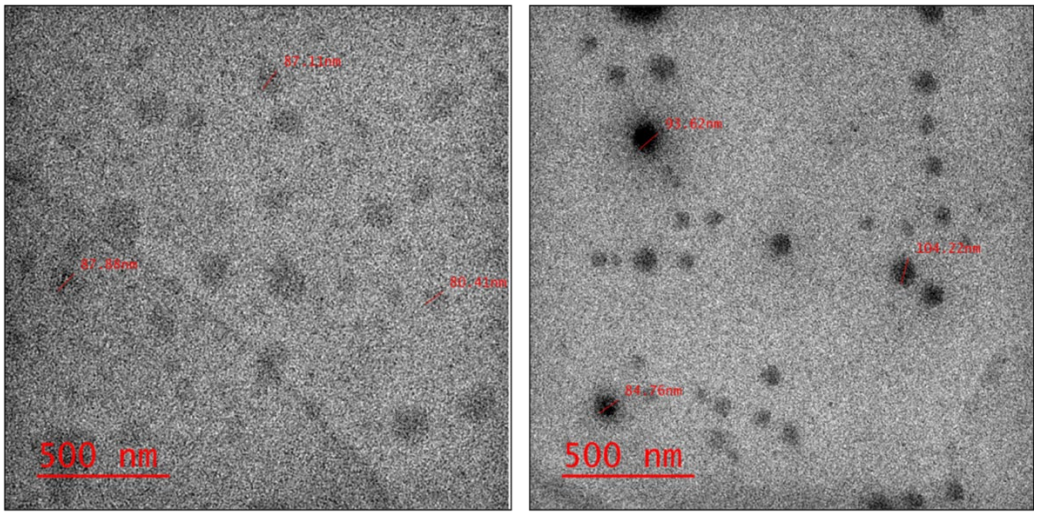

Figure 4.2 TEM images of (a) liposomes, and (b) liposomes encapsulated Zn-DTPA prepared by mechanical sonication.

The liposomes and lipo-Zn-DTPA prepared by lipid hydration method exhibited hydrodynamic diameters of 141 ± 3 nm and 143 ± 1 nm, respectively. As summarized in Table 4.1, hydrodynamic diameters of 172 ± 1 nm and 167 ± 1 nm were obtained for unloaded liposome and lipo-Zn-DTPA formed by reverse phase evaporation method, respectively. Larger particle diameters were obtained for unloaded liposomes 182 ± 2 nm, and lipo-Zn-DTPA 178 ± 1 nm that resulted from mechanical sonication. Liposomes and

lipo-Zn-DTPA prepared by the three methods exhibited a very narrow particle size distribution. As illustrated in Table 4.1, all samples showed a polydispersity of approximately 0.2 indicating a moderately polydispersed size distribution of the unloaded liposomes and lipo-Zn-DTPA [248].

Table 4.1 Hydrodynamic diameters of liposomes and liposomes encapsulated Zn-DTPA. Data are given as mean ± SD (n=10).

Sample	Hydrodynamic diameter (nm)	Polydispersity
Liposomes (Lipid hydration method)	141 ± 3	0.2
Liposomes encapsulated Zn-DTPA (Lipid hydration method)	143 ± 1	0.2
Liposomes (Reverse phase evaporation method)	172 ±1	0.2
Liposomes encapsulated Zn-DTPA (Reverse phase evaporation method)	167 ± 1	0.2
Liposomes (Mechanical sonication method)	182 ± 2	0.2
Liposomes encapsulated Zn-DTPA (Mechanical sonication)	178 ± 1	0.2

Based on the TEM images and DLS measurement all the lipo-Zn-DTPA were unilamellar ≤ 200 nm and have similar size distributions. The diameters of dry liposomes determined by TEM were smaller than the hydrodynamic dimeters of nanoparticles measured in aqueous suspension. This result was expected as DLS measures the size of the particle with the hydration layer [249]. However, in TEM, the particle size is observed more directly as the hydration layer does not form in dry nanoparticles that measured with TEM under vacuum. This resulted in a smaller particle size compared to the particle size obtained by DLS, thus TEM is more representative of the actual particle size. Liposomes formed using lipid hydration, reverse phase evaporation, or mechanical sonication methods have a small average size < 200 nm; smaller liposomes are more effective in the medical

application compared to larger liposomes as they can readily enter human cells through endocytosis [250,251]. Furthermore, nanoparticles smaller than 200 nm are less recognized by the lymphatic system compared to larger nanoparticles. Therefore, smaller particles can stay for a longer time in blood circulation; avoiding the immediate clearance by the lymphatic system than larger particles [252,253]. Hence, lipo-Zn-DTPA prepared by lipid hydration, reverse phase evaporation, or mechanical sonication methods could be suitable for our application. However, lipo-Zn-DTPA prepared by mechanical sonication were chosen for further experiments in this work for several reasons that will be discussed later in this manuscript.

To ensure the efficacy of removing radioactive actinides from human lungs, the loading capacity of Zn-DTPA in liposomes is an important factor. Although there are similarities among the three preparation methods, all of them were in fact evaluated to cross-check their loading capacity. The loading capacity of lipo-Zn-DTPA was evaluated *via* dialysis. Dialysis of plain Zn-DTPA or lipo-Zn-DTPA was continued for 48 hours to ensure all the plain or non-encapsulated Zn-DTPA was released through the dialysis membrane. As summarized in Table 4.2, the loading capacity (by mass) of lipo-Zn-DTPA that were prepared by lipid hydration, reverse phase evaporation, and mechanical sonication methods found to be 27 ± 4 mg/g, 72 ± 7 mg/g, and 41 ± 5 mg/g, respectively.

Table 4.2 Loading capacity and encapsulation efficiency of liposomes encapsulated Zn-DTPA. Data are given as mean ± SD (n=3).

Methods	Plain Zn-DTPA released in 48 h (control) mg	Free Zn-DTPA from liposomes (non-encapsulated mg	Encapsulated Zn-DTPA mg	Loading capacity mg/g	Encapsulation efficiency %
lipid hydration	94 ± 6	88 ± 6	6 ± 1	27 ± 4	6 ± 1
Reverse phase evaporation	95 ± 4	78 ± 5	16 ± 1	72 ± 7	17 ± 1
Mechanical sonication	100 ± 1	91 ± 1	9 ± 1	41 ± 5	10 ± 1

Lipid hydration method, also known as Bangham method, was the first method used for the formation of liposomes from a phospholipid. However, liposomes prepared by this method exhibit low encapsulation compared to those prepared by other methods [254]. This limitation has been confirmed by our findings as liposomes prepared by this method exhibit the lowest loading capacity of Zn-DTPA compared to those prepared by the two methods that have been used in this work. Liposomes can follow different formation mechanisms in each liposome preparation method. The energy input into lipid suspension in the form of sonication, homogenisation, shaking, or heating affects the arrangement of lipid molecules in the bilayered vesicles, which may lead to a different loading capacity [254]. Also, the lipid hydration process must be maintained above the phase-transition temperature to increase the fluidity of lipid for enhancing the loading capacity. In mechanical sonication method, during the hydration process the heat produced by the sonication probe is much higher than that applied in the lipid hydration method. This difference in temperature between the two methods may change the loading capacity of liposomes prepared by the mechanical sonication method compared to the lipid hydration

method. The reverse phase evaporation method exhibited the highest loading capacity among the three preparation methods, confirming observations reported by the literature [255]. However, the slow evaporation of the residual organic solvent that is mixed with the aqueous solution during the preparation of liposomes can affect the chemical and biological stability of the vesicle by altering its membrane permeability [256]. This can lead to leakage of the encapsulated drug and reduce the loading capacity. Moreover, the organic solvent can also induce toxic effects towards cells such as wall disruption, enzyme inhibition, and protein denaturation [257]. Thus, using another method to prepare liposomes-encapsulated pharmaceuticals in the absence of an organic solvent is preferable.

Although lipo-Zn-DTPA prepared by the mechanical sonication method showed a lower loading capacity compared to those prepared by the reverse phase evaporation method, it was chosen for the encapsulation of Zn-DTPA by lecithin liposomes in all subsequent experiments in this study for two reasons. Firstly, this method involves fewer steps during the preparation of lipo-Zn-DTPA, which makes those liposomes quickly available for the treatment of patients shortly after any nuclear accident. Secondly, liposomes formed using this method did not exhibit any significant difference in terms of liposome size (hydrodynamic diameter) and loading capacity compared to the reverse evaporation method. To increase the loading capacity of lipo-Zn-DTPA prepared using the mechanical sonication method, the initial Zn-DTPA concentration was increased progressively. Figure 4.3 shows that as the concentration of Zn-DTPA was increased from10 to 60 mg/mL, the loading capacity improved from 21 ± 8 mg/g to 75 ± 15 mg/g.

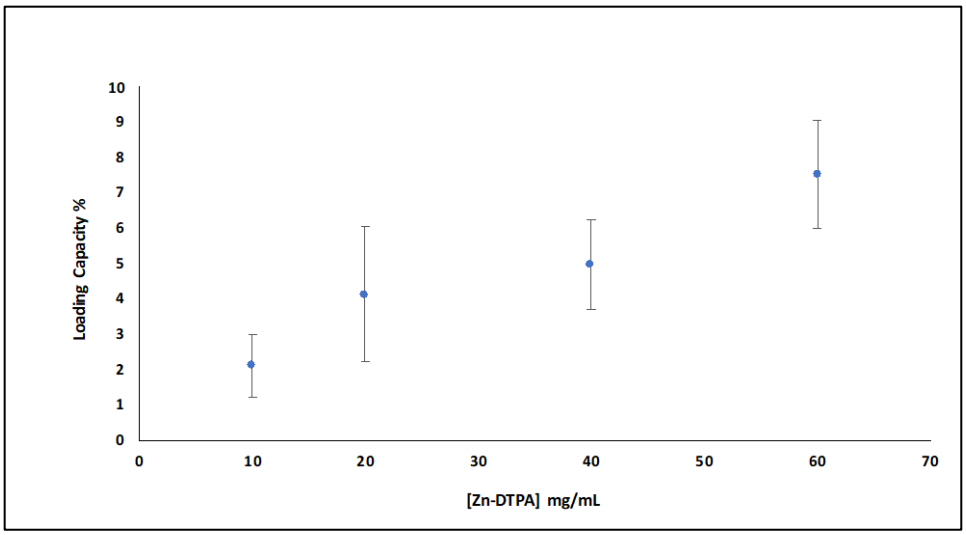

Figure 4.3 Loading capacity increases as a function of Zn-DTPA concentration. Data are presented as mean ± SD (n=3).

This loading capacity is lower than the capacity of PLGA nanoparticles 106 mg/g which were prepared in our lab for the decorporation of radioactive contaminants [258]. However, liposomes were prepared to overcome the limitations of PLGA nanoparticles regarding their larger hydrodynamic dimeter, leakage of Zn-DTPA, and residual organic solvents (acetone and dichloromethane) from the preparation [258]. Hence, lipo-Zn-DTPA were chosen for further experiments in this project. The encapsulation efficiency percentages of lipo-Zn-DTPA prepared using lipid hydration, reverse phase evaporation, and mechanical sonication methods found to be (6 ± 1)%, (17 ± 1)%, and (10 ± 1)%, respectively. The lowest, intermediate, and highest encapsulation efficiencies were obtained by lipid hydration, mechanical sonication, and reverse phase evaporation methods, respectively.

Figure 4.4 shows the dialysis release profile of lipo-Zn-DTPA (drug: lipid mass ratio of 0.2:1) for comparison with the profile for plain Zn-DTPA. Each *in vitro* drug

release experiment was performed using a dialysis tube in deionized water for 91 hours *via* dialysis at 25^{o}C ± 2^{o}C in order to test the extended drug release of liposomes. The release of Zn-DTPA from lipo-Zn-DTPA was slower compared to that from plain Zn-DTPA for the first two hours with a *p*-value of 0.01, which indicated a significant difference between the two dialysis release processes. The slow release was followed by a rapid release over the next 19 hours. Even though the initial concentrations of lipo-Zn-DTPA and plain Zn-DTPA were the same, the concentration of free Zn-DTPA in liposomes dialysis tube was lower than the plain Zn-DTPA concentration due to the encapsulation of some Zn-DTPA in the liposomes. The Zn-DTPA released from liposomes dialysis in the first 19 hours is attributed to the free/non-encapsulated Zn-DTPA. Hence, there was no significant difference between the two drug profiles in terms of the release half time where half of Zn-DTPA quantities were released. The release half times of Zn-DTPA from the control and the liposomes were 4.2 ± 0.3 and 6.5 ± 0.7 hours respectively, with a *p*-value of 0.28 indicating a non-significant difference between the two release half times. After 19 hours, the encapsulated Zn-DTPA started to be released from the liposomes in small amounts of 5 mg at 43 h, 3 mg at 67 h and 1 mg at 91 hours with a modest difference in release between the two drug release profiles.

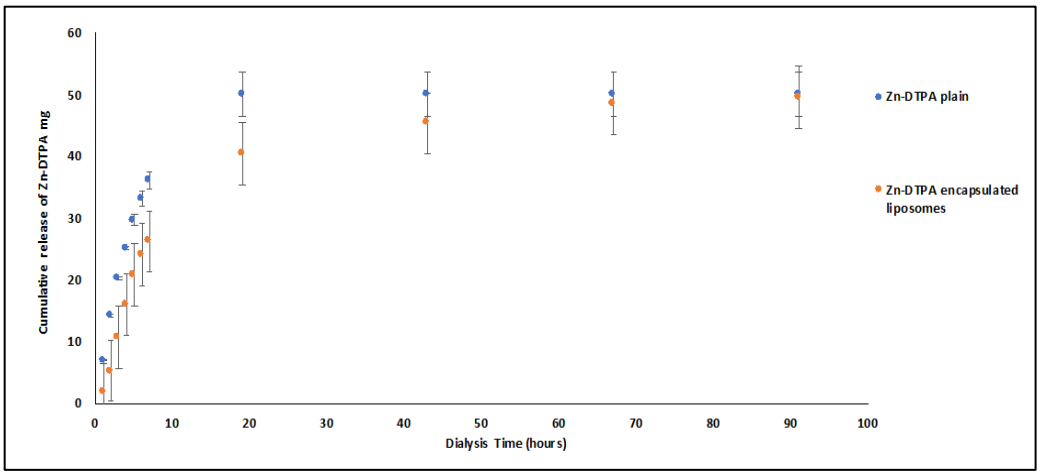

Figure 4.4 Dialysis release profiles of plain Zn-DTPA (control) and liposomes encapsulated Zn-DTPA in deionized water with LC-MS detection. Data are presented as mean ± SD (n=3).

Encapsulated molecules can be released from liposomes when the liposomes are either unstable or lose their stability temporarily. Zaboriva *et al.* reported the release of NaCl from liposomes during the dialysis of NaCl encapsulated liposomes in DDW that demonstrated the low stability of uncoated liposomes [259]. In this dialysis experiment, when the acceptor compartment was changed frequently, the Zn-DTPA concentration in the acceptor compartment became nearly zero. In this condition, liposomes could swell due to a difference in the salt concentrations inside the dialysis membrane from the surrounded acceptor compartment (DDW). This can decrease the van der Waals attraction between the lipid bilayer, increasing the membrane permeability which leads to the release of encapsulated Zn-DTPA [260]. Apparently, both plain Zn-DTPA and lipo-Zn-DTPA show extended dialysis through the membrane. One possible explanation for the delayed release of Zn-DTPA from the dialysis membrane is the slow diffusion rate of Zn-DTPA as the concentration gradient is the only source of potential energy that can affect the diffusion rate in this experiment. Another explanation is that the carboxylic groups of Zn-DTPA may

form H-bonds with the hydroxyl groups in the cellulose ester membrane resulting in slow drug release.

The stability of a drug delivery system is crucial in medical applications. The stability of lipo-Zn-DTPA in terms of drug content was studied at $25^{o}C \pm 2^{o}C$. In the drug release experiment *via* dialysis, the encapsulated Zn-DTPA got released from the liposomes. In the stability test, the free Zn-DTPA concentration was much higher (than that of the dialysis release experiment which was nearly zero) which protect liposomes of losing their stability. There was no separation between the free Zn-DTPA and lipo-Zn-DTPA. Separation of the suspension (0.5 mL) only occurred at regular intervals (from 0 to 100 hours) by centrifugation in microcentrifuge filter tubes. As shown in Figure 4.5, no release of encapsulated Zn-DTPA (5.9 ± 0.3 mg/L) from liposomes was observed because the free Zn-DTPA detectable in the filtrate remained the same even after 100-hour analysis. The concentration of Zn-DTPA encapsulated in the liposomes could therefore be calculated as the difference in concentration between the control sample (containing the original concentration of free Zn-DTPA) and the free Zn-DTPA detected in the liposome sample. This result could further suggest that liposomes can be stored at room temperature for at least five days without any leakage of Zn-DTPA.

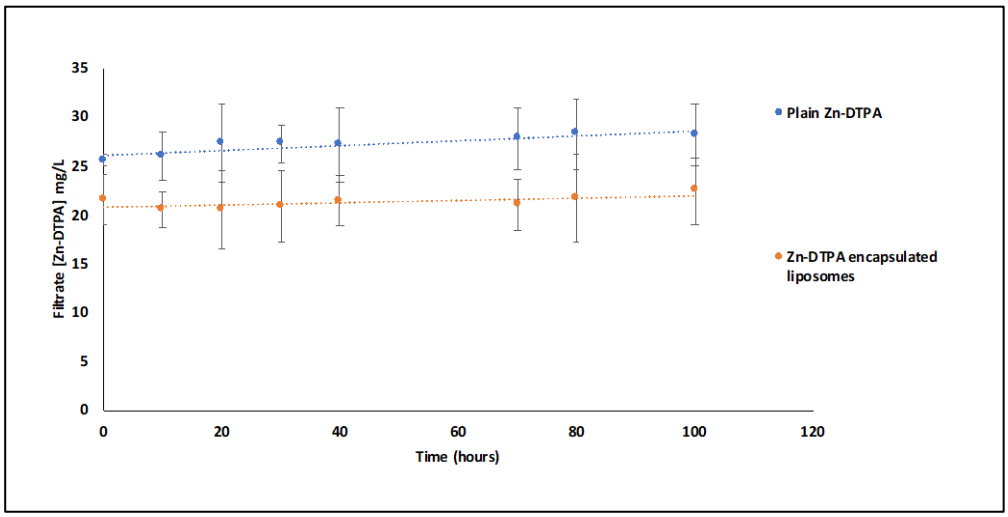

Figure 4.5 Stability of plain Zn-DTPA (control) and liposomes encapsulated Zn-DTPA in the presence of free Zn-DTPA at room temperature 25°C±2°C. Data are presented as mean ± SD (n=3).

Even though lipo-Zn-DTPA did not exhibit any leaking of the encapsulated drug during the above stability test, a stable solid dosage form of lipo-Zn-DTPA is required [261]. Liposomes stored as colloidal suspension may lose their stability, efficacy, and safety due to oxidation or hydrolysis of lipids, drug leakage, aggregation or fusion of the vesical [262]. Dry liposomes can overcome all of the above limitations that result from instability when storing liposomes in an aqueous environment. Lipo-Zn-DTPA were mixed with sucrose to protect liposomes during lyophilization (or freeze drying). Sugars may protect liposomes from being damaged during freezing due to the formation of a glassy matrix [263]. Also, sugars form H-bonds with the adjacent phosphate groups in lipids, increasing the distance between phosphate groups and thus decreasing the van der Waals interaction between the hydrocarbon chains of adjacent lipids. Kannan *et al.* observed that this interaction maximizes at a mass ratio of 5:1 sugar: lipid and not only protected the leakage of paclitaxel from pegylated liposomes, but it also prevented the aggregation of liposomes giving a monodispersed population of the liposomes after freeze-drying [242].

As illustrated in Table 4.3, the freeze-drying process did not affect the concentration of encapsulated Zn-DTPA in the lyophilized liposomes. That means the encapsulated Zn-DTPA did not leak out of the liposomes during the freeze-drying process; otherwise, the concentration of free Zn-DTPA in liposomes after lyophilization and reconstitution in water will be higher. Also, the non-lyophilized lipo-Zn-DTPA and lyophilized lipo-Zn-DTPA have almost the same concentration of Zn-DTPA with a *p*-value of 0.61 as determined after membrane disruption with Triton X-100 based on LC-MS analysis.

Table 4.3 Liposomes encapsulated Zn-DTPA before and after lyophilization. Data are given as mean ± SD (n=3).

Sample	Free Zn-DTPA (mg/L)	Encapsulated Zn-DTPA (mg/L)
Liposomes-encapsulated Zn-DTPA before lyophilization	28 ± 1	7 ± 2
Liposomes-encapsulated Zn-DTPA after lyophilization	27 ± 1	8 ± 1

As illustrated in Figure 4.6 (b), the shape and particle size of rehydrated lipo-Zn-DTPA did not change significantly after the freeze-drying process. They still exhibited a particle size in the range of 80-100 nm and a spherical shape similar to the non-lyophilized lipo-Zn-DTPA shown in Figure 6 (a). This observation agreed with results reported by Kannan V *et al*. and Glavas-Dodov, M *et al*. [242, 264].

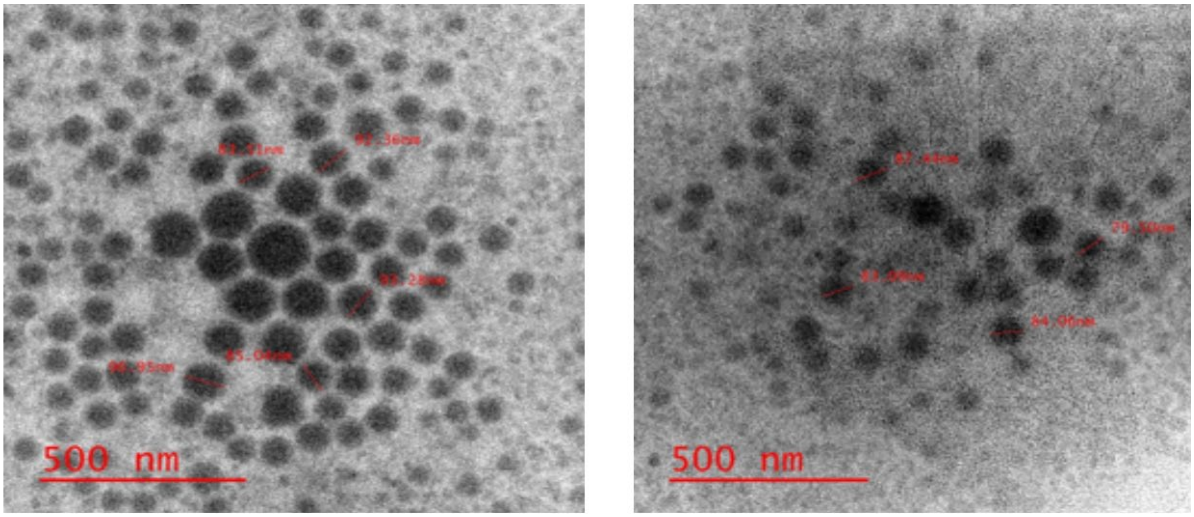

Figure 4.6 TEM images of liposomes encapsulated Zn-DTPA (a) before and (b) after lyophilization.

All the animal experiments were conducted in accordance to the guidelines set by The Canadian Council on Animal Care (CCAC). Mice were kept in a laboratory at a fixed temperature and humidity through the 12h/12h dark/light cycle. Laboratory rodent diet and water were provided *ad libitum*. Phan *et al.* had previously found that empty liposomes were safe and non-toxic in toxicological studies performed [42]. Hence, our lipo-Zn-DTPA were administered to rats (without involving empty liposomes) in our cytotoxicity study with relevance to pulmonary delivery. An aqueous solution of Zn-DTPA or lipo-Zn-DTPA were given to rats *via* intranasal instillation for five days to determine potential toxic effects to their respiratory system. During the toxicity study, Zn-DTPA did not exhibit adverse effects. Rats treated with lipo-Zn-DTPA experienced minimal inflammation characterized by perivascular lymphocytes inflammation. However, they recovered over the next several days without any reduction of the daily dose. Therefore, there was no serious adverse effect observed during the cytotoxicity study of our liposomes on rats

4.4 Conclusion

Lecithin has been successfully used for encapsulating the decorporation agent Zn-DTPA by formation of liposomes at low cost, compared to mixing phospholipids in the research lab. Mechanical sonication was chosen for the preparation of liposomes-encapsulated Zn-DTPA, with a particle size of 80-100 nm, due to its simple preparation even on a large production scale. The resultant lipo-Zn-DTPA exhibited a loading capacity of 41(±5) mg/g and an encapsulation efficiency of 10(±1)%. The lyophilized form of lipo-Zn-DTPA increases the stability during long-term storage. Lipo-Zn-DTPA did not show any significant adverse effects on the respiratory system based on our rat cytotoxicity study. The efficacy of lipo-Zn-DTPA for the decorporation of radioactive contaminants from the lungs will be tested soon on Long Evans rats.

4.5 Connection to Chapter 5

The resultant lipo-Zn-DTPA were found to be stable with no leakage or release of Zn-DTPA observed during the *in vitro* study. They were found to be safe and non-toxic as there was no observable serious adverse effect in rats based on our cytotoxicity study. According to literature, liposomes exhibit a prolonged release of various therapeutic agents. Hence, lipo-Zn-DTPA were chosen in this research work to test their efficacy in the decorporation of radioactive actinides that are deposited in the deep lungs (bronchioles and alveoli) using an animal model (Long Evans rats). Long Evans rats were contaminated with americium-241 (^{241}Am), curium-243 (^{243}Cm), curium-244 (^{244}Cm), and plutonium-238/239/240 ($^{238/239/240}$Pu) by intratracheal instillation at certain activity as illustrated in Table 4.4. Decorporation treatment was performed by the intratracheal instillation of either plain solution of Zn-DTPA, or lipo-Zn-DTPA (n = 6, 0.3 mL at 3.3 mg DTPA/mL) over eight days. Urine samples were collected every day to determine the excretion rate of the internalized ^{241}Am, $^{243/244}$Cm, and $^{238/239/240}$Pu.

Table 4.4 Amounts of actinides given into rats *via* intratracheal instillation.

Actinide	Activity/rat (Bq) (n=6)
^{241}Am	21.0
$^{243/244}$Cm	56.7
^{238}Pu	12.7
$^{239/240}$Pu	27.3

Chapter 5: Conclusion

Currently, animal experiments are being carried out to determine the efficacy of lipo-Zn-DTPA to eliminate the internalized ^{241}Am, $^{243/244}Cm$ and $^{238/239/240}Pu$ after intratracheal administration.

DTPA-H_5 loaded PEG-functionalized TiO_2 nanoparticles have been prepared to extend the release of DTPA and enhance its decorporation efficacy. However, the low loading capacity and the fast drug release of PEG-functionalized TiO_2 compared to PLGA nanoparticles and lecithin liposomes do not justify their use in the decorporation treatment.

PLGA nanoparticles have not been used for the decorporation of radioactive actinides previously. Based on our study, PLGA nanoparticles exhibited good loading capacity and extended release of Zn-DTPA with a release half time of 3.5 hours. However, the preparation of PLGA-encapsulated Zn-DTPA was lengthy (and the polymer is expensive). Inhalable drug encapsulated PLGA nanoparticles have been utilized to treat various lung diseases. Therefore, PLGA-encapsulated Zn-DTPA may be tested for the decorporation of internalized radioactive actinides in the near future if the lecithin liposomes decorporation results was not satisfactory.

In terms of decorporation efficiency reported so far in the scientific literature, liposomes are ranked as the best option for the decorporation of actinides as they show high capability in the decorporation of plutonium, curium, and americium. They show an extended release of many drugs and can stay for 24 hours in the lungs without triggering the immune system. Lecithin liposomes exhibited a good loading capacity and good stability in our study. However, our *in vitro* drug release experiment (dialysis) was not helpful to determine the extended release from liposomes and hence the release half-time

because liposomes lost their stability and released the encapsulated Zn-DTPA during this experiment. An *in vivo* experiment will be needed in order to demonstrate the extended drug release and determine the half-life after administration to rats.

In terms of safety, TiO_2 nanoparticles are considered to be safe in some studies but many studies mentioned that TiO_2 may be toxic and carcinogenic. However, attachment of PEG to the surface of TiO_2 nanoparticles reduces their toxicity. PLGA nanoparticles show negligible toxicity in all studies but can be used safely. Liposomes are considered to be the safest nanocarrier as liposome's composition is very similar to the cell membrane. Therefore, they do not show any toxicity on animal models either in the literature or in our own cytotoxicity study.

In this research project, DTPA-H_5 loaded PEG-TiO_2 nanoparticles, PLGA-encapsulated Zn-DTPA, and lipo-Zn-DTPA were prepared by non-covalent interactions (hydrogen bond, ionic attraction, van der Waals forces, and hydrophobic effect). However, according to the literature nanoparticles that have been attached covalently to DTPA exhibited slower release of DTPA compared to the PEG-TiO_2, PLGA, and lecithin liposomes prepared in our lab. Therefore, in the future, DTPA which has been attached covalently into nanoparticles will be prepared to extend the release of DTPA further for the decorporation of radioactive actinides.

5.1 Contribution to advancing knowledge

In this research project, three kinds of nanocarriers have been investigated for extended release of the decorporation agent DTPA. Specifically, inorganic nanoparticles (PEG-TiO_2), polymeric nanoparticles (PLGA), and lecithin liposomes have been designed

as DTPA carriers to reduce the intracellular deposits of radioactive actinides and thus the risk of radiation-induced diseases. From our consideration, titanium dioxide nanoparticles (TiO_2) might not be good enough for the decorporation of actinides from the lungs as there is a debate regarding the safety of TiO_2 nanoparticles in the respiratory system. However, here we used PEG to reduce any toxic effects that can be induced to the lungs by TiO_2. The fast release of DTPA and low loading capacity of PEG-TiO_2 could be overcome by the ability of PEG-TiO_2 to bind with actinides providing double therapeutic benefit as proposed in the literature. On the other hand, PLGA nanoparticles are a safe agent showing extended-release of Zn-DTPA in our *in vitro* study. This confirms a promising function of PLGA nanoparticles in extending drug release and could be used as a future reference for other drug studies that share a similar mechanism.

Although people have been preparing liposomes from a mixture of lipids, we proposed the use of soy lecithin to produce lipo-Zn-DTPA at a fairly low cost since lecithin is a common supplement readily available on the market. Lecithin liposomes were found to be stable and safe based on our stability and toxicity studies. Hence researchers can encapsulate drugs in liposomes prepared from soy lecithin, which is a more accessible method in treating radiation-exposed people compared to liposomes prepared from a mixture of several lipids. To determine whether lecithin liposomes can be a good candidate for the decorporation of actinides, they are tested further in animal contaminated with ^{241}Am, $^{243/244}Cm$ and $^{238/239/240}Pu$. Inhalable administration of lipo-Zn-DTPA was chosen due to its effectiveness in reducing the burden of radioactive actinides intrapulmonary as well as extrapulmonary. Unfortunately, those collected samples have not been analyzed yet

due to the impact of Covid-19. All of PEG-TiO_2, PLGA, and lecithin liposomes exhibited a certain degree of extended release of DTPA.

5.2 Breaking advances in actinide decorporation research

Actinides have been used widely in many applications ranging from energy production to life science. The decorporation of actinides is critical to minimize the radiotoxicity and chemotoxicity that can be induced inside the body. This requires the use of an effective agent that can bind effectively with actinides. However, the current decorporation agents are not sufficient in removing actinides that are deposited in tissues [265]. Moreover, several parameters could influence the complex formation between decorporation agents and actinides which need to be known to improve the decorporation therapy. Nanoparticles have been utilized as a delivery system for the decorporation of actinides. Chitosan nanoparticles have been used for the removal of radioactive actinides accumulated in the lungs due to their biocompatibility and resistance to radiation and oxidation. The decorporation agents were attached to the surface of chitosan nanoparticles. Chitosan nanoparticles combined with a hydroxypyridinone-derivative ligand showed high affinity in the decorporation of uranium and reactive oxygen species generated by uranium. However, these decorporation nanoparticles need further clinical studies to be available for the decorporation therapy of actinides. Polyethyleneimine (PEI) functionalized with either methylcarboxylates or methylphosphonates has been used successfully for the decorporation of thorium and plutonium. The success of the decorporation of actinides with the functionalized PEI is due to its ability to reach various tissues including lungs, bone, kidneys, and liver [266]. Although titanium dioxide nanoparticles exhibit high affinity

towards heavy metal ions and rare earth elements, their agglomeration due to the larger surface area limited their binding ability with actinides. However, this disadvantage can be solved by coating nanoparticles with a hydrophilic polymer such as polyethylene glycol. A recent study shows that polyethylene glycol coated titanium dioxide nanoparticles (PEG-TiO_2) can remove strontium-90 (^{90}Sr) and cesium-134 (^{134}Cs) from nuclear industrial wastewater [267]. In a study performed by Yuan, an open mesoporous silica structure (F-SiO_2) is grafted with various functional groups including amidoxime, phosphate, and amino. These porous microsphere materials were found to be very selective in the decorporation of uranium [268]. Currently, further studies are ongoing to develop more effective decorporation agents that can reduce the radiation diseases induced by actinides.

References:

[1] Williams P, COL L, FLETCHER S (2010). Health effects of prenatal radiation exposure. Leukemia. 7, 10-11.

[2] Taşoğlu A, Ates O, Bakaç M (2017). Prospective physics teachers' awareness of radiation and radioactivity. European Journal of Physics Education. 6, 1-14.

[3] Katsumura Y, Kudo H (2018) Radiation: Types and Sources. In: Kudo H. (eds) Radiation Applications. An Advanced Course in Nuclear Engineering. Springer, Singapore

[4] The United States Nuclear Regulatory Commission. What are the different types of radiation? October 19, 2018

[5] Ford J. (2004). Radiation, people, and the environment.

[6] Groen R, Bae J, Lim K (2012). Fear of the unknown: ionizing radiation exposure during pregnancy. American journal of obstetrics and gynecology. 206, 456-462.

[7] Durakovic A (2016). Medical effects of internal contamination with actinides: further controversy on depleted uranium and radioactive warfare. Environmental health and preventive medicine. 21, 111-117.

[8] Shimura T, Yamaguchi I, Terada H, Robert Svendsen E, Kunugita N (2015). Public health activities for mitigation of radiation exposure and risk communication challenges after the Fukushima nuclear accident. Journal of radiation research. 56, 422–429.

[9] Hasegawa A, Tanigawa K, Ohtsuru A, Yabe H, Maeda M et al (2015). Health effects of radiation and other health problems in the aftermath of nuclear accidents, with an emphasis on Fukushima. The Lancet, 386, 479-488

[10]https://www.nrcan.gc.ca/science-data/data-analysis/energy-data-analysis/energy-facts/uranium-and-nuclear-power-facts/20070

[11] Wood R, Sharp C, Gourmelon P, Le Guen B, Stradling G et al (2000). Decorporation treatment—medical overview. Radiation Protection Dosimetry. 87, 51–56.

[12] Canadian Nuclear Safety Commission. Radiation doses. September 12, 2019.

[13] Morgan W, Sowa M (2015). Non-targeted effects induced by ionizing radiation: mechanisms and potential impact on radiation induced health effects. Cancer Letters. 356, 17-21.

[14] Lissa R (2011). How does nuclear radiation affect the body? Psychology

[15] US Food and Drug Administration (2006). Guidance for industry internal radioactive contamination—Development of decorporation agents. Silver Spring, MD: US Food and Drug Administration.

[16] Ohmachi Y (2015). Decorporation agents for internal radioactive contamination. Yakugaku zasshi: Journal of the Pharmaceutical Society of Japan. 135, 557-563.

[17] Fattal E, Tsapis N, Phan G (2015). Novel drug delivery systems for actinides (uranium and plutonium) decontamination agents. Advanced drug delivery reviews. 90, 40-54

[18] Bunin D, Chang P, Doppalapudi R, Riccio E, An D et al (2013). Dose-dependent efficacy and safety toxicology of hydroxypyridinonate actinide decorporation agents in rodents: towards a safe and effective human dosing regimen. Radiation research. 179, 171–182.

[19] Huckle J, Sadgrove M, Leed M, Yang Y, Mumper R et al (2016). Synthesis and physicochemical characterization of a diethyl ester prodrug of DTPA and its investigation as an oral decorporation agent in rats. Association of Pharmaceutical Scientists. 18, 972-980.

[20] FDA (2004). Pentetate zinc trisodium injection 1000 mg for intravenous or inhalation administration

[21] FDA (2013). Highlights of Prescribing Information: Pentetate Zinc Trisodium Injection (Zn-DTPA) for Intravenous Injection or Inhalation Administration.

[22] Abergel R (2017). Chelation of actinides. Chapter 6. The Royal Society of Chemistry. United States.

[23] Jerrold T (2019). Radiation Exposure and Contamination. Merck & Co, Inc, Kenilworth, NJ, USA

[24] Taylor D, Stradling G, Hengé-Napoli M (2000). The scientific background to decorporation. Radiation Protection Dosimetry. 87, 11–8.

[25] Stradling G, Taylor D, Hengé-Napoli M, Wood R, Silk T (2000). Treatment for actinide-bearing industrial dusts and aerosols. Radiat Prot Dosim. 87, 41–50.

[26] US Food and Drug Administration (2015). Questions and answers on calcium-DTPA and zinc-DTPA (Updated)

[27] R Bailey B, Eckerman K, Townsend L (2003). An analysis of a puncture wound case with medical intervention. Radiation protection dosimetry. 105, 509-512.

[28] Stather J, Stradling G, Smith H (1982). Decorporation of 238 PuO 2 from the hamster by inhalation of chelating agents. Health physics. 42, 520-525.

[29] Grémy O, Tsapis N, Bruel S, Renault D, Van der Meeren A (2012). Decorporation approach following rat lung contamination with a moderately soluble compound of plutonium using local and systemic Ca-DTPA combined chelation. Radiation research. 178, 217-223.

[30] Fukuda S, Iida H (1987). Toxicological study of DTPA as a drug (III) Side effects of orally administered Zn-DTPA to beagles. Japanese Journal of Health Physics. 22, 439-444.

[31] Fukuda S, Iida H, Heish Y, Chen W (1990). Toxicological study of DTPA as a Drug (V): Toxicities of Ca-DTPA, Ca-EDTA and CBMIDA after Intravenous injection in beagle dogs. JJHP 25, 115-119.

[32] Zhang Y, Sadgrove M, Mumper R, Jay M (2013). Radionuclide decorporation: matching the biokinetics of actinides by transdermal delivery of pro-chelators. The AAPS journal. 15, 1180-1188.

[33] Stevens E, Rosoff B, Weiner M, Spencer H (1962). Metabolism of the chelating agent diethylenetriamine pentaacetic acid (C14DTPA) in man. Proceedings of the Society for Experimental Biology and Medicine.111, 235-238.

[34] Durbin P (2008). Lauriston S. Taylor Lecture: the quest for therapeutic actinide chelators. Health physics. 95, 465-492.

[35] Bulman R, Griffin R, Russell A (1979). An examination of some complexing agents for the ability to remove intracellularly deposited plutonium. Health physics. 37, 729-734.

[36] Stradling G, Stather J, Sumner S, Moody J, Strong J (1984). Decorporation of inhaled americium-241 dioxide and nitrate from hamsters using ZnDTPA and Puchel. Health physics. 46, 1296-1300.

[37] Volf V, Peter E (1984). DTPA is superior to its lipophilic derivative Puchel in removing ^{234}Th, ^{238,239} Pu and ^{241}Am from Chinese hamsters and rats. Health physics. 46, 422.

[38] Bruenger F, Kuswik-Rabiega G, Miller S (1992). Decorporation of aged americium deposits by oral administration of lipophilic polyamine carboxylic acids. Journal of medicinal chemistry. 35 112-118.

[39] Shankar G, Potharaju S, Green C (2014). Evaluating the Toxicity of Novel Z n-DTPA Tablet Formulation in Dogs and Rats. Drug development research. 75, 37-46.

[40] Reddy J, Cobb R, Dungan N, Matthews L, Aiello K et al (2012). Preclinical toxicology, pharmacology, and efficacy of a novel orally administered diethylenetriaminepentaacetic acid (DTPA) formulation. Drug Development Research. 73, 232-242.

[41] Wilson J, Cobb R, Dungan N, Matthews L, Eppler B (2015). Decorporation of systemically distributed americium by a novel orally administered diethylenetriaminepentaacetic acid (DTPA) formulation in beagle dogs. Health physics. 108, 308-318.

[42] Phan G, Gall B, Manceau J, Fanet M, Benech H et al (2004). Targeting of diethylene triamine pentaacetic acid encapsulated in liposomes to rat liver: an effective strategy to prevent bone deposition and increase urine elimination of plutonium in rats. International Journal of Radiation Biology. 80, 413-22.

[43] Phan G, Le Gall B, Grillon G, Rouit E, Fouillit M et al (2006). Enhanced decorporation of plutonium by DTPA encapsulated in small PEG-coated liposomes. Biochimie. 88, 1843-1849.

[44] Phan G, Herbet A, Cholet S, Benech H, Deverre J et al (2005). Pharmacokinetics of DTPA entrapped in conventional and long-circulating liposomes of different size for plutonium decorporation. Journal of controlled release. 110, 177-188.

[45] Keuth J, Nitschke Y, Mulac D, Riehemann K, Rutsch F et al (2020). Reversion of arterial calcification by elastin-targeted DTPA-HSA nanoparticles. European Journal of Pharmaceutics and Biopharmaceutics.

[46] Sabu C, Pramod K (2020). Advanced Nanostructures for Oral Insulin Delivery. In Nanoscience in Medicine Vol. 1 (pp. 187-212). Springer, Cham.

[47] Zhang L, Liu T, Xiao Y, Yu D, Zhang N (2015). Hyaluronic acid-chitosan nanoparticles to deliver Gd-DTPA for MR cancer imaging. Nanomaterials. 5, 1379-1396.

[48] Martínez Martínez T, García Aliaga Á, López González I, Abellá Tarazona A, Ibañez Ibañez M et al (2020). Fluorescent DTPA-Silk Fibroin Nanoparticles Radiolabeled with ^{111}In: a Dual Tool for Biodistribution and Stability Studies. ACS Biomaterials Science & Engineering.

[49] Perrie Y, Rades T (2012). FASTtrack Pharmaceutics: Drug Delivery and Targeting. Pharmaceutical press.

[50] Zuo Z, Lee V (2007). Controlled drug delivery: Pharmacokinetic considerations, methods and
systems. Wiley Encyclopedia of Chemical Biology. 1-10.

[51] Kaur G, Grewal J, Jyoti K, Jain U, Chandra R et al (2018). Oral controlled and sustained drug delivery systems: Concepts, advances, preclinical, and clinical status. In Drug Targeting and Stimuli Sensitive Drug Delivery Systems (pp. 567-626). William Andrew Publishing.

[52] Patel J, Patel A (2016). Artificial neural networking in controlled drug delivery. In Artificial Neural Network for Drug Design, Delivery and Disposition (pp. 195-218). Academic Press.

[53] Chen E, Liu W, Megido L, Díez P, Fuentes M et al (2018). Understanding and utilizing the biomolecule/nanosystems interface. In Nanotechnologies in Preventive and Regenerative Medicine (pp. 207-297). Elsevier.

[54] Raja M, Lim P, Wong Y, Xiong G, Zhang Y et al (2019). Polymeric Nanomaterials: Methods of Preparation and Characterization. In Nanocarriers for Drug Delivery (pp. 557-653). Elsevier.

[55] Zhang X, Cresswell M (2015). Inorganic Controlled Release Technology: Materials and Concepts for Advanced Drug Formulation. Butterworth-Heinemann.

[56] Mehtani D, Seth A, Sharma P, Maheshwari N, Kapoor D et al (2019). Biomaterials for Sustained and Controlled Delivery of Small Drug Molecules. In Biomaterials and Bionanotechnology (pp. 89-152). Academic Press.

[57] Siegel R, Rathbone M (2012). Overview of controlled release mechanisms. In Fundamentals and applications of controlled release drug delivery (pp. 19-43). Springer, Boston, MA.

[58] D'Souza, S (2014). A review of in vitro drug release test methods for nano-sized dosage forms. Advances in Pharmaceutics.2014.

[59] Heng D, Cutler D, Chan H, Yun J, Raper J et al (2008). What is a suitable dissolution method for drug nanoparticles? Pharmaceutical Research. 25, 1696-1701.

[60] Shen J, Burgess D (2013). In Vitro Dissolution Testing Strategies for Nanoparticulate Drug Delivery Systems: Recent Developments and Challenges. Drug delivery and translational research. 3, 409–415.

[61] Chidambaram N, Burgess D (1999). A novel in vitro release method for submicron-sized dispersed systems. AAPS PharmSciTech. 1, 32-40.

[62] Xu X, Khan M, Burgess D (2012). A two-stage reverse dialysis in vitro dissolution testing method for passive targeted liposomes. International journal of pharmaceutics. 426, 211-218.

[63] Hua S. (2014). Comparison of in vitro dialysis release methods of loperamide-encapsulated liposomal gel for topical drug delivery. International journal of nanomedicine. 9, 735–744.

[64] Haney P, Herting K, Smith S (2013). Molecular weight cut-off (MWCO) specifications and rates of buffer exchange with Slide-A-Lyzer Dialysis Devices and Snakeskin Dialysis Tubing. Thermo Fischer Scientific. 4, 100.

[65] Tangri P, Khurana S (2011). Approaches to pulmonary drug delivery systems. International Journal of Pharmaceutical Sciences and Research. 2, 1616.

[66] Patil J, Sarasija S (2012). Pulmonary drug delivery strategies: A concise, systematic review. Lung India: Official Organ of Indian Chest Society. 29, 44.

[67] Nikolić V, Ilić-Stojanović S, Petrović S, Tačić A, Nikolić, L (2019). Administration routes for nano drugs and characterization of nano drug loading. In Characterization and Biology of Nanomaterials for Drug Delivery (pp. 587-625). Elsevier.

[68] Abdelaziz H, Freag M, Elzoghby A (2019). Solid Lipid Nanoparticle-Based Drug Delivery for Lung Cancer. In Nanotechnology-Based Targeted Drug Delivery Systems for Lung Cancer (pp. 95-121). Academic Press.

[69] Ingle A, Shende S, Pandit R, Paralikar P, Tikar S et al (2016). Nanotechnological applications for the control of pulmonary infections. In The Microbiology of Respiratory System Infections (pp. 223-235). Academic Press.

[70] Lizio R, Klenner T, Borchard G, Romeis P, Sarlikiotis A et al (2000). Delivery of the GnRH antagonist centrolix by intratracheal instillation in Anesthetized rats. European Journal of Pharmaceutical Sciences. 9, 253–8.

[71] Yurdasiper A, Arıcı M, Ozyazici M (2018). Nanopharmaceuticals: Application in inhaler systems. In Emerging Nanotechnologies in Immunology (pp. 165-201). Elsevier.

[72] Paranjpe M, Müller-Goymann C (2014). Nanoparticle-mediated pulmonary drug delivery: a review. International Journal of Molecular Sciences. 15, 5852-5873.

[73] Gupta R, Xie H (2018). Nanoparticles in daily life: applications, toxicity and regulations. Journal of Environmental Pathology, Toxicology and Oncology. 37, 209-230.

[74] Rizvi S, Saleh A (2018). Applications of nanoparticle systems in drug delivery technology. Saudi Pharmaceutical Journal. 26, 64-70.

[75] Yadav H, Almokdad A, Sumia I, Debe M (2019). Polymer-based nanomaterials for drug-delivery carriers. In Nanocarriers for Drug Delivery (pp. 531-556). Elsevier.

[76] Minelli C, Sikora A, Garcia-Diez R, Sparnacci K, Gollwitzer C (2018). Measuring the size and density of nanoparticles by centrifugal sedimentation and flotation. Analytical Methods. 10, 1725-1732.

[77] Toy R, Hayden E, Shoup C, Baskaran H, Karathanasis E (2011). The effects of particle size, density and shape on margination of nanoparticles in microcirculation. Nanotechnology. 22, 115101.

[78] Kumar B, Jalodia K, Kumar P, Gautam H (2017). Recent advances in nanoparticle-mediated drug delivery. Journal of Drug Delivery Science and Technology. 41, 260-268.

[79] Mu Q, Jiang G, Chen L, Zhou H, Fourches D et al (2014). Chemical basis of interactions between engineered nanoparticles and biological systems. Chemical Reviews.114, 7740-7781.

[80] Prokop A, Davidson J (2008). Nanovehicular intracellular delivery systems. Journal of Pharmaceutical Sciences. 97, 3518-3590.

[81] Panyam J, Labhasetwar V (2003). Biodegradable nanoparticles for drug and gene delivery to cells and tissue. Advanced Drug Delivery Reviews. 55, 329-347.

[82] Bantz C, Koshkina O, Lang T, Galla H, Kirkpatrick C et al (2014). The surface properties of nanoparticles determine the agglomeration state and the size of the particles under physiological conditions. Beilstein Journal of Nanotechnology. 5, 1774-1786.

[83] Kou L, Sun J, Zhai Y, He Z (2013). The endocytosis and intracellular fate of nanomedicines: Implication for rational design. Asian Journal of Pharmaceutical Sciences. 8, 1-10.

[84] Suk J, Xu Q, Kim N, Hanes J, Ensign L (2016). PEGylation as a strategy for improving nanoparticle-based drug and gene delivery. Advanced Drug Delivery Reviews. 99, 28-51.

[85] Choi J, Seo K, Yoo J (2012). Recent advances in PLGA particulate systems for drug delivery. Journal of Pharmaceutical Investigation. 42, 155-163.

[86] Du Y, Ren W, Li Y, Zhang Q, Zeng L et al (2015). The enhanced chemotherapeutic effects of doxorubicin loaded PEG coated TiO 2 nanocarriers in an orthotopic breast tumor bearing mouse model. Journal of Materials Chemistry B. 3, 1518-1528.

[87] Suarez S, O'Hara P, Kazantseva M, Newcomer C, Hopfer R et al (2001). Respirable PLGA microspheres containing rifampicin for the treatment of tuberculosis: screening in an infectious disease model. Pharmaceutical Research. 18. 1315-1319.

[88] Rudokas M, Najlah M, Alhnan M, Elhissi A (2016). Liposome delivery systems for inhalation: a critical review highlighting formulation issues and anticancer applications. Medical Principles and Practice. 25, 60-72.

[89] Pitt J (2009). Principles and applications of liquid chromatography-mass spectrometry in clinical biochemistry. The Clinical Biochemist Reviews. 30, 19.

[90] Kang J (2012). Principles and applications of LC-MS/MS for the quantitative bioanalysis of analytes in various biological samples. Tandem Mass Spectrometry–Applications and Principles, 441-492.

[91] Sudhakar P, Latha P, Reddy P (2016). Phenotyping crop plants for physiological and biochemical traits. Academic Press.

[92] Kumar P, Dinesh S, Rini R (2016). LCMS—a review and a recent update. The Journal of Pharmacy and Pharmaceutical Sciences. 5, 377-391.

[93] Korfmacher W (2005). Foundation review: principles and applications of LC-MS in new drug discovery. Drug discovery today. 10, 1357-1367.

[94] Kontogianni V (2014). Novel techniques towards the identification of different classes of polyphenols. In Polyphenols in Plants (pp. 159-185). Academic Press.

[95] https://www.agilent.com/cs/library/support/documents/a05296.pdf

[96] http://www.ecs.umass.edu/eve/background/methods/chemical/Openlit/Chromacademy%20LCMS%20Intro.pdf

[97] Crutchfield C, Lu W, Melamud E, Rabinowitz J (2010). Mass spectrometry-based metabolomics of yeast. In Methods in enzymology (Vol. 470, pp. 393-426). Academic Press.

[98] Brandt A, Meeßen J, Jänicke R, Raguse M (2017). Simulated space radiation: impact of four different types of high-dose ionizing radiation on the lichen Xanthoria elegans. Astrobiology. 17, 136-144.

[99]Azzam E, Jay-Geran J, Pain D (2012). Ionizing radiation-induced metabolic oxidative stress and prolonged cell injury. Cancer Letters. 327(1-2): 48-60.

[100] Panganiban R, Snow A, Day R (2013). Mechanisms of Radiation Toxicity in Transformed and Non-Transformed Cells. The International Journal of Molecular Sciences. 14, 15931-15958.

[101] Gebicki J (2016). Oxidative stress, free radicals and protein peroxides. Archives of Biochemistry and Biophysics. 595, 33-39.

[102] U.S. Department of Health and Human Services: Calcium-DTPA and Zinc-DTPA Information Page. [https://www.fda.gov/drugs/emergencypreparedness/bioterrorismanddrugpreparedness/ucm130311.htm (accessed September 23, 2016)]

[103] Chen S, Lai EPC, Ko R, Li CS, Wyatt H (2016). Inhalable Chitosan Tripolyphosphate Nanoparticles for Extended Release of DTPA into Lung Fluid. Nanomedicine: Nanotechnology, Biology and Medicine. 1, 000106.

[104] Aime S, Caravan P (2009). Biodistribution of gadolinium-based contrast agents, including gadolinium deposition. Journal of Magnetic Resonance Imaging. 30, 1259-1267.

[105] Sorour M, Hani H, Shaalan H, El-Sayed M (2016). Experimental screening of some chelating agents for calcium and magnesium removal from saline solutions. Desalination and water Treatment. 57, 22799-22808.

[106] Gervelas C, Serandour A, Geiger S, Grillon G, Fritsch P (2007). Direct lung delivery of a dry powder formulation of DTPA with improved aerosolization properties: effect on lung and systemic decorporation of plutonium. The Journal of Controlled Release. 118, 78-86.

[107] Patel A, Woods A, Riffo-Vasquez Y, Babin-Morgan A, Jones M, et al (2016). Lung inflammation does not affect the clearance kinetics of lipid nanocapsules following pulmonary administration. Journal of Controlled Release. 235, 24–33.

[108] Wang A, Marinakos S, Badireddy A, Powers C, Houck K (2013). Characterization of physicochemical properties of nanomaterials and their immediate environments in high-throughput screening of nanomaterial biological activity. WIREs Nanoscience and Nanotechnology. 5, 430-448.

[109] Choi H, Stathatos E, Dionysiou D (2006). Solgel preparation of mesoporous photocatalytic TiO2 films and TiO2/Al2O3 composite membranes for environmental applications. Applied Catalysis B. 63, 60-67.

[110] Aitken R, Chaudhry M, Boxall A, Hull M (2006). Manufacture and use of nanomaterials: current status in the UK and global trends. Occupational Medicine. 56, 300–306.

[111] Briffa S, Lynch L, Trouillet V, Bruns B, Hapiuk, D, et al (2017). Development of scalable and versatile nanomaterial libraries for nanosafety studies: polyvinylpyrrolidone (PVP) capped metal oxide nanoparticles. RSC Advances. 7, 3894-3906.

[112] Yin Z, Wu L, Yang H, Su H (2013). Recent progress in biomedical applications of titanium dioxide. Physical Chemistry Chemical Physics.15, 4844-4858.

[113] Heredia-Cervera E, González-Azcorra S, Rodríguez-Gattorno R, López T, Ortiz-Islas E, et al (2009). Controlled Release of Phenytoin from Nanostructured TiO2 Reservoir. Science of Advanced Materials. 1, 63-68.

[114] Uddin M, Mondal D, Morris C, Lopez U, Diebold R, et al (2011). An in vitro controlled release study of valproic acid encapsulated in a titania ceramic matrix. Applied Surface Science. 257, 7920-7927.

[115] Qin L, Sun X, Li Q, Cao H, Wang X, et al (2011). Highly water-dispersible TiO2 nanoparticles for doxorubicin delivery: effect of loading mode on therapeutic efficacy. The Journal of Materials Chemistry. 21, 18003-18010.

[116] Wu T, Yamauchi C, Hong Y, Yang Y, Liang T, Funatsu T, et al (2011). Biocompatible, surface functionalized mesoporous titania nanoparticles for intracellular imaging and anticancer drug delivery. Chemical Communications. 47, 5232-5234.

[117] Peters R, Bemmel V, Herrera R, Helsper J, Marvin H, et al (2014). Characterization of Titanium Dioxide Nanoparticles in Food Products: Analytical Methods To Define Nanoparticles. The Journal of Agricultural and Food Chemistry. 62, 6285-6293.

[118] Diasanayakea B, Senadeeraa C, Sarangikaa B, Ekanayakea C, Thotawattagea B, et al (2016). TiO2 as a low cost, multi functional material. Materials Today: Proceedings. 3, S40-S47.

[119] Kaida K, Kobayashi M, Adachi A, Suzuki F (2004). Optical characteristics of titanium oxide interference film and the film laminated with oxides and their application for cosmetics. Journal of Cosmetic Science. 55, 219-220.

[120] Hongbo S, Magaye R, Castranova V, Zhao J (2013). Titanium_dioxide_nanoparticles: a review of current toxicological data. Particle and Fibre Toxicology. 10, 15.

[121] Genç L, Kutlu H, Guney G (2015). Vitamin B12-loaded solid lipid nanoparticles as a drug carrier in cancer therapy. Pharmaceutical Development and Technology. 20, 337-344.

[122] Gosecki M, Gadzinowski M, Gosecka M, Basinska T, Slomkowski S (2016). Polyglycidol, Its Derivatives, and Polyglycidol-Containing Copolymers—Synthesis and Medical Applications. Polymers. 8, 227.

[123] Sawhney A, Pathak C, Hubbell J (1993). Interfacial photopolymerization of poly(ethylene glycol)-based hydrogels upon alginate poly(L-lysine) microcapsules for enhanced biocompatibility. Biomaterials. 14, 1008–1016.

[124] Cui Y, Liu H, Zhou M, Duan Y, Li N, et al (2011). Signaling pathway of inflammatory responses in the mouse liver caused by TiO2 nanoparticles. Journal of Biomedical Materials Research A. 96A, 221-229.

[125] Pan, Z, Lee W, Slutsky L, Clark R, Pernodet N, et al (2009). Adverse effects of titanium dioxide nanoparticles on human dermal fibroblasts and how to protect cells. Small. 5, 511–520.

[126] Venkatasubbu G, Ramasamy S, Ramakrishnan V, Kumar J (2013). Folate targeted PEGylated titanium dioxide nanoparticles as a nanocarrier for targeted paclitaxel drug delivery. Advanced Powder Technology. 24, 947-954.

[127] Steele T, Huang C, Widjaja E, Boey F, Loo J, et al (2011). The effect of polyethylene glycol structure on paclitaxel drug release and mechanical properties of PLGA thin films. Acta Biomaterialia. 7,1973-1983.

[128] Alsudir S, Lai E (2017). Selective detection of ZnO nanoparticles in aqueous suspension by capillary electrophoresis analysis using dithiothreitol and L-cysteine adsorbates. Talanta. 169,115-122.

[129] Marques M, Loebenberg R, Almukainzi M (2011). Simulated biological fluids with possible application in dissolution testing. Dissolution Technologies. 18, 15-28.

[130] Sato H, Kubota Y, Takahashi S, Matsuoka O (1989). Effects of H_5-DTPA and Ca-DTPA on the Removal of ^{59}Fe from Rats Injected with ^{59}Fe-iron Dextran. Hoken Butsuri. 24, 109-114.

[131] Miller S, Wang X, Bowman B (2010). Pharmacological properties of orally available, amphipathic polyaminocarboxylic acid chelators for actinide decorporation. Health Physics. 99, 408-412.

[132] Zhou S, Zhang B, Sturm E, Teagarden D, Schöneich C (2010). Comparative evaluation of disodium edetate and diethylenetriaminepentaacetic acid as iron chelators to prevent metal -catalyzed destabilization of a therapeutic monoclonal antibody. The Journal of Pharmaceutical Sciences. 99, 4239-4250.

[133] Siepmann F, Muschert S, Flament M, Leterme P, Gayot A (2006). Controlled drug release from Gelucire-based matrix pellets: experiment and theory. The International Journal of Pharmaceutics. 317, 136-143.

[134] Vora A, Rega A, Dollimore D, Alexander K (2002). Thermal Stability of folic acid. Thermochem.392, 209-220.

[135] Hastings C, Roched E, Ruiz-Hernandez E, Schenke-Laylandf K, Walsh C J, et al (2015). Drug and cell delivery for cardiac regeneration. Advanced Drug Delivery Reviews. 84, 85-106.

[136] Barbosa G, Silva P, Luz G, Brasil L (2015). Nanotechnology applied in drug delivery, World Congress on Medical Physics and Biomedical Engineering, Toronto, IFMBE Proceedings. 51, 911.

[137] Stoicea N, Fiorda J, Joseph N, Shabsigh M, Arias C, et al (2017). Advanced Analgesic Drug Delivery and Nanobiotechnology. 77, 1069-1076.

[138] Maudens P, Seemayer C, Thauvin C, Gabay C, Jordan O, et al (2018). Nanocrystal–Polymer Particles: Extended Delivery Carriers for Osteoarthritis Treatment. Small. 14, 1703108.

[139] Soppimath K, Aminabhavi T, Kulkarni A, Rudzinski W (2001). Biodegradable polymeric nanoparticles as drug delivery devices. Journal of Controlled Release. 70, 1-20.

[140] Lee, J (2014). Nanoparticle-assisted controlled drug release. Journal of Nanomedicine and Biotherapeutic Discovery. 4, 133.

[141] Sharma N, Madan P, Lin S (2016). Effect of process and formulation variables on thepreparation of parenteral paclitaxel-loaded biodegradablepolymeric nanoparticles: A co-surfactant study. Asian Journal of Pharmaceutical Sciences. 11, 404-416.

[142] Makadial H, Siegel S (2011). Poly lactic-co-glycolic acid as biodegradable controlled drug delivery carrier. Polymers. 3, 1377-1397.

[143] Héloïse R, Fabienne D, Véronique P, Robert L, Daniel G (2017). Nanoparticle-based drug delivery systems: a commercial and regulatory outlook as the field matures. Journal Expert Opinion on Drug Delivery. 14, 851-864.

[144] Shweta S, Ankush P, Shivpoojan K, Rajat S (2016). PLGA-based Nanoparticles: A New Paradigm in Biomedical Applications.Trends in Analytical Chemistry. 80, 30-40

[145] Hines D, Kaplan D (2013). Poly (lactic-co-glycolic acid) controlled release systems: experimental and modeling insights. Critical Review Drug Carrier Systems. 3, 257-276.

[146] Zohreh H, Fatemeh A, Ahad M, Mohammad R, Maryam H (2016). Evaluation of anti-cancer activity of PLGA nanoparticles containing crocetin. Artificial Cells, Nanomedicine, and Biotechnology. 45, 955-960.

[147] McCall R, Sirianni R (2013). PLGA nanoparticles formed by single-or double-emulsion with vitamin E-TPGS. Journal of Visualized Experiments. (82), e51015.

[148] Yadav R, Ali M, Kumar A, Pandey B (2017). Mechanism of carcinogenesis after exposure of actinide radionuclides. Journal of Radiation and Cancer Research. 8, 20-34.

[149] Gilbert E (2009). Ionizing Radiation and Cancer Risks: What Have We Learned From Epidemiology. International Journal of Radiation Biology. 85, 467-482.

[150] Ansoborlo E, Prat O, Moisy P, Den C, Auwer P, et al (2006). Actinide speciation in relation to biological processes. Biochimie. 88, 1605-1618.

[151] Gorden A, Xu J, Raymond K, Durbin P (2003). Rational design of sequestering agents for plutonium and other actinides. Chemical Reviews.103, 4207-4282.

[152] Centers for Disease Control and Prevention. Emergency Preparedness and Response: DTPA. http://emergency.cdc.gov/radiation/dtpa.asp(accessed Sep 23, 2016)

[153] Oliveri V, Vecchio G (2016). Prochelator strategies for site-selective activation of metal chelators. Journal of Inorganic Biochemistry.162, 31-43.

[154] Flora S, Pachauri V (2010). Chelation in Metal Intoxication. International Journal of Environmental Research and Public Health. 7, 2745-2788.

[155] Rump A, Stricklin D, Lamkowski A, Eder S, Abend M, et al (2017). Advances in The Incorporation of Radionuclides After Wounding by a "Dirty Bomb": The Impact of Time for Decorporation Efficacy and a Model for Cases of Disseminated Fragmentation Wounds. Advances in Wound Care. 6,1-9.

[156] Grémy O, Laurent D, Coudert S, Griffiths N, Miccoli L (2016). Decorporation of Pu/Am Actinides by Chelation Therapy: New Arguments in Favor of an Intracellular Component of DTPA Action. Radiation Research. 185, 568-579.

[157] Konzen K, Brey R (2015). Development of the plutonium-DTPA biokinetic model. Health Physics. 108, 565-573.

[158] Lee W, Loo C, Traini D, Young P (2015). Inhalation of nanoparticle-based drug for lung cancer treatment: Advantages and challenges. Asian journal of pharmaceutical sciences.10, 481-489.

[159] Capstick T, Clifton I (2012). Inhaler Technique and Training in People with Chronic Obstructive Pulmonary Disease and Asthma: Effects of Particle Size on Lung Deposition. Expert Review of Respiratory Medicine. 6, 91-103.

[160] Tena A, Clarà P (2012). Deposition of Inhaled Particles in the Lungs. Archivos de Bronconeumogia. 48, 240-246.

[161] Tsapis N (2014). Spray-drying from fundamentals to pulmonary administration of therapeutic molecules. Review Farmacologia de Chile. 7, 33-40.

[162] Bhatia J (2015). New model tackles sticky problem of getting drugs past mucus. Nature Medicine. 21, 301.

[163] Lai S, Wang Y, Hanes J (2009). Mucus-penetrating nanoparticles for drug and gene delivery to mucosal tissues. Advanced Drug Delivery Reviews. 61,158-171.

[164] Yu T, Wang Y, Y M, Schneider C, Zhong W, et al (2012). Biodegradable mucus-penetrating nanoparticles composed of diblock copolymers of polyethylene glycol and poly (lactic-co-glycolic acid). Drug Delivery and Translational Research. 2, 124-128.

[165] Modi S, Anderson B (2013). Determination of drug release kinetics from nanoparticles: overcoming pitfalls of the dynamic dialysis method. Molecular Pharmaceutics. 10, 3076–3089.

[166] Van Eerdenbrugh, Alonzo D, Taylor L (2011). Influence of particle size on the ultraviolet spectrum of particulate-containing solutions: implications for in-situ

concentration monitoring using UV/vis fiber-optic probes. Pharmaceutical Research. 28, 1643-1652.

[167] Xie L, Beyer S, Vogela V, Wacker M, Mantele W (2015). Assessing the drug release from nanoparticles: Overcoming the shortcomings of dialysis by using novel optical techniques and a mathematical model. International Journal of Pharmaceutics. 488, 108-119.

[168] Zambito Y, Pedreschi E, Di Colo G (2012). Is dialysis a reliable method for studying drug release from nanoparticulate systems?—A case study. International Journal of Pharmaceutics. 434, 28-34

[169] Sethi M, Sukumar R, Karve S, Werner M, Wang E, et al (2014). Effect of drug release kinetics on nanoparticle therapeutic efficacy and toxicity. Nanoscale. 6, 2321-2327.

[170] Liu J, Qiu Z, Wang S, Zhou L, Zhang S (2010). A modified double-emulsion method for the preparation of daunorubicin-loaded polymeric nanoparticle with enhanced in vitro anti-tumor activity. Biomedical Materials. 5, 10.

[171] Garcia M, Foged C, Nielsen HM (2015). Improved insulin loading in poly(lactic-co-glycolic) acid (PLGA) nanoparticles upon self-assembly with lipids. International Journal of Pharmaceutics. 482, 84–91.

[172] Quintana J, Reemtsma T (2007). Rapid and sensitive determination of ethylenediaminetetraacetic acid and diethylenetriaminepentaacetic acid in water samples by ion-pair reversed-phase liquid chromatography–electrospray tandem mass spectrometry. Journal of Chromatography A. 1145, 110-116.

[173] Wang G, Tomasella F (2016). Ion-pairing HPLC methods to determine EDTA and DTPA in small molecule and biological pharmaceutical formulations. Journal of Pharmaceutical Analysis. 6, 150-156.

[174] Lim Y, Tiemann K, Hunstad D, Elsabahy M, Wooley K (2016). Polymeric Nanoparticles in Development for Treatment of Pulmonary Infectious Diseases. Nanomedicine and Nanobiotechnology. 8, 842–871.

[175] Fredenberga S, Wahlgrenb M, Reslowc M, Axelssona A (2011). The mechanisms of drug release in poly (lactic-co-glycolic acid)-based drug delivery systems—A review. International Journal of Pharmaceutics. 415, 34-52.

[176] Danhier F1, Ansorena E, Silva JM, Coco R, Le Breton A, et al (2012). PLGA-based nanoparticles: an overview of biomedical applications. Journal of Controlled Release. 161, 505-22.

[177] Tang J, Li J, Li G, Zhang H, Wang L, Li D, Ding J (2017). Spermidine-mediated poly (lactic-co-glycolic acid) nanoparticles containing fluorofenidone for the treatment of idiopathic pulmonary fibrosis. International Journal of Nanomedicine. 12 6687–6704.

[178] Haji Mansor M, Najberg M, Contini A, Alvarez-Lorenzo C, Garcion E, et al (2018). Development of a non-toxic and non-denaturing formulation process for encapsulation of SDF-1α into PLGA/PEG-PLGA nanoparticles to achieve sustained release. European Journal of Pharmaceutics and Biopharmaceutics. 125, 38-50.

[179] Swed A, Cordonnier T, Dénarnaud A, Boyer C, Guicheux J, et al (2015). Sustained release of TGF-β1 from biodegradable microparticles prepared by a new green process in CO_2 medium. International Journal of Pharmaceutics. 493, 357-65.

[180] Roberts RA, Shen T, Allen IC, Hasan W, DeSimone JM, et al (2013). Analysis of the murine immune response to pulmonary delivery of precisely fabricated nano- and microscale particles. PLoS One. 8, e62115.

[181] Kothalawala N, Mudalige T, Sisco P, Linder S Novel analytical methods to assess the chemical and physical properties of liposomes. Journal of Chromatography B. 2018, 1091, 14-20.

[182] Has C, Sunthar P. A. comprehensive review on recent preparation techniques of liposomes. Journal of Liposome Research. 2019, 29, 1-30.

[183] Soema P, Willems G, Jiskoot W, Amorij J, Kersten G. Predicting the influence of liposomal lipid composition on liposome size, zeta potential and liposome-induced dendritic cell maturation using a design of experiments approach. European Journal of Pharmaceutics and Biopharmaceutics. 2015, 94, 427-435.

[184] Li J, Wang X, Zhang T, Wang C, Huang Z et al. A review on phospholipids and their main applications in drug delivery systems. Asian Journal of Pharmaceutical Sciences. 2015, 10, 81-98.

[185] Akbarzadeh A, Rezaei-Sadabady R, Davaran S, Joo S, Zarghami N. Liposome: classification, preparation, and applications. Nanoscale Research Letters. 2013, 8,102.

[186] Shehata T, Ogawara K, Higaki K, Kimura T. Prolongation of residence time of liposome by surface-modification with mixture of hydrophilic polymers. International Journal of Pharmaceutics. 2008, 359, 272-279.

[187] Pradeep P, Manisha S, Monica Amala Nayaki J, Sivaraman D, Selvaraj R et al. Potential antioxidant and anti-inflammatory action of Hypericum hookerianum extracts in a liposome system evaluated with zebrafish embryos. Journal of microencapsulation. 2019, 36, 513-522.

[188] Oskoueian E, Karimi E, Noura R, Ebrahimi M, Shafaei N et al. Nanoliposomes encapsulation of enriched phenolic fraction from pistachio hulls and its antioxidant, anti-inflammatory, and anti-melanogenic activities. Journal of microencapsulation. 2020, 37, 1-13.

[189] Ghorbanzade T, Jafari S, Akhavan S, Hadavi R. Nano-encapsulation of fish oil in nano-liposomes and its application in the fortification of yogurt. Food Chemistry. 2017, 216, 146-152.

[190] Xia S, Tan C, Zhang Y, Abbas S, Feng B. Modulating effect of lipid bilayer–carotenoid interactions on the property of liposome encapsulation. Colloids and Surfaces B: Biointerfaces. 2015, 128,172-180.

[191] Yalcin T, Ilbasmis-Tamer S, Ibisoglu B, Ozdemir A, Ark M et al. Gemcitabine hydrochlorideloaded liposomes and nanoparticles: comparison of encapsulat ion efficiency, drug release, particle size, and cytotoxicity. Pharmaceutical Development and Technology. 2018, 23, 76-86.

[192] Taylor T, Weiss J, Davidson P, Bruce B. Liposomal nanocapsules in food science and agriculture. Critical Reviews in Food Science and Nutrition. 2005, 45, 587-605.

[193] Chan J, Zhang L, Yuet K, Liao G, Rhee J et al. PLGA–lecithin–PEG core-shell nanoparticles for controlled drug delivery. Biomaterials. 2009, 30, 1627-1634.

[194] Zhan C, Santamaria C, Wang W, McAlvin J, Kohane D. Long-acting liposomal corneal anaesthetics. Biomaterials. 2018, 181, 372-377.

[195] Ortega V, Giorgio S, de Paula E. Liposomal formulations in the pharmacological treatment of leishmaniasis: a review. Journal of Liposome Research. 2017, 27, 234-248.

[196] Çoban Ö, Değim Z, Yılmaz Ş, Altıntaş L, Arsoy T et al. Efficacy of targeted liposomes and nanocochleates containing imatinib plus dexketoprofen against fibrosarcoma. Drug development research. 2019, 80, 556-565.

[197] Adu-Frimpong M, Firempong C, Omari-Siaw E, Wang Q, Mukhtar Yet al (2019). Preparation, optimization, and pharmacokinetic study of nanoliposomes loaded with triacylglycerol-bound punicic acid for increased antihepatotoxic activity. Drug development research. 80, 230-245.

[198] Jahadi M, Khosravi-Darani K. Liposomal encapsulation enzymes: from medical applications to kinetic characteristics. Mini-reviews in Medicinal Chemistry.2017, 17, 366-370.

[199] Silva-Weiss A, Quilaqueo M, Venegas O, Ahumada M, Silva W. Design of dipalmitoyl lecithin liposomes loaded with quercetin and rutin and their release kinetics from carboxymethyl cellulose edible films. Journal of Food Engineering. 2018, 224,165-173.

[200] Emami S, Azadmard-Damirchi S, Peighambardoust S, Valizadeh H, Hesari J. Liposomes as carrier vehicles for functional compounds in the food sector. Journal of Experimental Nanoscience. 2016, 11, 737-759.

[201] Belfiore L, Saunders D, Ranson M, Thurecht K, Storm G et al. Towards clinical translation of ligand-functionalized liposomes in targeted cancer therapy: challenges and opportunities. Journal of Controlled Release. 2018, 277,1-13.

[202] Barenholz Y. Doxil® — the first FDA-approved nano-drug: Lessons learned. Journal of Controlled Release. 2012,160,117-134.

[203] McAlvin J, Padera R, Shankarappa S, Reznor G, Kwon A. Multivesicular liposomal bupivacaine at the sciatic nerve. Biomaterials. 2014, 35, 4557-4564.

[204] Silverman J, Deitcher S. Marqibo® (vincristine sulfate liposome injection) improves the pharmacokinetics and pharmacodynamics of vincristine. Cancer Chemotherapy and Pharmacology. 2013, 71, 555-564.

[205] Franco M, Oliveira M. Liposomes co-encapsulating anticancer drugs in synergistic ratios as an approach to promote increased efficacy and greater safety. Anti-Cancer Agents Med Chem. 2019, 19, 17-28.

[206] Chang H, Yeh M. Clinical development of liposome-based drugs: formulation, characterization, and therapeutic efficacy. International Journal of Nanomedicine. 2011, 7, 49-60.

[207] Hajdo L, Szulc A, Klajnert B, Bryszewska M. Metabolic limitations of the use of nucleoside analogs in cancer therapy may be overcome by application of nanoparticles as drug carriers: A review. Drug Development Research. 2010, 71, 383-394.

[208] Singh S. Liposome encapsulation of doxorubicin and celecoxib in combination inhibits the progression of human skin cancer cells. International Journal of Nanomedicine. 2018, 13, 11-13.

[209] Zununi V, Salehi R, Davaran S, Sharifi S. Liposome-based drug co-delivery systems in cancer cells. Materials Science and Engineering C. 2017, 71, 1327-1341.

[210] Ivanova V, Garbuzenko O, Reuhl K, Reimer D, Pozharov V et al. Inhalation treatment of pulmonary fibrosis by liposomal prostaglandin E2. European Journal of Pharmaceutics and Biopharmaceutics. 2013, 84, 335-344.

[211] Kan P, Chen K, Hsu C, Lin Y. Inhaled liposomal treprostinil shows sustained pharmacokinetic profile, lower irritation, and potentials of reducing dosing frequency. American Journal of Respiratory and Critical Care Medicine. 2018, 197, A3753.

[212] Jhan S, Pethe A.M. Double-loaded liposomes encapsulating lycopene β-cyclodextrin complexes: preparation, optimization, and evaluation. Journal of Liposome Research. 2019, 29, 1-13.

[213] Nguyen T, Nguyen T, Nguyen D. Development and in vitro evaluation of liposomes using soy lecithin to encapsulate paclitaxel. International Journal of Biomaterials. 2017

[214] Daraee H, Etemadi A, Kouhi M, Alimirzalu S, Akbarzadeh A. Application of liposomes in medicine and drug delivery. Artificial Cells, Nanomedicine, and Biotechnology. 2016, 44, 381-391.

[215] Zamboni W. Concept and clinical evaluation of carrier mediated anticancer agents. Oncologist. 2008, 13, 248-260.

[216] Patil Y, Jadhav S. Novel methods for liposome preparation. Chemistry and Physics of Lipids. 2014, 177, 8-18.

[217] Zhao X, Lai E. Titania and zinc oxide nanoparticles: coating with polydopamine and encapsulation within lecithin liposomes — water treatment analysis by gel filtration chromatography with fluorescence detection. Separations. 2018, 5, 13.

[218] Food and Drug Administration. Guidance for industry on pentetate calcium trisodium and pentetate zinc trisodium for treatment of internal contamination with plutonium, americium, or curium; availability. Federal register. 2003, 68, 53984-8.

[219] Dumit S, Avtandilashvili M, McComish S, Strom D, Tabatadze G. Validation of a system of models for plutonium decorporation therapy. Radiation and Environmental Biophysics. 2019, 58, 227-235.

[220] Kastl M, Giussani A, Blanchardon E, Breustedt B, Fritsch P. Developing a physiologically based approach for modeling plutonium decorporation therapy with DTPA. International Journal of Radiation Biology. 2014, 90, 1062-1067.

[221] Grappin L, Berard P. Autorisation de mise sur le marche du Ca- DTPA. Radioprotection. 2008, 43, 465-6.

[222] Yu L, Meng F, Guo M, Yang Y, He J et al. Developing a robust LC-MS/MS method to quantify Zn-DTPA, a zinc chelates in human plasma and urine. Biomedical Chromatography. 2018, 32, e4298.

[223] Grémy O, Miccoli L, Lelan F, Bohand S, Cherel M et al. Delivery of DTPA through liposomes as a good strategy for enhancing plutonium decorporation regardless of treatment regimen. Radiation Research. 2018, 189, 477-489.

[224] Rump A, Becker B, Eder S, Lamkowski A, Abend M, Port M. Medical management of victims contaminated with radionuclides after a "dirty bomb" attack. Military Medical Research. 2018, 5, 27.

[225] Lahrouch F, Siberchicot B, Fèvre J, Leost L, Aupiais J et al. Carboxylate- and phosphonate-modified polyethylenimine: toward the design of Actinide decorporation agents. Inorganic Chemistry. 2019

[226] Ali M, Sadhu B, Boda A, Tiwari N, Das A et al. Thorium decorporation efficacy of rationally-selected biocompatible compounds with relevance to human application. Journal of Hazardous Materials. 2019, 365, 952-961.

[227] Miccoli L, Ménétrier F, Laroche P, Gremy O. Chelation treatment by early inhalation of liquid aerosol DTPA for removing plutonium after rat lung contamination. Radiation Research. 2019, 192, 630-639.

[228] Yan T.T, Lin G.A, Wang M.J, Lamkowski A, Port M et al. Pharmacological treatment of inhalation injury after nuclear or radiological incidents: The Chinese and German approach. Military Medical Research. 2019, 6, 10.

[229] Miller G, Klumpp J.A, Poudel D, Weber W, Guilmette R.A et al. Americium systemic biokinetic model for rats. Radiation Research. 2019, 192, 75-91.

[230] Cipolla D. Will pulmonary drug delivery for systemic application ever fulfill its rich promise? Expert Opinion on Drug Delivery. 2016,13,1337-1340.

[231] Taylor K, Taylor G, Kellaway I, Stevens J. The influence of liposomal encapsulation on sodium cromoglycate pharmacokinetics in man. Pharmaceutical Research. 1989, 6, 633-636.

[232] Mehta P, Ghoshal D, Pawar A, Kadam S, Dhapte-Pawar V. Recent advances in inhalable liposomes for treatment of pulmonary diseases: Concept to clinical stance. Journal of Drug Delivery Science and Technology. 2020, 56, 101509.

[233] Clancy J, Dupont L, Konstan M, Billings J, Fustik S et al. Phase II studies of nebulised Arikace in CF patients with Pseudomonas aeruginosa infection. Thorax. 2013, 68, 818-825.

[234] Rudokas M, Najlah M, Alhnan M, Elhissi A. Liposome delivery systems for inhalation: a critical review highlighting formulation issues and anticancer applications. Medical Principles and Practice. 2016, 25, 60-72.

[235] Grémy O, Tsapis N, Chau Q, Renault D, Abram M et al. Preferential decorporation of americium by pulmonary administration of DTPA dry powder after inhalation of aged PuO2 containing americium in rats. Radiation research. 2010, 174, 637-644.

[236] Podlipec R, Strancar J. Interaction of liposomes on endothelial cells. University of Ljubljana, Slovenia. (2010).

[237] Grémy O, Laurent D, Coudert S, Griffiths N, Miccoli L. Decorporation of Pu/Am actinides by chelation therapy: new arguments in favor of an intracellular component of DTPA action. Radiation Research. 2016, 185, 568-579.

[238] Dumit S, Avtandilashvili M, Strom D, McComish S, Tabatadze G. Improved modeling of plutonium-DTPA decorporation. Radiation Research. 2019, *191*, 201-210.

[239] Bangham A, Standish M, Watkins J. Diffusion of univalent ions across the lamellae of swollen phospholipids. Journal of Molecular Biology.1965, 13, 238-252.

[240] Cortesi R, Esposito E, Gambarin S, Telloli P, Menegatti E, Nastruzzi C. Preparation of liposomes by reverse-phase evaporation using alternative organic solvents. Journal of Microencapsulation. 1999, 16, 251-256.

[241] Dwivedi C, Sahu R, Tiwari S, Satapathy T, Roy A. Role of liposome in novel drug delivery system. Journal of Drug Delivery and Therapeutics. 2014, 4,116-129.

[242] Kannan V, Balabathula P, Thoma L, Wood G. Effect of sucrose as a cryoprotectant on the integrity of paclitaxel-loaded liposomes during lyophilization. Journal of Liposome Research. 2015, 25, 270-278.

[243] Szebeni J, Muggia F, Gabizon A, Barenholz Y. Activation of complement by therapeutic liposomes and other lipid excipient-based therapeutic products: prediction and prevention. Advanced Drug Delivery Reviews. 2011, 63, 1020-1030.

[244] Takahashi N, Higashi K, Ueda K, Yamamoto K, Moribe K. Determination of nonspherical morphology of doxorubicin-loaded liposomes by atomic force microscopy. Journal of Pharmaceutical Sciences.2018, 107, 717-726.

[245] U.S. Food and Drug Administration. Non-binding recommendations for liposomal doxorubicin hydrochloride evaluation. Silver Spring, MD: FDA. 2017.

[246] U.S. Food and Drug Administration. Draft guidance of liposome drug products chemistry, manufacturing, and controls; human pharmacokinetics and bioavailability; and labeling documentation. Silver Spring, MD: FDA. 2015.

[247] Muraki Y, Yamasaki M, Takeuchi H, Tohyama K, Sano N et al. Fluorescent imaging analysis for distribution of fluorescent dye labeled-or encapsulated-liposome in monocrotaline-induced pulmonary hypertension model rat. Chemical and Pharmaceutical Bulletin. 2018, c17-00811.

[248] Danaei M, Dehghankhold M, Ataei S, Hasanzadeh Davarani F, Javanmard R, et al. Impact of particle size and polydispersity index on the clinical applications of lipidic nanocarrier systems. Pharmaceutics. 2018, 10, 57.

[249] Maguire C, Rösslein M, Wick P, Prina-Mello A. Characterisation of particles in solution–a perspective on light scattering and comparative technologies. Science and Technology of Advanced Materials. 2018, 19, 732-745.

[250] Machy P, Leserman L. Small liposomes are better than large liposomes for specific drug delivery in vitro. Biochimica et Biophysica Acta. 1983, 730, 313-320.

[251] Hood R, Andar A, Omiatek D, Vreeland W, Swaan, P. Pharmacy-on-a-chip: microfluidic synthesis of pegylated and folate receptor-targeted liposomes for drug delivery. 16th International Conference on Miniaturized Systems for Chemistry and Life Sciences. 2012.

[252] Rizvi S, Saleh A. Applications of nanoparticle systems in drug delivery technology. Saudi Pharmaceutical Journal. 2018, 26, 64-70.

[253] Prokop A, Davidson J. Nanovehicular intracellular delivery systems. Journal of Pharmaceutical Sciences. 2008, 97, 3518-3590.

[254] Mozafari M. Liposomes: an overview of manufacturing techniques. Cellular and Molecular Biology Letters. 2005, 10, 711-719.

[255] Dua J, Rana A, Bhandari A. Liposome: methods of preparation and applications. International Journal of Pharmaceutical Sciences and Research. 2012, 3, 14-20.

[256] Shi N, Qi X. Preparation of drug liposomes by reverse-phase evaporation. Liposome-Based Drug Delivery Systems. In book: Liposome-Based Drug Delivery Systems.2018, 1-10.

[257] Dwivedi A. Residual solvent analysis in pharmaceuticals. Pharmaceutical technology. 2002, 14, 26-28.

[258] Almalki M, Lai E E, Ko R, Li C. Encapsulation of Zn-DTPA into poly lactic-co-glycolic acid nanoparticles via a modified double emulsion method for extended release into lung fluid. Journal of Nanomedicine. 2018, 2, 1009.

[259] Zaborova O, Filippov S, Chytil P, Kováčik L, Ulbrich K et al. A novel approach to increase the stability of liposomal containers via in prep coating by poly [N-(2-hydroxypropyl)methacrylamide] with covalently attached cholesterol groups. Macromolecular Chemistry and Physics. 2018, 219, 1700508.

[260] Petrache H, Tristram-Nagle S, Harries D, Kucerka N, Nagle J et al. Swelling of phospholipids by monovalent salt. Journal of Lipid Research. 2006, 47, 302-309.

[261] Misra A, Jinturkar K, Patel D, Lalani J, Chrougule M. Recent advances in liposomal dry powder formulations: Preparation and evaluation. Expert Opinion on Drug Delivery. 2009, 6, 71-88.

[262] Franzé S, Selmin F, Samaritani E, Minghetti P, Cilurzo F. Lyophilization of liposomal formulations: still necessary, still challenging. Pharmaceutics. 2018, 10, 139.

[263] Koster K, Webb M, Bryant G, Lynch D. Interactions between soluble sugars and POPC (1-palmitoyl-2-oleoylphosphatidylcholine) during dehydration: vitrification of sugars alters the phase behavior of the phospholipid. Biochimica et Biophysica Acta. 1994, 1193, 143-150.

[264] Glavas-Dodov M, Fredro-Kumbaradzi E, Goracinova K, Simonoska M, Calis S et al (2005). The effects of lyophilization on the stability of liposomes containing 5-FU. International Journal of Pharmaceutics. 291, 79-86.

[265] Pallares R, Abergel R (2020). Transforming lanthanide and actinide chemistry with nanoparticles. Nanoscale. 12, 1339-1348.

[266] Abergel R, Kozimor S (2020). Innovative f-Element Chelating Strategies. inorganic Chemistry. 59, 4-7.

[267] Dakroury G, Abo-Zahra S (2020). The use of titanium oxide/polyethylene glycol nanocomposite in sorption of ^{134}Cs and ^{60}Co radionuclides from aqueous solutions. Journal of Radioanalytical and Nuclear Chemistry. 324, 1351-1364.

[268] Yuan L, Gao G, Feng C, Chai Z, Shi W (2020). A new family of actinide sorbents with more open porous structure: Fibrous functionalized silica microspheres. Chemical Engineering Journal. 385, 123892.